

# UC San Diego

## Research Theses and Dissertations

### Title

Biomechanics of Thunniform Swimming: Electromyography, Kinematics, and Caudal Tendon Function in the yellowfin tuna *Thunnus albacares* and the skipjack tuna *Katsuwonus pelamis*

### Permalink

<https://escholarship.org/uc/item/7cv071z7>

### Author

Knower, Andrea T.

### Publication Date

1998

Peer reviewed

## INFORMATION TO USERS

This manuscript has been reproduced from the microfilm master. UMI films the text directly from the original or copy submitted. Thus, some thesis and dissertation copies are in typewriter face, while others may be from any type of computer printer.

**The quality of this reproduction is dependent upon the quality of the copy submitted.** Broken or indistinct print, colored or poor quality illustrations and photographs, print bleedthrough, substandard margins, and improper alignment can adversely affect reproduction.

In the unlikely event that the author did not send UMI a complete manuscript and there are missing pages, these will be noted. Also, if unauthorized copyright material had to be removed, a note will indicate the deletion.

Oversize materials (e.g., maps, drawings, charts) are reproduced by sectioning the original, beginning at the upper left-hand corner and continuing from left to right in equal sections with small overlaps. Each original is also photographed in one exposure and is included in reduced form at the back of the book.

Photographs included in the original manuscript have been reproduced xerographically in this copy. Higher quality 6" x 9" black and white photographic prints are available for any photographs or illustrations appearing in this copy for an additional charge. Contact UMI directly to order.

# UMI

A Bell & Howell Information Company  
300 North Zeeb Road, Ann Arbor MI 48106-1346 USA  
313/761-4700 800/521-0600



UNIVERSITY OF CALIFORNIA, SAN DIEGO

Biomechanics of Thunniform Swimming:  
Electromyography, Kinematics, and Caudal Tendon Function  
in the yellowfin tuna *Thunnus albacares*  
and the skipjack tuna *Katsuwonus pelamis*

A dissertation submitted in partial satisfaction of the  
requirements for the degree Doctor of Philosophy  
in Marine Biology

by

Andrea Torrence Knowler

Committee in charge:

Robert E. Shadwick, Chair  
Jeffrey B. Graham  
Gerald L. Kooyman  
Michael I. Latz  
Richard L. Lieber  
Richard H. Rosenblatt

1998

**UMI Number: 9907823**

---

**UMI Microform 9907823**  
**Copyright 1998, by UMI Company. All rights reserved.**

**This microform edition is protected against unauthorized  
copying under Title 17, United States Code.**

---

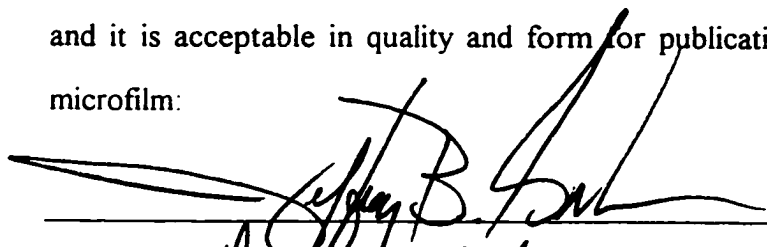
**UMI**  
**300 North Zeeb Road**  
**Ann Arbor, MI 48103**

**Copyright**

**Andrea Torrence Knower, 1998**

**All rights reserved**

The dissertation of Andrea Torrence Knowler is approved,  
and it is acceptable in quality and form for publication on  
microfilm:

  
\_\_\_\_\_  
Michael A. Katz  
\_\_\_\_\_  
Richard H. Rosenblatt  
\_\_\_\_\_  
R. L. Leber  
\_\_\_\_\_  
A. P. Kayman  
\_\_\_\_\_  
R. K. Shadworth  
\_\_\_\_\_

Chair

University of California, San Diego

1998

iii

I dedicate this work to my husband,  
Michael C. Clifton,  
without whose never-ending love, support,  
humor, and faith in me  
this milestone in my life could not have been achieved.



## Table of Contents

Signature Page .....	iii
Dedication .....	iv
Table of Contents .....	v
List of Symbols, Definitions, and Abbreviations .....	viii
List of Figures and Tables .....	x
Acknowledgments .....	xii
Vita, Publications, and Fields of Study .....	xvi
Abstract .....	xx
1. Introduction .....	1
2. Electromyography: red muscle activation patterns during steady swimming in yellowfin and skipjack tunas .....	11
A. Abstract .....	11
B. Introduction .....	13
C. Materials and methods .....	17
1. Fish .....	17
2. Water tunnel .....	17
3. Surgical procedures .....	18
a. Anaesthesia .....	18
b. EMG methodology .....	18
c. Tail tendon buckle .....	19
4. Swimming protocols .....	20
5. Analysis .....	21
a. Selection criteria .....	21
b. EMG processing .....	21
D. Results .....	23
1. Muscle morphology .....	23
2. Swimming velocities and tailbeat frequencies .....	24
3. Electromyography and tail tendon forces .....	25
4. Activity of superficial red muscle .....	28

E. Discussion.....	30
1. Muscle activation in tunas: comparison of yellowfin and skipjack.....	30
2. Muscle activation in tunas vs. other species of fish.....	33
3. Comparison of muscle activation in medial and superficial red muscle.....	36
F. References.....	52
3. Kinematics.....	56
A. Abstract.....	56
B. Introduction.....	57
C. Materials and methods.....	62
1. Experimental protocol.....	62
2. Analysis.....	62
D. Results.....	65
1. Description of propagating waves of midline curvature and lateral displacement.....	65
2. Phase relationships among traveling waves of muscle activation, midline curvature, and lateral displacement of the midline.....	66
3. Rates of traveling waves of activation, curvature, and displacement.....	67
4. Kinematic reference for peak force at the tail blade.....	68
E. Discussion.....	69
1. Significance of muscle activation-midline curvature phase.....	69
2. Kinematic parameters compared with other teleosts and a previous study of yellowfin.....	71
3. Significance of muscle activation and midline curvature rates in tunas.....	72
4. Kinematic reference for when peak force occurs at the tail blade.....	73
F. References.....	89
4. Forces measured in the caudal tendons of swimming tunas, and the functional role of the tendons as force transmitters.....	91
A. Abstract.....	91
B. Introduction.....	93
C. Materials and methods.....	98
1. <i>In vivo</i> experiments.....	98
a. Experimental protocol.....	98
b. Analysis.....	100
2. <i>In vitro</i> experiments.....	100

a. Experimental protocol .....	100
b. Analysis .....	102
D. Results.....	103
1. Relationship between force and swimming speed .....	103
2. Relationship between muscle activation and tendon force development.....	104
3. Biomaterial properties of tendons .....	105
E. Discussion.....	108
1. <i>In vivo</i> force measurements .....	108
2. Calculation of tendon strain energy <i>in vivo</i> and its possible importance .....	110
3. <i>In vitro</i> biomaterial properties: comparison of tuna and mammalian tendons .....	112
F. References.....	129
5. Summary and conclusions.....	131

## List of Symbols, Definitions, and Abbreviations

$\varepsilon$	strain: relative length change ( $= \Delta l/l_0$ )
$\lambda_b$	propulsive wavelength (= wavelength of the propagating lateral displacement wave)
$\sigma$	stress: force per unit cross-sectional area
COT	cost of transport: the total metabolic energy required to travel a unit distance
cruising	aerobic swimming
duty cycle	the proportion of the tailbeat period when muscle is active (= EMG burst duration/T)
E	elastic modulus: an indicator of material stiffness ( $=\Delta\sigma/\Delta\varepsilon$ )
EMG	electromyogram
H	hysteresis: the proportion of strain energy dissipated as heat during a loading/unloading cycle
kinematics	the study of motions through time
$l_0$	rest length (e.g., of tendon or muscle)
L	forklength; nose = 0, tail fork = 1 L
lateral displacement	excursion of a point on the midline (backbone) to the left or right of the swimming track
medial red muscle	aerobic muscle located near the backbone; anatomically, an integral component of the nested myotome cones
midline curvature	reciprocal of the radius of curvature of a bend in the backbone
myotome	muscle corresponding to a vertebral segment (one myotome per segment)

myoseptum	collagenous connective tissue sheet separating myotomes, and onto which muscle fibers of the myotome attach
N	Newton
negative work	externally generated work absorbed by muscle
Pa	Pascal
positive work	work generated by muscle on its surroundings
stride length	distance traveled in one tailbeat ( $= T * U$ )
superficial red muscle	triangular wedge of aerobic muscle under the skin, running along the lateral midline of the body
swimming track	the path of forward motion of the body through the water
T	tailbeat period: the time required to complete one tailbeat cycle; the reciprocal of TBF.
tailbeat cycle	2 consecutive tail sweeps, where a tail sweep is when the tail traverses from one side to the other
TBF	tailbeat frequency (Hz): number of tailbeat cycles per second; the reciprocal of T.
U	swimming speed
VDA	video dimension analyzer
XSA	cross-sectional area

## List of Figures and Tables

<u>Chapter</u>		
1.	Fig. 1.1	Types of axial propulsion mechanisms in fishes..... 7
	Fig. 1.2	The tuna “engine” is spatially separated from the “propeller” ..... 8
	Fig. 1.3	Schematic of how EMGs and caudal tendons forces are recorded ..... 9
2.	Fig. 2.1	Side view of yellowfin and skipjack tuna; hemi-cross sections of yellowfin and skipjack muscle..... 38
	Fig. 2.2	Tailbeat frequency as a function of water velocity..... 40
	Fig. 2.3	Examples of EMG traces..... 41
	Fig. 2.4	EMG onsets and offsets plotted in absolute time and normalized to tailbeat period, at various TBFs ..... 43
	Fig. 2.5	EMG duty cycle as a function of muscle location..... 45
	Fig. 2.6	Summary of red muscle activation data for 4 yellowfin and 3 skipjack across all swimming speeds, with superimposed force traces ..... 46
	Fig. 2.7	Comparison of medial and superficial red muscle activity..... 48
	Fig. 2.8	Comparison of tuna red muscle activation patterns with those of other species ..... 50
3.	Fig. 3.1	Montages of captured video fields ..... 75
	Fig. 3.2	Traveling waves of midline curvature and lateral displacement... 77
	Fig. 3.3	Amplitude envelopes of midline curvature and lateral displacement ..... 79
	Fig. 3.4	Phase of muscle activation, midline curvature, and lateral displacement at 3 axial locations..... 80
	Table 3.1	Phase delays among midline curvature, lateral displacement, and EMG onset ..... 83
	Table 3.2	Propagation rates of waves of muscle activation, midline curvature, and lateral displacement ..... 85
	Fig. 3.5	Occurrence of peak force in the caudal tendons relative to lateral movements of the peduncle and tail tip..... 86
	Table 3.3	Phase relationship between when the tail tip crosses the swimming track and peak force..... 88
4.	Fig. 4.1	<i>Post mortem</i> photograph of buckle force transducer on caudal tendons ..... 115
	Fig. 4.2	Representative tendon buckle force traces at different TBFs ..... 116
	Fig. 4.3	Peak caudal tendon forces at cruising speeds and restrained burst speeds ..... 118

Fig. 4.4	Summary of muscle activation patterns with superimposed force traces .....	120
Table 4.1	Percentage of peak force registered in the caudal tendons prior to activation of red muscle at 0.65 L .....	122
Fig. 4.5	Sample stress vs. strain curves for yellowfin and skipjack caudal tendons .....	124
Table 4.2	Biomaterial properties of caudal tendons when mechanically loaded to <i>in vivo</i> cruising forces .....	125
Table 4.3	Biomaterial properties of caudal tendons when mechanically loaded to maximal burst swimming forces.....	127
Table 4.4	Percentage of total mechanical energy output per tail sweep invested in loading the caudal tendons.....	128

## Acknowledgments

In this day and age, it is probably impossible to complete any doctoral science project successfully without the help of numerous people. This project has certainly been no exception, especially given the challenges of conducting field research far from the parent institution.

First I wish to thank my committee for their support and advice over the years. I consider myself fortunate to have had a committee comprised of members with such a diverse yet complementary array of expertise. My research and writing skills both have benefited greatly from the guidance of Drs. Shadwick, Graham, Kooyman, Rosenblatt, Latz, and Lieber, and I thank you all.

In particular, I could not have asked for a better major advisor than Dr. Robert Shadwick. He's one of the smartest guys I know, yet one of the most modest, and he's one of the few researchers I've met who knows how to teach-- and teach well. I'll be happy if I manage to retain a quarter of what he's taught me over the years. I thank him not only for sharing his expertise with me, but also for giving me free rein when I needed it, and for helping me muck out the tunnel and dissect tunas when that was on the agenda. I also appreciate his efforts to introduce me to other experts in the field of biomechanics.

I would also like to thank the National Marine Fisheries Service Honolulu Lab for allowing us to maintain the water tunnel at their Kewalo Research Facility for so many years. The people there were very accommodating, and in particular, I'd like to thank Dr. Rich Brill, Ray Sumida, and the late Shige Yano. Captain Sadami Tsue and the crew of the *F/V Corsair* went to great lengths to find tunas and deliver them safely to us. In addition, thanks to Dr. Chris Boggs for allowing me to tag along on



his tuna long-lining cruise to conduct muscle physiology experiments on BIG tunas. The Captain and crew of the *Townsend Cromwell* were some of the most helpful and friendly of any research vessel I've been on.

I owe thanks to many folks here at the Scripps Institution of Oceanography (SIO) and UCSD. One of the most important was Dr. Art Yayanos, for without his efforts, I would not have been able to attend Scripps in the first place, so I thank him whole-heartedly. Michael Clifton, Dr. Bob Guza, and Bill Boyd (all from the Center for Coastal Studies) provided me with new perspectives on research and much-needed electronics assistance. Dr. Lieber in Orthopedics was kind enough to make his lab and equipment available to me to do the *in vitro* tendon biomaterial testing experiments for Chapter 4, and Scott Lundberg devoted several hours of his time to teaching me how to use the software. Outside of Scripps, Dr. Clem Wardle (SOAFD Marine Laboratory, Aberdeen, UK) worked with us for several weeks in Honolulu and provided valuable advice on making EMG electrodes and video filming techniques. Dr. Andy Biewener (University of Chicago) provided the tendon buckles and helped us develop the surgical techniques for using them. Various people at Scripps took time off from their own work to help out with my experiments in Hawaii, including Drs. Chin Lai, Steve Katz, Bob Shadwick, and Jeff Graham. In particular, I am indebted to my fellow tuna researchers, Drs. Keith Korsmeyer and Heidi Dewar. They got me started with the nitty-gritty of tunnel operations and endured many long, hot hours in the shack for my benefit. Back at Scripps, the staffs of the Marine Biology Research Division, Center for Marine Biotechnology and Biomedicine, and the SIO Graduate Department could always be counted on both for their help and their sense of humor. Many thanks to Sharon Williams for somehow managing to find funding for me when it didn't seem possible.

I cannot over-emphasize the importance of my all my friends, near and far, throughout the years of thick and thin, fun and not-so-fun. They played an integral part in my success. Dr. Steve Katz was like an adjunct advisor to me, and I am most grateful for the many, many hours he invested in sharing his eclectic knowledge. He is one of the most gifted teachers I've met. Just as important was his unique sense of humor. My cohorts in the Shadwick lab, Drs. Jen Nauen and Greg Szulgit, are my best friends and were it not for their support, good nature in putting up with me, and encouragement, it would have been very difficult if not impossible to have completed my doctoral work. It's hard to imagine a more convivial atmosphere and a more interesting group than has existed in the Shadwick Lab for the last six years.

My heartfelt thanks go out to all my family for encouraging me through all these years and having faith in me no matter what. I was particularly touched by the amount of time and effort many of them took out of their own busy schedules to send me care packages, survival kits, and other tokens of their love and affection, especially during the last few months of writing when I needed the support the most. They were always there for me and were very understanding of the long times which passed between visits to the east coast. Thank you, thank you all for your love.

Major funding was required for this project and was provided by the National Science Foundation (OCE91-03739 and IBN95-14203), the San Diego Chapter of Sigma Xi, the SIO Tuna Endowment, the SIO Graduate Department, and the UCSD Academic Senate. I also received salary support through a Research Assistantship to the Center for Coastal Studies and a Sea Grant Traineeship to Dr. Tim Baumgartner (Marine Life Research Group, SIO).

I thank the Inter-American Tropical Tuna Commission for permission to adapt tuna illustrations from their book *Tuna and Billfish-Fish Without a Country* (by J. Joseph, W. Klawe, and P. Murphy) for figures in Chapters 1 and 2 of this dissertation.

Most of all, my love and thanks to my husband Michael, for seeing me through this and making my life more wonderful than I ever thought it could be.

## Vita

**Personal:** Born 21 November 1961, Columbia, SC, USA.

### Education:

1983 B.A. Biology, Cornell University, Ithaca, NY.

1998 Ph.D. Marine Biology, Scripps Institution of Oceanography,  
University of California, San Diego, La Jolla, CA.

### Professional Experience:

1979-82: Laboratory Technician, Hynson, Westcott, and Dunning; Department  
(Summers) of Research and Development, Baltimore, MD.

1981-83: Laboratory Technician, New York State College of Veterinary  
Medicine, Cornell University, Ithaca, NY.

1983-1985: Research Chemist, Uniformed Services University of the Health  
Sciences, F. Edward Hebert School of Medicine, Department of  
Pediatrics, Bethesda, MD.

1985-1988: Assistant Director of Cell Biology/Research Biochemist,  
Westinghouse Bio-Analytic Systems Company, Rockville, MD.

1988-1991: Senior Technical Associate, Hybridoma Network Laboratory of the  
Center for Advanced Biotechnology and Medicine, Rutgers  
University, Piscataway, NJ.

1991-1995: Research Assistant, Marine Biology Research Division, Center for  
Marine Biotechnology and Biomedicine, and Center for Coastal  
Studies, Scripps Institution of Oceanography, University of California,  
San Diego, La Jolla, CA.

1994: Teaching Assistant, Dept. of Biology, University of California, San  
Diego, La Jolla, CA. Comparative Physiology.

1995-1997: Sea Grant Trainee, Marine Life Research Group, Scripps Institution of  
Oceanography, University of California, San Diego, La Jolla, CA.

### Research Cruise Experience:

- Aug. 1989: Research Associate on research cruise aboard NOAA ship *Oregon II*. National Oceanic and Atmospheric Administration, National Marine Fisheries Service, Environmental Process Division, Sandy Hook, NJ. Project studying seabed oxygen metabolism in the New York Bight around the Twelve-Mile Dump Site.
- July 1990: Research Associate on research cruise aboard Texas A & M's R/V *Gyre*. National Oceanic and Atmospheric Administration, National Marine Fisheries Service, Environmental Process Division, Sandy Hook, NJ. Project studying seabed oxygen metabolism at varying depths in the Gulf of Mexico.
- July 1993: Research Associate on research tuna long-lining cruise, NOAA ship *Townsend Cromwell*, Hawaiian islands. Studying muscle morphology and twitch kinetics in large yellowfin tunas.
- 1994 : Technician aboard R/V *Cape Hatteras*: collecting and processing (Aug. - Oct.) CTD data for multi-institutional Coastal Ocean Processes (CoOP) Project, sponsored by the National Science Foundation.

### Publications:

- Feuerstein, G., Powell, J. A., Knowler, A. T. and Hunter, K. W. (1985). Monoclonal antibodies to T-2 toxin: *In vitro* neutralization of protein synthesis inhibition and protection of rats against lethal toxemia. *J. Clin. Invest.* **76**:2134-2138.
- Graham, C. E., Knowler, A. T. and Hunter, K. W. (1985). *Leishmania mexicana*: Expression of heat shock genes during differentiation. *J. Cell Biol.* **101**(5-2):76a. (Abstract)
- Hunter, K. W., Jr, Brimfield, A. A., Knowler, A. T., Powell, J. A. and Feuerstein, G. Z. (1990). Reversal of intracellular toxicity of the tricothecene mycotoxin T-2 with monoclonal antibody. *J. Pharmacol. Exp. Ther.* **255**(3): 1183-1187.
- Knowler, T., Carlson, J., Yarmush, D. M., Yarmush, M. L. and Granzow, R. (1991). The characterization of antibody-antigen interactions by a novel biosensor: Biacore. *Biophysical Journal* **59**(2, pt. 2): 170A. (Abstract)

- Knower, T., Lai, N. C., Shadwick, R. E., Graham, J. B., Shabetai, R. and Bhargava, V. (1992). Biomechanical properties of the elasmobranch pericardial septum. *Amer. Zool.* **32(5)**: 56A. (Abstract)
- Lai, N. C., Kim, B. U., Knower, T., Graham, J. B. and Shabetai, R. (1992). Atrial pressure recordings verify vis-a-tergo cardiac filling in the elasmobranch heart. *Amer. Zool.* **32(5)**: 39A. (Abstract)
- Shadwick, R. E., Knower, T. and Fonseca, M. (1992). The mechanical organization of muscle and tendon in yellowfin tuna. *Amer. Zool.* **32(5)**: 159A. (Abstract)
- Knower, T., Shadwick, R. E., Biewener, A. A., Korsmeyer, K. and Graham, J. B. (1993). Direct measurement of tail tendon forces in swimming tuna. *Amer. Zool.* **33(5)**: 30A. (Abstract)
- Knower, T., Shadwick, R. E., Wardle, C. S., Korsmeyer, K. and Graham, J. B. (1993). The timing of red muscle activation in swimming tuna. *Amer. Zool.* **33(5)**: 30A. (Abstract)
- Korsmeyer, K. E., Lai, N. C., Knower, T., Dewar, H., Shadwick, R. E. and Graham, J. B. (1993). Cardiovascular function in swimming yellowfin tuna (*Thunnus albacares*). *Amer. Zool.* **33(5)**: 44A. (Abstract)
- Graham, J. B., Dewar, H., Lai, N. C., Korsmeyer, K. E., Fields, P. A., Knower, T., Shadwick, R. E., Shabetai, R. and Brill, R. W. (1994). Swimming physiology of pelagic fishes. In *Mechanics and Physiology of Animal Swimming* (ed. L. Maddock, Q. Bone and J. M. V. Rayner), pp. 63-74. Cambridge: Cambridge University Press.
- Korsmeyer, K. E., Lai, N. C., Dewar, H., Knower, T., Shadwick, R. E. and Graham, J. B. (1994). Cardiovascular responses to exercise in yellowfin tuna. *The Physiologist* **37**: A-93. (Abstract)
- Shadwick, R. E., Steffensen, J. F., Katz, S. L. and Knower, T. (1997). Muscle dynamics in fish during steady swimming. *Amer. Zool.* (in press)
- Knower, T., Shadwick, R. E., Katz, S. L., Graham, J. B. and Wardle, C. S. (1997). Red muscle activation patterns in yellowfin (*Thunnus albacares*) and skipjack (*Katsuwonus pelamis*) tunas during steady swimming. *J. exp. Biol.* (accepted with revisions)

**Fields of Study:**

Major Field: Marine Biology

Studies in Biomechanics.  
Dr. Robert E. Shadwick

Studies in Biology of Fishes.  
Dr. Richard H. Rosenblatt

Studies in Muscle Physiology.  
Dr. Richard L. Lieber

Studies in Natural History.  
Dr. Paul K. Dayton

Studies in Research Cruise Operations and Techniques.  
Dr. Kenneth L. Smith

## ABSTRACT OF THE DISSERTATION

Biomechanics of Thunniform Swimming:  
Electromyography, Kinematics, and Caudal Tendon Function  
in the yellowfin tuna *Thunnus albacares*  
and the skipjack tuna *Katsuwonus pelamis*

by

Andrea Torrence Knowler

Doctor of Philosophy in Marine Biology

University of California, San Diego, 1998

Professor Robert E. Shadwick, Chair

This research project was undertaken on two species of tropical tuna: the yellowfin *Thunnus albacares* and the skipjack *Katsuwonus pelamis*, to explore the dynamic physiological design features of tunas which underly the highly-developed thunniform propulsion mechanism. To achieve an integrated understanding of tuna swimming mechanics, a combination of electromyography, kinematics, and direct force measurements was used to probe the dynamic function of the myotomal red muscle as fish swam over a range of sustained, aerobic swimming speeds in a large water tunnel.



In both species, onset of red muscle activation proceeds sequentially in a rostral-caudal direction, while deactivation is nearly simultaneous at all sites, coincident with peak force in the caudal tendons. In yellowfin, there is complete segregation of contralateral activity, while in skipjack there is slight overlap. In both species, all red muscle on one side is active simultaneously for part of each cycle. Comparison with other fish species shows that the tuna EMG patterns culminate a spectrum of activation patterns underlying swimming modes from anguilliform to thunniform.

Coupling kinematics with EMG data revealed that muscle activation occurs after the midline has reached its maximum convexity at any given axial location; therefore, it was concluded that midline curvature is not an accurate indicator of local strain in the myotomal cone muscle. Activation and curvature waves travel down the body at the same rate, so muscle function is predicted not to vary by axial location. In yellowfin, peak force occurs in the caudal tendons as the tail tip crosses the midpoint of its sweep; in skipjack, when the tip is about three-quarters through its sweep.

Internal force measurements were made for the first time in any fish species by fitting a stainless steel buckle force transducer around the pair of deep caudal tendons on one side. At cruising speeds, mean forces were 1.3-3.8 N in yellowfin and 1.6-4.1 N in skipjack. At restrained burst speeds, forces were approximately 10 times higher. The biomaterial properties of the tendons show that they function as inextensible linkages, rather than biological springs, in transferring muscle force to the tail.

# Chapter 1: Introduction

Scientists have long been intrigued by the mechanics of fish locomotion. With the great diversity of fish species and the habitats they exploit comes a wide variety of body morphologies and lifestyles, resulting in different swimming modes. For those species that swim by axial locomotion (that is, by bending of the backbone), the kinematics of these swimming modes has been broadly categorized (Breder, 1926; Webb, 1993) to describe a progression from undulatory to oscillatory body movements used for propulsion (Fig. 1.1). In all cases, a wave of sequential muscle activation passes from head to tail down the body, and the resulting muscle contractions cause a posteriorly-progressing bending wave that pushes the fish forward through the water. What differs across the spectrum of swimming mechanisms is the degree of undulation (or lateral movement) along the body and the location where internal muscle force is directed on the body to produce thrust (indicated by black shading in the figure). For example, in eels (anguilliform mode), the body height is nearly uniform along the entire length, and muscle contractions cause sequential bending of body segments to push directly against the water. In fact, if the “tail” end were removed, an eel would still be able to swim. However, with ensuing modes in the progression (subcarangiform to carangiform to thunniform), body morphologies have a more distinctive tail, and thrust production is directed farther and farther back on the body, generated by more oscillatory movements of the

posterior region while side to side lateral motion of the anterior region is minimized. This trend culminates in the thunniform swimming mode (named for the tunas), in which most of the body is held relatively rigid while lateral movement and thrust production are focused almost exclusively at the high aspect ratio, lunate tail. Indeed, if the tail is cut off a tuna, it cannot swim, but sinks. Thus, tunas represent an extreme end (opposite eels) of the kinematic progression of axial swimming styles, using a highly specialized mode of swimming that enables them to move quickly through the water. This research project was undertaken to explore the dynamic physiological design features of tunas which underly the highly-developed thunniform propulsion mechanism.

From a physiological standpoint, tunas are fascinating subjects because of their ability to excel in two areas that for many vertebrates remain mutually exclusive: they achieve some of the fastest burst speeds known, yet also have long endurance for sustained swimming. As Joseph *et al.* (1988) noted, they are both accomplished sprinters and marathon runners. Some of the physiological features enabling tunas to be such successful pelagic swimmers include a streamlined, fusiform body plan externally and several uncommon anatomical features internally. One of these features is a large, red (aerobic) muscle mass positioned near the backbone. Most fishes have only a thin wedge of red muscle running superficially along the lateral midline of the body. The internal location in tunas, along with counter-current vasculature, allows the red muscle to maintain temperatures several degrees above

ambient, which contributes to increased muscle performance. In addition, the red muscle near the backbone is incorporated within the nested structure of myotome cones, contiguous with the surrounding rings of white (anaerobic) muscle (see Chapter 2, Fig. 2.1, for further details). The myotomes in tunas are highly elongated, which directs the force produced by the anteriorly-situated muscle mass rearward to the tail. The unusual anatomical arrangement of red muscle makes it possible to probe the dynamic function of the myotomal cone muscle at steady, cruising speeds, without exhausting the fish. This is an attractive feature of studying tunas, as attempting a similar study of the nested myotomes in other fishes would require eliciting anaerobic burst swimming speeds.

Another anatomical feature which sets tunas apart from most other teleosts is the presence of thick tendons spanning the peduncle to connect the force-producing muscle mass with the tail. Most fishes have muscle instead of tendon connecting all the way to the caudal fin. Because a force transducer can be fitted onto the tuna tendons, they are the key feature enabling experimental measurements of internal muscle force during swimming. This study is the first in any fish species to measure such forces directly. These measurements permit quantification of the anteriorly-generated muscle force reaching the tail for external thrust production.

Thunniform swimming is the most derived form within the spectrum of axial swimming modes. This study of swimming mechanics focuses on understanding how the tuna muscle and tendon physiology functions to produce the highly-adapted

locomotion of these pelagic swimmers. In particular, because the major cross-sectional area of the force-producing muscle “engine” is located anteriorly in tunas, spatially separated from the thrust-producing “propeller” (Fig. 1.2), this study addresses the following questions: 1) what are the characteristics of tuna muscle activation leading to force production; 2) how much force is produced; and 3) how is this force directed down the body and transferred across the peduncle to the tail?

Studies were undertaken on two species of tropical tuna, the yellowfin tuna *Thunnus albacares* and the skipjack tuna *Katsuwonus pelamis*, and were carried out at the National Marine Fisheries Service Kewalo Research Facility in Honolulu, Hawaii. Both these species are readily available in waters near this laboratory. The facility was also large enough to accommodate the large water tunnel treadmill built by Dr. J. B. Graham (Graham *et al.* 1990; Dewar and Graham, 1994; Graham *et al.* 1994). Such a tunnel is key to the success of a project of this nature because it allows the fish to swim at controlled velocities while maintaining station. This allows the investigator to have monitoring wires extending from the free-swimming fish to amplifiers and computers, and to film the fish using a fixed-position video camera.

Success of this project was also dependent upon the development of surgical protocols which would enable instrumentation of fish with several electrodes and a force transducer simultaneously, without impairing the fish’s swimming ability. Fortunately, this was accomplished in these highly active fish. Thus, with the

combination of the Kewalo Facility, the large water tunnel, and the surgical expertise, it was possible to surmount many of the challenges to working with tunas.

To achieve an integrated understanding of tuna swimming mechanics, a combination of tools was used to probe dynamic muscle function. These included electromyography, kinematics, and direct internal measurements of muscle force. A series of electromyogram (EMG) electrodes was inserted down the length of the red muscle to measure activation patterns, and a force transducer was fitted onto the caudal tendons (Fig. 1.3). Instrumented fish were videotaped as they swam over a range of sustained aerobic swimming speeds in the water tunnel, with all signals recorded simultaneously to computer. The following chapters discuss the parallel experiments conducted on yellowfin tuna and skipjack tuna:

Chapter 2 describes the temporal activation patterns recorded from a series of EMG electrodes implanted down the length of red muscle. The time course of muscle activation is expressed relative to the production of peak force recorded from the caudal tendon transducer.

Chapter 3 analyzes the kinematics of tuna swimming by relating muscle activation, midline curvature, and lateral movement. An analysis of tail tip position relative to development of peak force at the tail is also given.

Chapter 4 quantifies the *in vivo* forces measured by the caudal tendon transducer during swimming. The *in vitro* biomaterial properties of the tendons are

then examined, and a prediction is made for how the tendons function in the transmission of muscle force to the tail blade to produce thrust.

The work concludes with a summary that attempts to synthesize the findings on muscle activation, kinematics, and force production into a description of physio-mechanical events which produce thunniform swimming.

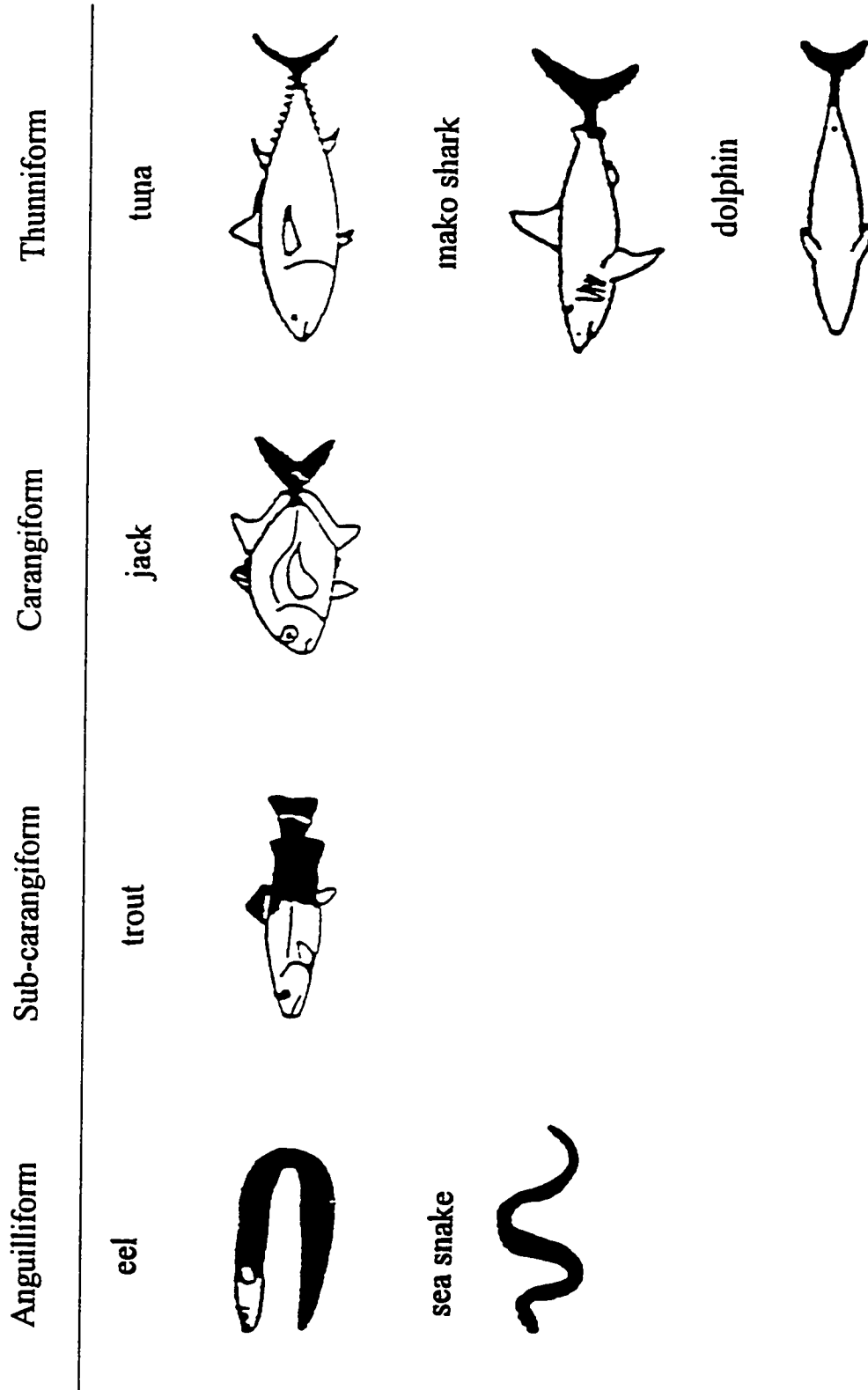


Fig. 1.1. Types of axial propulsion mechanisms in fishes (with reptilian and mammalian representatives that also use these mechanisms). The portion of the body used for thrust production is indicated in black. (Adapted from Webb and Blake, 1995.)



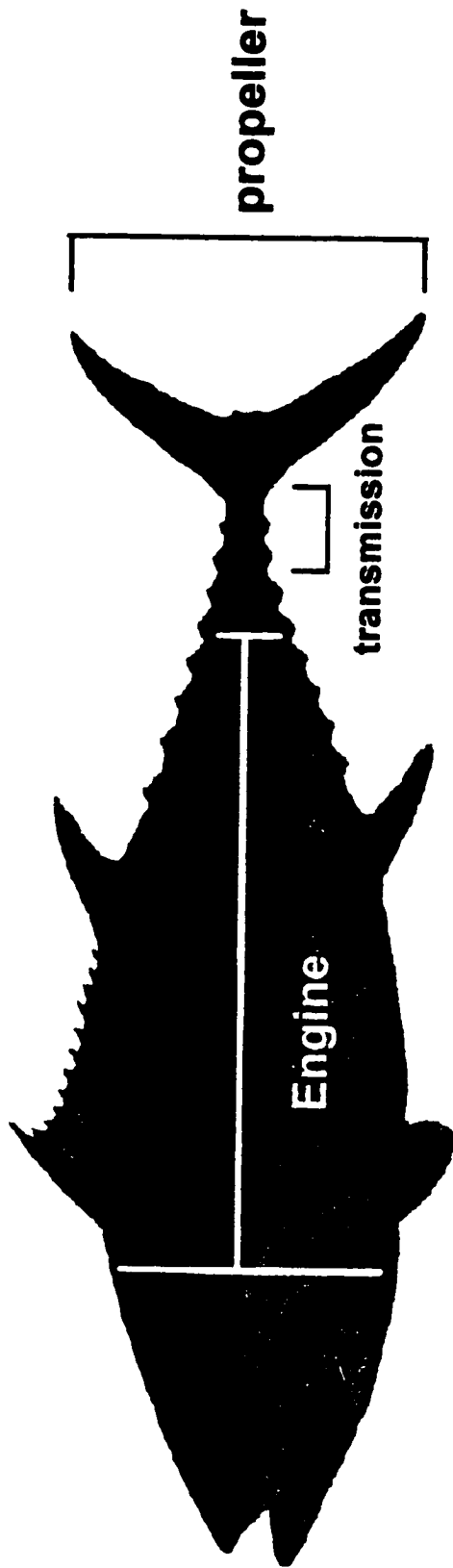


Fig. 1.2. The tuna "engine" is spatially separated from the "propeller". (Illustration of the yellowfin tuna *Thunnus albacares* adapted from Joseph *et al.* 1988.)

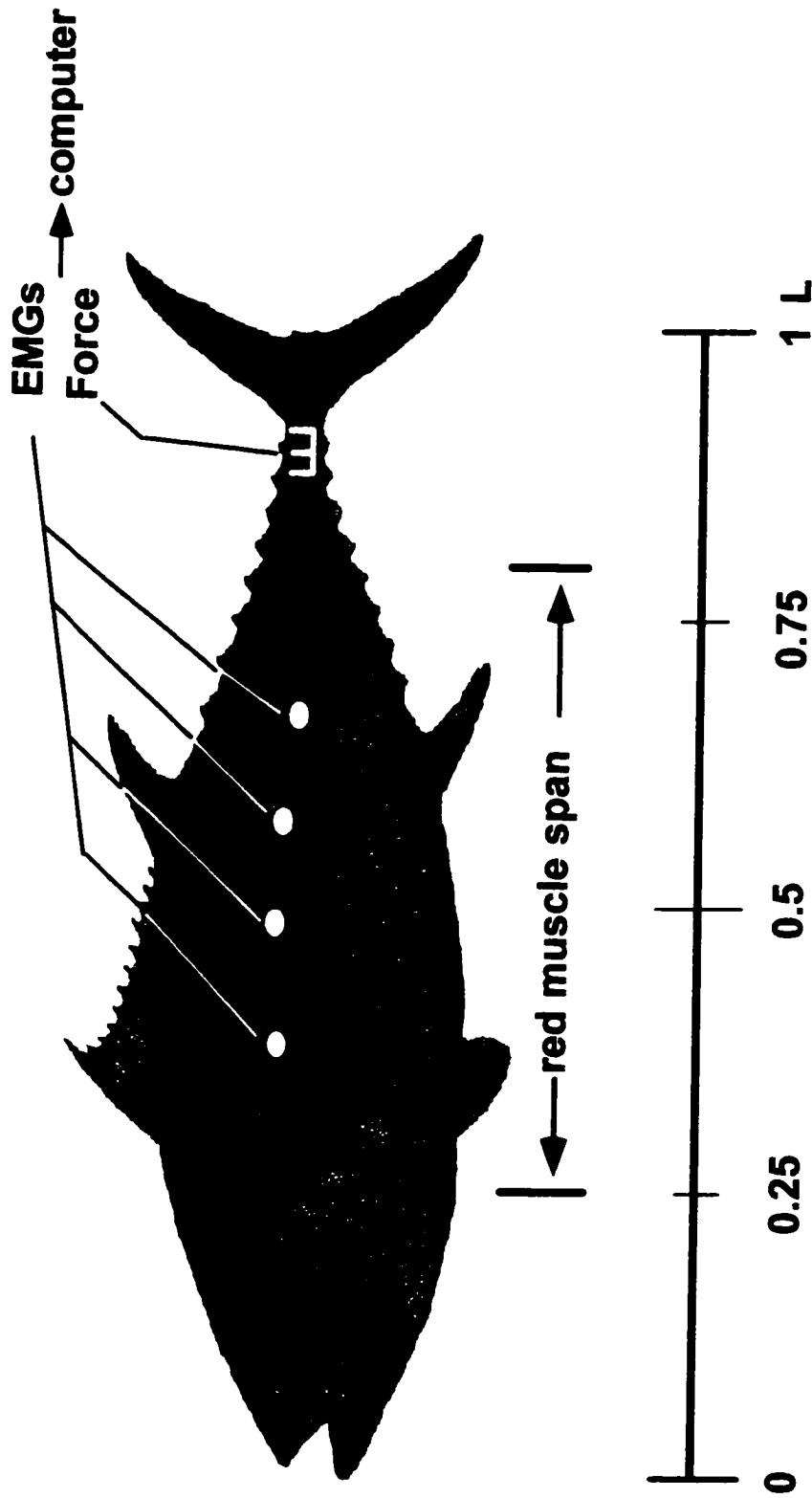


Fig. 1.3. Schematic indicating how electromyograms (EMG) and caudal tendon forces are recorded from the left side of a tuna. Total forklength ( $L$ ) and the portion of  $L$  spanned by the red muscle are also shown. (Illustration of the yellowfin tuna *Thunnus albacares* adapted from Joseph *et al.* 1988.)

## References

- Breder, C. M. (1926). The locomotion of fishes. *Zoologica* 4, 159-297.
- Dewar, H. and Graham, J. B. (1994). Studies of tropical tuna swimming performance in a large water tunnel: I. Energetics. *J. exp. Biol.* 192, 13-31.
- Graham, J. B., Dewar, H., Lai, N. C., Korsmeyer, K. E., Fields, P. A., Knowler, T., Shadwick, R. E., Shabetai, R. and Brill, R. W. (1994). Swimming physiology of pelagic fishes. In *Mechanics and Physiology of Animal Swimming* (ed. L. Maddock, Q. Bone and J. M. V. Rayner), pp. 63-74. Cambridge: Cambridge University Press.
- Graham, J. B., Dewar, H., Lai, N. C., Lowell, W. R. and Arce, S. M. (1990). Aspects of shark swimming performance determined using a large water tunnel. *J. exp. Biol.* 151, 175-192.
- Joseph, J., Klawe, W. and Murphy, P. (1988). *Tuna and Billfish-Fish Without a Country*. La Jolla: Inter-American Tropical Tuna Commission.
- Webb, P. W. (1993). Swimming. In *The Physiology of Fishes* (ed. D. H. Evans), pp. 47-73. Boca Raton: CRC Press.
- Webb, P. W. and Blake, R. W. (1985). Swimming. In *Functional Vertebrate Morphology* (ed. M. Hildebrand, D. M. Bramble, K. F. Liem and D. B. Wake), pp. 110-128. Cambridge, MA and London, England: Belknap Press of Harvard Univ. Press.

## **Chapter 2: Electromyography: red muscle activation patterns during steady swimming in yellowfin and skipjack tunas.**

### **Abstract**

Tunas are exceptional swimmers, able to attain some of the fastest speeds known among fishes, as well as having strong endurance to cover vast distances during migrations. These extreme abilities make them enticing subjects for a study of dynamic swimming design. To learn about the swimming muscle function in two species of tuna (yellowfin: *Thunnus albacares* and skipjack: *Katsuwonus pelamis*), a series of electromyogram (EMG) electrodes was implanted down the length of the body in the medial red (aerobic) muscle. (In one individual from each species, EMG wires were also inserted into the superficial red muscle.) Additionally, a buckle force transducer was fitted around the caudal tendons on the same side of the peduncle. Recordings of muscle activity and caudal tendon forces were made while fish swam over a range of steady, sustainable cruising speeds in a large water tunnel treadmill. In both species, onset of red muscle activation proceeds sequentially in a rostro-caudal direction, while offset (or deactivation) is nearly simultaneous at all sites. This results in EMG burst duration decreasing towards the tail. Muscle duty cycle at each location remains a constant proportion of the tailbeat period (T), independent of

swimming speed, and peak force is registered in the tail tendons just as all the muscle on that side deactivates. Average duty cycles in skipjack are longer than those in yellowfin. In yellowfin medial red muscle, there is complete segregation of contralateral activity, while in skipjack there is slight overlap, as the anterior muscle on one side is activated 0.15 T before the posterior muscle on the opposite side is deactivated. In both species, all medial red muscle on one side is active simultaneously for part of each cycle, lasting 0.18 T in yellowfin and 0.11 T in skipjack. Preliminary findings concerning superficial red muscle activation indicate that in skipjack, stimulation of medial and superficial muscle in the same transverse plane is nearly synchronous. In yellowfin, superficial activation precedes medial by varying degrees (by as much as 0.08 T), depending on axial location. In comparison with EMG patterns from other species of fish, the tuna medial red EMG patterns culminate a progression encompassing the spectrum of swimming modes from anguilliform to thunniform.

## Introduction

Scientists have long been intrigued by the mechanics of axial fish locomotion, and have pursued its study via two primary approaches. One is hydrodynamical, describing swimming performance based on the effects that the moving body imparts on the surrounding water (e.g., Lighthill, 1969; Webb, 1975), while the other examines features of the body design itself. Within the latter category, some investigators have studied body morphology to make inferences about swimming mode (e.g., Wainwright, 1983; Westneat *et al.* 1993), but the approach of the present study has been to focus on the dynamic physiology of the fish's swimming mechanism, by probing its muscle function. With this method, one tries to understand how a particular swimming mode results from the sequence of muscle activation along the fish's body and the subsequent interactions between this contracting muscle and the body's structural elements.

To do this, two species of tropical tuna were studied : the yellowfin *Thunnus albacares* (Bonnaterre) and the skipjack *Katsuwonus pelamis* (Linnaeus). From a design point of view, tunas present a fascinating subject for study because of their demonstrated prowess in swimming. Tunas are known to achieve some of the fastest swimming speeds of any fish [e.g., yellowfin: 70 km/hr (Magnuson, 1978)], but they also excel in endurance, as they must swim continuously to ram ventilate and to counteract their negative buoyancy (Magnuson, 1978). Some species cover vast distances during migrations, as illustrated by the bluefin's trans-Pacific crossings [e.g.

Japan to Baja California: 9700 km (Lindsey, 1978)]. The overall goal of this research is to understand the design features of the tuna “power plant” which make this level of swimming performance possible, by analyzing muscle activation patterns, kinematics, and caudal tendon forces in swimming tunas. The present chapter focuses on the first component: muscle activation, or electromyography.

What are some important features of the tuna body plan? Externally, tunas feature a shape which one might regard as the epitome of design for a fast-swimming animal: a highly streamlined body with smooth skin and recesses for retracting many of the fins; the largest cross-sectional area of muscle mass concentrated near the body’s midlength; narrow-necking just forward of the tail fin for reduced drag; and a large aspect-ratio lunate tail to provide lift-based thrust (Fig. 2.1A). Internally, they manifest the same highly segregated anatomic division between red (slow, aerobic) and white (fast, anaerobic) muscle types seen commonly in other fish: the greatest proportion of the muscle mass is comprised of white muscle arranged in nested cones of myotomes, flanked by a thin triangular wedge of longitudinally-oriented red muscle located laterally (just under the skin) along each side of the body. Where tunas differ from most other fish is in having an additional mass of red muscle located medially, near the backbone (Fig. 2.1B). This internal mass is an integral part of the nested myotome cones, with the concentric rings of red muscle continuous with the surrounding white. Because red, aerobic muscle is used to power sustained swimming, this rare anatomical placement provided a unique opportunity to probe the function of this complicated nested cone structure without exhausting the fish. (In

most species of fish, the white muscle is the only avenue for studying the nested myotomes, so prolonged steady swimming conditions are difficult to achieve.)

Tunas were instrumented with a series of electromyogram (EMG) electrodes to record the temporal sequence of red muscle activation as they swam in a water tunnel. Prior to this study, the only data on muscle activity in tunas demonstrated the sequential recruitment of aerobic to anaerobic fiber types with increasing swimming speed, as observed in other fishes (Rayner and Keenan, 1967; Brill and Dizon, 1979). However, one of the goals of the present study was to characterize the temporal sequence of muscle activation down the body, about which nothing is currently known in tunas. Yellowfin and skipjack exhibit subtle morphological differences externally and internally (Fig. 2.1), so another goal of this study was to determine if these design differences are manifested in different dynamic behaviors of their muscle.

Another unusual feature of tuna anatomy is the presence of robust tendons spanning the caudal peduncle to connect the body's muscle mass with the tail blade. Unlike the majority of fishes, in which muscle extends all the way to the tail blade, in tunas the caudal myotomes have been reduced to a series of concentric myoseptal sheaths forming two major deep and two major superficial tendons on each side of the caudal peduncle (Fierstine and Walters, 1968). This anatomy made it possible to do something never done before in any fish: to fit an "E"-shaped buckle force transducer around the deep tendons of one side to measure forces directly during swimming. The details of how these tendons transmit muscle force to the tail blade



will be covered in Chapter 4, but for now, the time of peak force has been used as a convenient reference to normalize muscle activation state from tailbeat-to-tailbeat.

To summarize the goals of this study on electromyography: by instrumenting yellowfin and skipjack tunas with EMG electrodes and a caudal tendon force transducer, and swimming them over a range of steady, sustained speeds in a water tunnel, we would: 1) determine the sequential activation patterns down the length of the red muscle; 2) relate these timings to the occurrence of peak force recorded from the tail tendons; 3) compare the patterns observed in the medial and superficial red muscle masses; 4) compare EMGs of yellowfin and skipjack; and 5) compare these tunas' EMG patterns with those of other fish species.

## Materials and Methods

### Fish:

All experiments were conducted at the National Marine Fisheries Service-Kewalo Research Facility in Honolulu, Hawaii. Yellowfin and skipjack tunas, ranging in size from 35-55 cm (1-2 kg), were caught by local fishermen using barbless hooks. After transfer to circular holding tanks (7 m diameter by 1 m deep) with continuous aeration and seawater flow (temperature range ~ 22-27° C), they were fed daily with chopped squid. Fish were allowed to acclimate for at least one week before being used in experiments. All care and experimental procedures were conducted in accordance with approved animal protocols.

### Water Tunnel:

The water tunnel has been described previously (original in Graham *et al.* 1990; modifications for tunas in Dewar and Graham, 1994a; Graham *et al.* 1994). Briefly, the 3000-liter capacity tunnel was filled with fresh seawater before each experiment. The water was saturated with oxygen and adjusted to a temperature of approximately 23° C (near ambient). The working section measured 113 cm L x 22.5 cm W x 32.5 cm H (cross-sectional area = 731 cm<sup>2</sup>). Water flow speeds were calculated from a regression of voltage output from the propeller motor with output from a flowmeter, as described in Graham *et al.* 1994. The greatest cross-sectional

area of each of the fish used was less than 10% of the cross-sectional area of the tunnel's working section; therefore, no water velocity corrections were necessary to compensate for the solid blocking effect of the body.

#### Surgical Procedures:

Anaesthesia: A fish was dip-netted from a holding tank and transferred to a plastic bag containing an oxygenated solution of MS-222 [Finquel™: methane tricaine sulfonate (Argent Chemical Laboratories), 1:1000 (w/v) in sea water] buffered with sodium bicarbonate or Tris base (~pH 7.8). This served to anaesthetize the fish quickly to minimize struggling while it was rushed from the tank to the tunnel.

Surgery was performed in a chamois cradle on top of the working section of the tunnel, the fish being ventilated with a more dilute solution of oxygenated, buffered MS-222 (1:17,500) (Korsmeyer *et al.* 1997).

EMG Methodology: After the fish was anaesthetized, 2 to 6 electromyogram (EMG) electrodes were implanted along the length of the medial red muscle (i.e., the red portion of the nested myotome cones, near the backbone; Fig. 2.1B) of the left side, using a 22G needle. In some experiments, a second set of electrodes was implanted in the lateral wedge of superficial red muscle, in the same transverse plane as the medial electrodes. Initially, bipolar hook type electrodes were used, constructed of 34G teflon-coated copper wire (Belden Wire and Cable #8057) with the ends bared a couple of mm. However, monopolar electrodes (referenced to a common wire implanted under the skin just behind the top of the skull) were used

later to take advantage of the much stronger signal-to-noise ratio, after verifying that they gave the same burst timings as the bipolar. After suturing the wires to the skin to prevent slippage, and collecting all wires into one slim bundle to pass out of the tunnel working section, the electrodes were connected to preamplifiers (Grass Instrument Co., model P15), then amplifiers (Axon Instruments, Inc., CyberAmp 320 or A-M Systems Differential AC Amplifier, model 1700), and the signals recorded to computer via an analog-to-digital (A/D) board (Axon Instruments, Inc., model TL-2). Typical frequency bandwidth for EMG recordings was 30-1000 Hz, similar to the range (20-2000 Hz) recommended by Winter (1990).

Tail Tendon Buckle: The tendon buckle force transducers [designed by A.A. Biewener (Biewener *et al.* 1988)] were constructed as a stainless steel "E" shape with a strain gauge mounted on the middle arm and coated with epoxy for waterproofing the leads. All buckles were 15 mm long, but two widths were available (5.0 or 6.5 mm) to accommodate the tendons from different sized fish. To implant the buckle, a small incision was made in the anaesthetized fish just above the fleshy keel on the left side of the peduncle (the same side as the EMG electrodes). The pair of deep lateral tendons on that side were separated from the superficial subcutaneous sheath and threaded through the buckle such that they passed behind the middle arm (see Chapter 4, Fig. 4.1). The skin was sutured and then externally sealed with tissue adhesive (3M Vetbond™) so as to enclose the buckle completely, leaving only the 2 lead wires to exit the incision. These wires were sutured to the skin near the second dorsal fin and connected outside the tunnel to a strain gauge conditioning amplifier

(Measurements Group, Inc., Model 2310 or the CyberAmp 320, with the transducer as one quarter of a Wheatstone bridge) and thence to the computer via the A/D interface. The strain gauges respond linearly to force changes and are not limiting in their frequency response for the types of experiments presented herein (Biewener *et al.* 1988). For the present study, the only analysis done on the force signals was to determine the time of peak force within each tailbeat, to use as the time reference for standardizing tailbeat-to-tailbeat muscle activation phase.

### Swimming Protocols:

After surgery, the MS-222 ventilating solution was replaced with fresh seawater until the fish started to revive, at which point it was lowered into the working section of the tunnel. The flow was adjusted until the fish swam steadily, which generally took 10-30 min. Signals were recorded at a sampling rate of 500 Hz or (in one experiment) 2000 Hz. (Several sampling rates between 500 Hz and 10 kHz were tested, to verify that burst onsets and offsets were not being clipped. Burst durations were equivalent at all these rates.) Recordings were made over the range of speeds at which the individual fish would swim steadily. Using a 45<sup>o</sup>-angled mirror above the working section, video recordings were made of the fish's dorsal aspect and synchronized with the EMG and force recordings on the computer with a flashing red diode (see Chapter 3 for details of kinematics). For the present study, the videos were used to select sequences of steady swimming for EMG analysis. The selection criteria were that the fish had to be away from the walls and holding station within the

flow (i.e., no drifting forward or back, left or right) for at least 10 consecutive tailbeats.

At the end of each experiment, the fish was euthanized by a sharp blow to the head. It was then dissected to verify correct EMG electrode placement in the red muscle, to determine exact myotome locations of the electrodes, and to verify correct buckle placement on the tendons.

Analysis:

Selection criteria: To obtain the most accurate information possible on muscle activation timing, it was necessary for any given fish to meet all of the following criteria before being selected for analysis: steady swimming over a range of water velocities (as evidenced by consistent beat-to-beat frequencies, while swimming in the center of the flow); correctly placed EMG electrodes with clean signals at several body locations; and a successful tendon force signal. Preliminary analyses were done on 6 yellowfin and 8 skipjack to ascertain how well these criteria were met. Ultimately, the data from 4 yellowfin (40-44 cm; 1174-1391 g) and 3 skipjack (38-41 cm; 803-1055 g) were found to satisfy these stringent requirements and are presented in this chapter.

EMG processing: During the experiments, filtering was kept to a minimum to ensure accurate EMG burst timings. However, due to the conductive nature of seawater, and the length of EMG wires required to reach from the fish to the preamplifiers (~ 1.5 m), some EMG records had noise which required post-

experimental processing to clarify burst onsets and offsets (i.e., the times when electrical activity starts and stops). This was done with AcqKnowledge<sup>®</sup> software (BIOPAC Systems, Inc.), which has several finite impulse response (FIR) filters, thresholding, and peak detection capabilities. The typical protocol was as follows: For each speed, steady swimming segments of 10-30 consecutive tailbeats were selected from the files, based on the video. Each EMG train was first subjected to a high-pass filter (30 Hz cut-off) to eliminate possible movement artifacts; rectified; then put through a low-pass filter (10 Hz cut-off) to define a general envelope for each burst. Finally, a voltage threshold level was set (based on the signature of the high-pass filtered, rectified signal) so that onset and offset times of the burst envelopes could be selected automatically by the program. These times were then imported into a spreadsheet program (Microsoft Excel) to calculate average burst durations, relative onset and offset times down the length of the body, and the temporal relation between muscle activation and peak force registered by the tendon transducer. To allow comparisons among fish, muscle activation onset and offset times were expressed as proportion of tailbeat period (T), using the time of peak force registered by the force transducer as the reference point. (It was first verified that the peak force times in the buckle signals consistently matched the same kinematic reference in the video, beat-to-beat, independent of tailbeat frequency. See Chapter 3.) EMG locations were expressed as proportion of body forklength (L), with the nose being 0 and the tail fork 1.

## Results

### Muscle morphology:

Figure 2.1A shows body plans of a yellowfin and a skipjack tuna, depicting the longitudinal extent of the medial red muscle. Figure 2.1B shows several muscle cross sections from each species, which illustrate the continuity within the nested cones between white muscle and medial red muscle. In yellowfin, the red muscle near the backbone extends from approximately 0.26 L to 0.80 L (largest cross-sectional area at 0.56 L); in skipjack, from 0.28 L to 0.77 L (largest cross-sectional area at 0.50 L). These ranges are comparable to those Graham *et al.* (1983) found in similar-sized specimens: 0.30-0.85 L in yellowfin and 0.32-0.80 L in skipjack. In the size range of fish used for this study, the region which was large enough to target consistently with EMG wires was somewhat shorter than the ranges given above: approximately 0.35-0.65 L.

The cross sections in Fig. 2.1B also illustrate that in the lateral wedge of superficial red muscle, there is a transition from a dark red color anteriorly (matching that of the medial red muscle) to a lighter color towards the tail. This color gradation occurs in both species but to differing degrees. In yellowfin, the lateral wedge is solid dark red from 0.29 L to 0.45 L; beyond this, all the way to 0.75 L, the outer third to half of the wedge exhibits a lighter color, though not as light as the surrounding white muscle. In skipjack, however, the dark red color disappears from the lateral wedge much sooner. The wedge is entirely dark red from 0.28 L to 0.37 L, exhibits



decreasing amounts of dark red between 0.40 and 0.58 L, and is completely similar in color to the surrounding myotomal white muscle posterior of 0.60 L. That this lighter color may denote some intermediate, faster fiber type is supported by Bone's (1978a) histological examinations of muscle in *Katsuwonus*, which showed that this light-colored lateral wedge of muscle was quite similar to the surrounding myotomal white muscle in terms of mitochondrial density, lack of lipid, and low degree of vascularization.

#### Swimming velocities and tailbeat frequencies:

The present results represent data collected from similarly-sized yellowfin and skipjack tunas swimming at sustained speeds powered only by the red, aerobic muscle. In early experiments, EMG electrodes were implanted into white, anaerobic muscle, but no activity was observed during steady swimming. Furthermore, none of the fish could be enticed to swim at burst speeds (which would require the recruitment of white muscle) when flow was increased in the water tunnel. White muscle activity was observed only when fish gave brief, erratic bursts.

Although there was variability in the speed range over which individual fish would swim steadily, skipjack typically preferred to swim against faster water velocities than did yellowfin. However, in the range of speeds where skipjack and yellowfin swimming overlapped, the two species used similar tailbeat frequencies (TBFs) for a given water velocity. This is illustrated in Fig. 2.2. On average, the yellowfin we analyzed swam between 46 and 105 cm/s (1.1 - 2.7 L/s), using TBFs of

2.4 to 3.6 Hz. The range encompassed by the skipjack, on the other hand, was 60 to 140 cm/s (1.5 - 3.7 L/s), with TBFs of 2.8 to 4.8 Hz. The data for both these species fall in the same range of TBFs found by Dewar (1993) and Dewar and Graham (1994b) for unanaesthetized, uninstrumented tunas of comparable size swimming in this same tunnel. Therefore, the surgical procedures and implanted wires did not adversely affect the swimming behavior of these fish in this regard. Both species exhibited a linear relationship between TBF and swimming speed, which is typical of steady swimming in many fish.

#### Electromyography and tail tendon forces:

Figure 2.3A illustrates 16 consecutive tailbeats of unprocessed EMG signals from the medial red muscle at 0.40, 0.52, and 0.63 L in one side of a swimming skipjack tuna. Fig. 2.3B shows the same at 0.26, 0.43, 0.52, and 0.67 L during 4 consecutive tailbeats in a swimming yellowfin, except that time is expanded and the EMG traces have been high-pass filtered and rectified (showing the first steps in post-experimental processing). In both cases, the force signal from the transducer on the tail tendons (on the same side of the body) is shown at the bottom. The long sequence of steady tailbeats illustrated in Fig. 2.3A is typical of the prolonged steady swimming bouts routinely recorded from fish in the tunnel, and which were chosen for analysis. The expanded view of 4 tailbeats in Fig. 2.3B facilitates an examination of EMG burst characteristics. The trends are the same for both species: during each tailbeat, the muscle mass on one side is activated sequentially down the length of the

fish, the anterior muscles turning on before the posterior. The EMG offsets are nearly synchronous, and the force peaks in the tendons on that side just as the muscles are turning off. The diagonal lines in the figure point out how burst duration decreases at more posterior locations on the fish.

When muscle activity is plotted in absolute time at different swimming speeds, it becomes apparent that burst duration at any given location also decreases with increased speed. Fig. 2.4A shows EMG onset and offset times at different TBFs for a 44 cm yellowfin and a 38 cm skipjack. To standardize beat-to-beat EMG timings, the time at which peak force occurred within each cycle was used as the zero time reference, since it had been determined from kinematics that this event always occurs at the same point in the tail sweep, regardless of swimming speed (Chapter 3). (In Fig. 2.4A, peak force time in the preceding tailbeat is set to 0 seconds, with the next cycle of EMGs following.) The distance between the onset and offset regression lines (which are extrapolated to the approximate full extent of the medial red muscle) represents burst duration; the wedge shape illustrates that burst duration decreases posteriorly. In addition, it can be seen that as the fish swims faster, the slopes of the onset lines become increasingly steep, denoting the increased velocities required to propagate the muscle activation wave down the body to produce more rapid body undulations. These findings confirm preliminary data reported previously (Knower *et al.* 1993).

However, in order to compare muscle activity from different fish across a range of swimming speeds, it is easier to visualize trends by expressing activation

times in terms of duty cycles-- i.e., normalized to the period of time required to complete one tailbeat ( $T$ ). Thus, in Fig. 2.4B (which shows data from the same yellowfin and skipjack in Fig. 2.4A), normalized onset and offset times have been plotted relative to when peak force occurs on the same side, which has arbitrarily been set at  $0.5 T$ . (In Fig. 2.4B and all remaining figures, the time of peak force occurring at the culmination of the EMG sequence within a tailbeat has been used as the standardizing time reference. When  $T = 0$  and  $1$ , peak force is registered in the tail tendons on the opposite side.) Now muscle activation states at different TBFs still show the wedge shape but are superimposed. This demonstrates that, as in other fishes, the duty cycle at a given muscle location on the body remains essentially constant for any cruising speed powered by the red, aerobic muscle. Another way of looking at this is illustrated by Fig. 2.5, which shows muscle duty cycle as a function of longitudinal location on the body for 4 yellowfin and 3 skipjack, across all swimming speeds. On average, the skipjack duty cycles at each location are longer than those of the yellowfin.

Fig. 2.6 shows combined data from 4 yellowfin (A) and 3 skipjack (B), with force traces superimposed to illustrate the relation between medial red muscle activation and tendon force development and relaxation. (Each force trace is a typical example from one tailbeat, and is included mainly as a visual reference to illustrate how EMG times relate to peak force times.) The EMG onset and offset points from all fish fall close to the linear regression lines, indicating good agreement among fish as well as among speeds. The anterior muscles are active longer than the posterior

ones, but there is a time when all the muscle on one side of the body is active simultaneously, lasting approximately 0.18 T in yellowfin and 0.11 T in skipjack (data extrapolated between 0.25 and 0.80 L). This corresponds to 36% and 22%, respectively, of the duration of one tail sweep (i.e., half a tailbeat cycle). In skipjack, muscle activation starts in the anterior muscle slightly before (0.08 T) peak caudal tendon force is reached on the opposite side, whereas in yellowfin, it starts 0.08 T after contralateral peak force. Skipjack exhibit a brief overlap between the end of posterior muscle activity on one side and the start of anterior activity on the opposite side (about 0.15 T), whereas in yellowfin, there is no overlap in any muscle activity between the two sides. [Throughout this paper, muscle “activity” refers strictly to the electrical stimulation (EMG) of the muscle only.]

Activity of superficial red muscle:

Although these studies concentrated on the medially-located red muscle of the nested myotome cones, preliminary EMG data were also collected from the lateral wedge of superficial red muscle in 1 yellowfin and 1 skipjack. Fig. 2.7 shows a comparison of activation patterns recorded from medial and superficial electrode locations paired in the same transverse planes. In the 43 cm yellowfin (Fig. 2.7A), the first 4 of 5 superficial electrodes were active at cruising swimming speeds (posterior-most active site at 0.52 L), while the last one at 0.67 L only showed activity during brief bursts of non-steady tailbeats. This behavior correlated with the visual appearance of the superficial muscle, which graded from a dark red color at the first 4

locations to a lighter color posteriorly. In the 38 cm skipjack, however (Fig. 2.7B), only the first two superficial electrodes (at 0.33 and 0.41 L) registered muscle activity at cruising speeds, reflecting the more anteriorly-located transition from dark red to lighter-colored muscle in this species compared with the yellowfin. The absence of activity in the posterior locations at steady cruising speeds lends support to the visual and histological data (Bone, 1978a) suggesting that this muscle is comprised of an intermediate fiber type which is only recruited at faster speeds.

Comparing the timing between the medial and superficial red muscle masses, it was observed in the skipjack that the two masses within a transverse plane were activated simultaneously. In the yellowfin, on the other hand, a curious pattern was seen in that the sequential rostro-caudal activation of the superficial red muscle did not appear to be linear--e.g., the superficial muscle at 0.43 L turned on quite a bit earlier (about 0.08 T, relative to its medial partner) than that at either 0.26 L or 0.52 L. The burst offsets of the superficial muscle in both species, however, coincided approximately with the timing of their medially-located counterparts.

## Discussion

The overall goal of this research is to understand the physiological design features of the tuna “power plant” which define the thunniform mode of swimming. The present study has for the first time elucidated the temporal patterns of red muscle activation in two species of tuna, providing the foundation for this quest. Invasive measurements on free-swimming tunas have been limited in the past, as the high metabolic rates and delicate skin of these endothermic fish make handling and successful anaesthesia difficult. With new surgical procedures developed during this project (and Korsmeyer *et al.* 1997), it became possible to successfully instrument fish with several EMG electrodes and a tendon force transducer simultaneously. Using a large water tunnel enabled the recording of measurements from instrumented fish swimming at controlled, steady speeds for hours at a time. This information has made possible the first detailed examination of how the tuna muscle “engine” functions dynamically.

### Muscle activation in tunas: comparison of yellowfin and skipjack:

The main discussion will consider only the results from the medial red muscle, as this was the primary focus. The general trends describing sequential muscle activation in yellowfin and skipjack are similar: both species exhibit decreasing duty cycles towards the tail, duty cycle is independent of swimming speed, and peak force in the caudal tendons coincides with near-simultaneous muscle deactivation on that

side. A persistent question in studies of axial fish locomotion in any species is whether each entire myotome is activated as a unit, or if muscle is activated more according to longitudinal position of the vertebral segments. It was not possible to resolve this issue in the present tuna study. The extremely elongated myotomes in these species translate to a maximum of 13 (yellowfin) or 17 (skipjack) “rings” of nested cones when viewed in cross section (personal observations). Because of the small sizes of fish used in this study, each myotome was only 1-3 mm thick, which made it impossible to distinguish differences in EMG signatures between adjacent myotomes when an array of electrodes was inserted into a given cross section (unpublished results). However, the EMG data indirectly support the idea that the medial red muscle mass is activated according to longitudinal position (vertebral segment), rather than myotome-to-myotome. In all experiments, a sequential train of EMG onset times was consistently recorded down the body, irrespective of which myotome rings the electrodes were in (determined by *post mortem* dissections). If each myotome were activated as a unit, one would expect to see non-sequential patterns of rostral-caudal activation onsets in at least some of the experiments (e.g., more posterior locations being activated prior to anterior ones), but such patterns were not observed. Segmental activation in tunas would be in contrast to the results of Jayne and Lauder (1995b), who found that in largemouth bass, the central portion of each myotome was activated simultaneously as a unit. However, in contrast to the present study, their data were obtained from white muscle activated during bouts of unsteady, burst-and-glide swimming. In addition, with the large number of



motoneurons supplying any single myotome (Bone, 1978b; Johnston, 1983), many different activation patterns are conceivable in different species of fish.

Although yellowfin and skipjack are clearly very similar in their EMG trends, there are subtle differences between the two species. As can be seen in Fig. 2.6, the sequential train of EMG onsets travels down the body faster in the yellowfin than in the skipjack, as evidenced by the steeper slope of the yellowfin onset regression line. The yellowfin offsets are nearly simultaneous, while the skipjack offsets exhibit a slight rostral-caudal delay. Additionally, the trends indicated in Fig. 2.5 (as well as Fig. 2.6) are that duty cycles at any given muscle location are longer in skipjack than in yellowfin. The combination of these factors results in complete contralateral segregation of muscle activity in yellowfin, but slight activation overlap in skipjack (the anterior muscle at 0.25 L turns on 0.15 T before activity at 0.80 L on the opposite side has finished). Finally, all the muscle on one side is simultaneously active for a longer proportion of the tail sweep in yellowfin [36% (or 0.18 T) vs. 22% (0.11 T) in skipjack].

What are the consequences of these differing EMG patterns on swimming mode? The yellowfin mechanism involves a design that approaches near-synchronous muscle activation (and, hence, force production) on each side, and because there is no overlap in contralateral activity, this would suggest that yellowfin use a stiffer swimming mode than skipjack. (See section below on comparisons with other fishes). EMG patterns are dictated partially by body morphology. Skipjack are more elongate than yellowfin, have less body depth, have a smaller tail span and area (Magnuson,

1978), and have much smaller pectoral fins. The last point is particularly pronounced in the size range of fish used for this study: small yellowfin have much larger pectorals relative to their body size than do skipjack, and therefore derive more hydrodynamic lift (Beamish, 1978). Consequently, skipjack require a faster minimum swimming velocity to maintain hydrostatic equilibrium (Fig. 2.2). Additionally, the higher sustained velocities observed in skipjack may explain why their lateral wedge of superficial muscle is more largely comprised of an intermediate (faster) fiber type. The fact that these two tuna species have subtle differences in their body morphologies may explain some of the equally subtle differences observed in the EMG patterns used to activate the muscle. In summary, although these two tuna species are more similar than different, it is interesting that these morphological design differences can be correlated with dynamic design differences in muscle activation patterns and, ultimately, swimming mode.

#### Muscle activation in tunas vs. other species of fish:

Having ascertained the temporal course of red muscle activation in yellowfin and skipjack, it is possible to make predictions about the thunniform swimming mode, based on comparisons with EMG data from other species of fish. In 1926, Breder published a now-familiar classification scheme for describing different swimming modes, based on the kinematics of movement. For fishes which swim by axial locomotion, this scheme describes a progression from fish without tail blades, which use whole-body undulations to press against the water (anguilliform swimmers), to

those employing more oscillatory movements, where most thrust is developed at the posterior end of the body (carangiform swimmers) (Lindsey, 1978; Webb, 1993). At the opposite end of the spectrum from eels (anguilliform swimmers), the thunniform swimmers (e.g., tunas; sharks in the family *Lamnidae*) exploit a more lift-based propulsion where body motion is almost entirely restricted to oscillation of a lunate tail (Lighthill, 1969). The kinematic details of these swimming modes are dependent on parameters such as muscle activation pattern, body morphology, and physical interactions with the water. It turns out that many of these underlying components, including EMG patterns, also show a recognizable progression of trends, parallel to the kinematic spectrum. Several authors have reviewed EMG patterns found in anguilliform, subcarangiform, and carangiform fishes (e.g., Videler, 1993; Wardle and Videler, 1994; van Leeuwen, 1995; Wardle *et al.* 1995; Gillis, 1996; Jayne and Lauder, 1996; Shadwick *et al.* 1997). Data from a few representative species are presented with the tuna data in Fig. 2.8.

To standardize EMG times within a tailbeat cycle, the time of peak force production at the tail was again used as the reference. For the tunas, this reference was provided directly by the buckle force transducer on the caudal tendons. To transform EMG data from other species in the literature, a kinematic reference for peak force was used, based on the assumption that this event occurs as the tail tip sweeps across the swimming track (as predicted by Lighthill, 1971; Wardle, 1985). Activation patterns during cruising swimming are presented from the aerobic muscle on one side only. The examples shown are representatives of: anguilliform (eel:

Gillis, pers. comm.), subcarangiform (largemouth bass: Jayne and Lauder, 1995a&c), carangiform (mackerel/saithe: Wardle and Videler, 1993), and thunniform (skipjack and yellowfin tunas) swimmers.

Several patterns emerge across this spectrum. With changes in swimming mode from whole-body undulations to tail oscillations come decreasing duty cycles at more posterior body locations and decreasing levels of contralateral muscle activity. The tuna EMG patterns culminate this progression by further separating the activity between left and right sides. Progressing from anguilliform to thunniform, burst duration grades from being nearly constant down the length of the body (eel) to being long rostrally and short caudally (mackerel, tunas). Also, muscle activation begins earlier within the tailbeat in swimming modes that involve more of a propulsive wave on the body (eel, bass), and there is a greater degree of simultaneous activity on both sides (at different longitudinal sites). With a progression to stiffer modes of swimming, in which most body motion is concentrated near the tail (mackerel, tunas), there is less overlap in activity between sides: EMG onsets begin later in the tailbeat cycle, while burst offsets at all locations become more nearly synchronous and coincide more closely with time of peak force. This trend in dynamic swimming design towards simultaneity of muscle activation (and force production) culminates in the yellowfin swimming design, in which there is a long portion of the tail sweep during which all muscle is active, resulting from complete segregation of activity side-to-side (all muscle activation for each side is accomplished within half a tailbeat period). This mode of muscle activation is at the opposite extreme from the

anguilliform mode. The fact that yellowfin EMG onsets start later in the tailbeat cycle (relative to other fishes) could be a consequence of faster intrinsic contraction kinetics. On the other hand, it may well be explained by the fact that this medial cone muscle has different linkages to the backbone than the superficial muscle (see below).

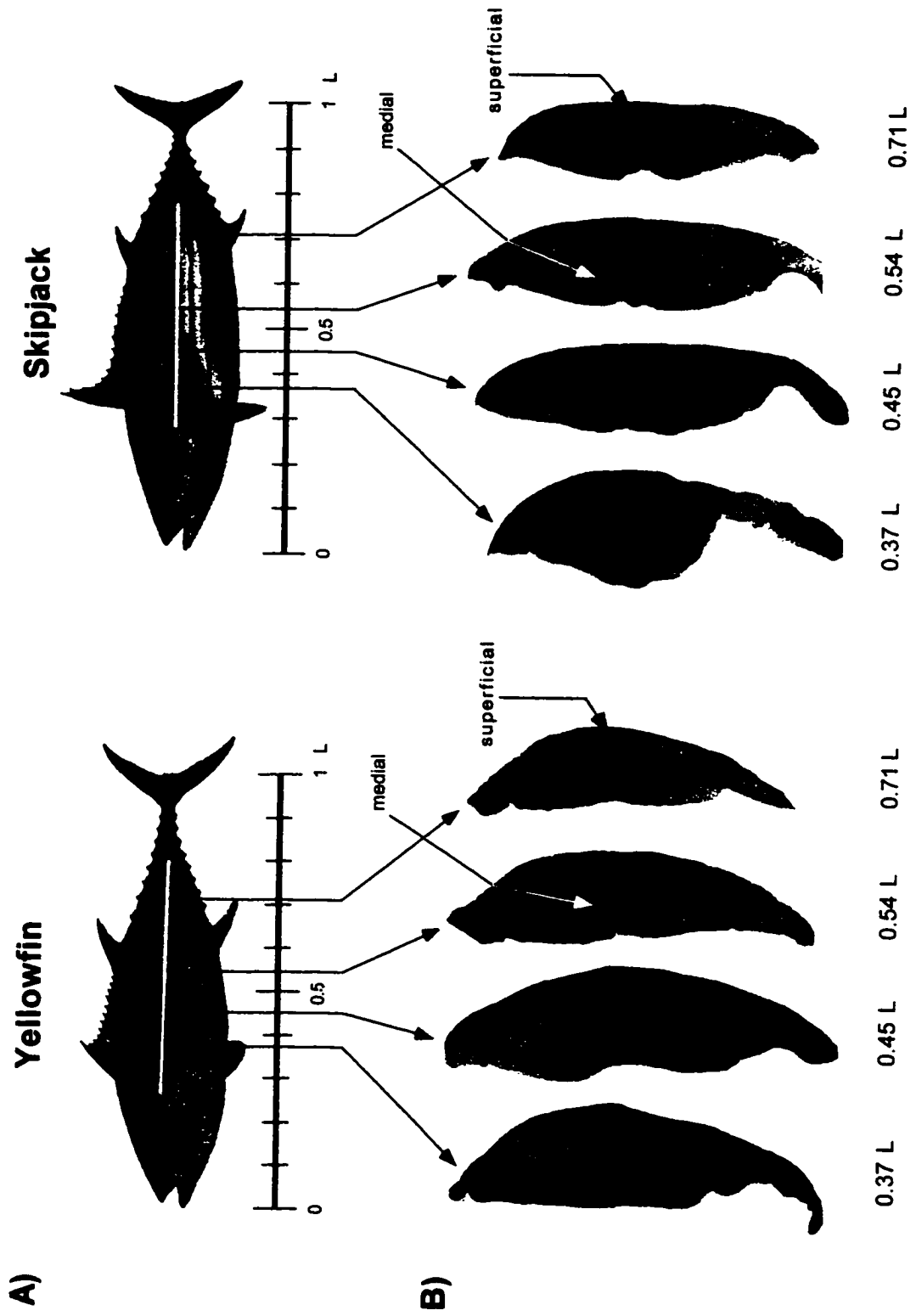
#### Comparison of muscle activation in medial and superficial red muscle:

Although the EMG experiments presented herein have concentrated on the medial red muscle, preliminary data on the superficial muscle have nevertheless afforded some tantalizing contrasts. Fig. 2.1B illustrates that anteriorly, the dark red coloration is continuous between the medial and superficial red muscle masses. However, the anatomical division between the nested cones and the lateral wedge is visually very distinct. In skipjack, it is difficult to make inferences about superficial vs. medial red muscle timing down the entire body length, because superficial muscle activity at cruising speeds is restricted to such a limited region (corresponding to the range of dark red coloration). In yellowfin, on the other hand, Fig. 2.7 shows that this anatomical distinction is reflected in differing activation patterns: the superficial muscle is activated earlier than its medial counterpart within any transverse plane, while the offsets occur simultaneously. However, the velocity of this superficial activation wave does not appear to be constant, as the mid-body muscle locations have a greater phase lag between superficial and medial muscle than do the anterior and posterior locations. There is no visible color difference between the medial and

superficial red muscle where these recordings were made, although fiber type differences cannot strictly be ruled out without biochemical assays.

What might explain this phase lag between superficial and medial red muscle masses at the same longitudinal site? The most likely answer is differences in fiber orientation and anatomical linkages. The medial fibers run in helical trajectories across myotome cones (Alexander, 1969), whereas the superficial fibers have a more parallel orientation. Also, the fibers of the superficial and medial muscle within a given axial plane connect to the backbone at different locations, owing to the highly elongated and folded structure of the myotome cones. Superficial muscle contractions should produce bending locally (as has been demonstrated in other fishes: Rome and Sosnicki, 1991; Coughlin *et al.* 1996; Shadwick *et al.* 1997), while contraction of myotomal cone fibers may produce bending at more posterior locations. Thus, temporal differences in activation between superficial and medial muscle within a transverse plane would be necessary to achieve coordinated body bending (Rome and Sosnicki, 1991). Preliminary studies in our laboratory using sonomicrometry in swimming yellowfin and skipjack suggest this may be the case, in that the two muscle masses appear to shorten out of phase. More data are needed before this question can be answered fully, but the tuna body plan is ideal for exploring the functional aspects of these different muscle masses simultaneously during sustained swimming.

- Fig. 2.1A: Side view of the yellowfin tuna *Thunnus albacares* and the skipjack tuna *Katsuwonus pelamis*, showing the longitudinal extent of the medial red muscle (indicated by the white bar on the body). The scale bar underneath shows one forklength (L). (Adapted from paintings by George Mattson in Joseph *et al.* 1988.)
- 2.1B: Hemi-cross sections of yellowfin and skipjack muscle at several axial locations, showing the distribution of medial and superficial red muscle. Also shown is the color gradation in the superficial muscle of both species from dark red (matching the medial color) to a lighter color at more posterior locations. Views are of the anterior faces of slices from the left side of the body. (Note: the skipjack cross section at 0.71 L is somewhat splayed at the horizontal septum: the medial red muscle is actually continuous on either side of the horizontal septum *in vivo*.)





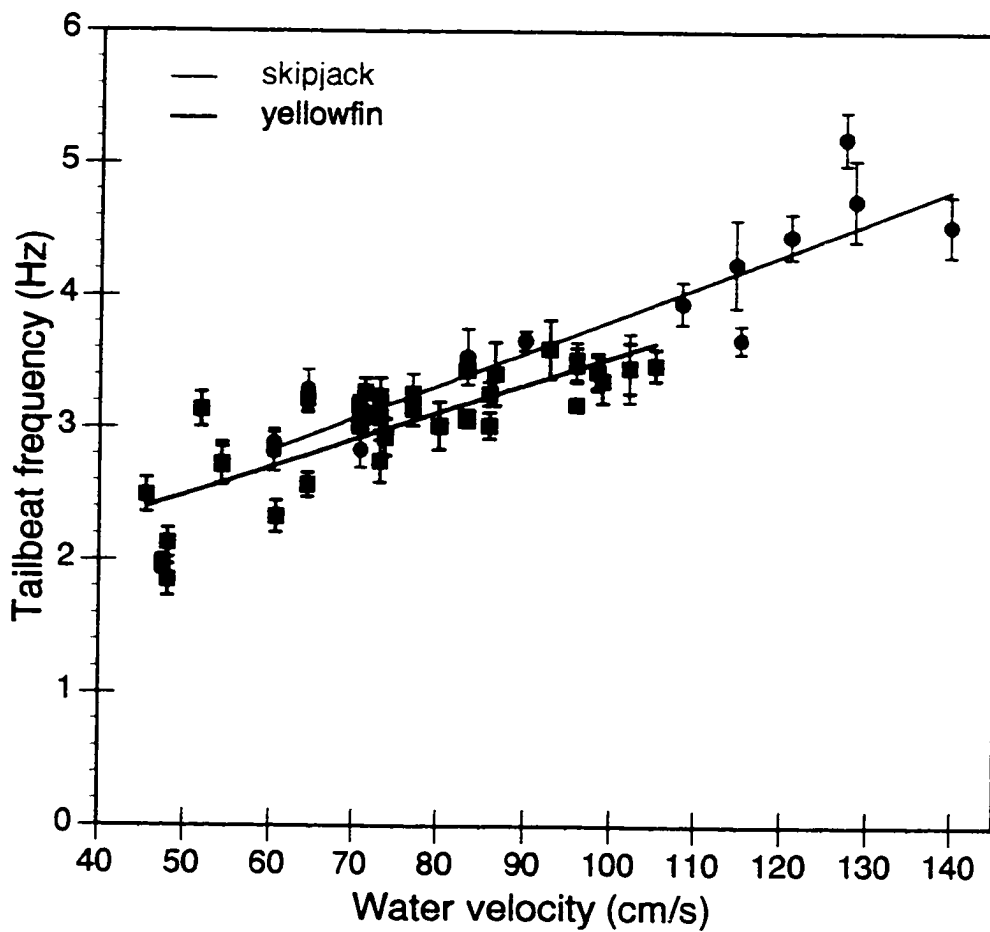
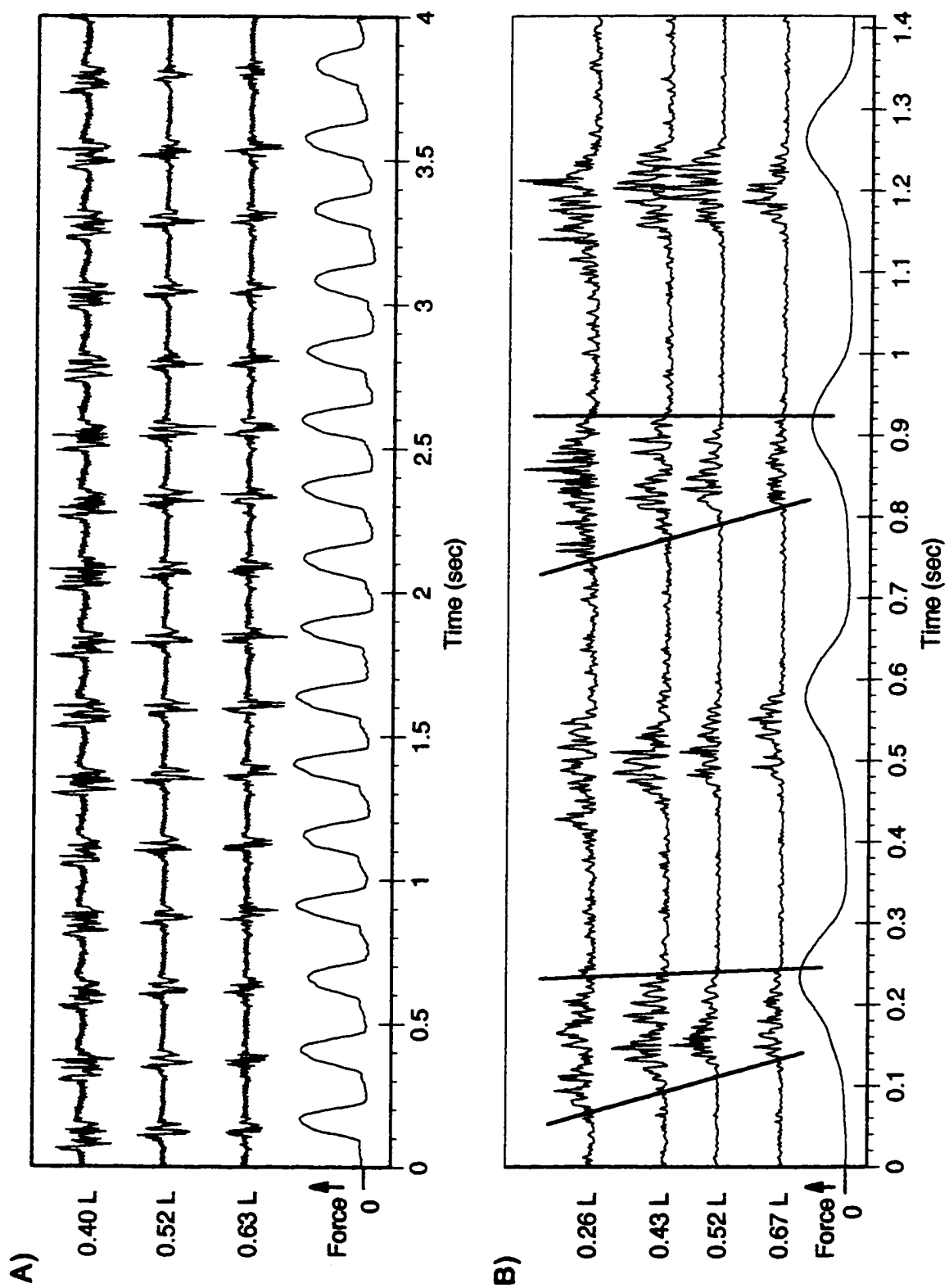


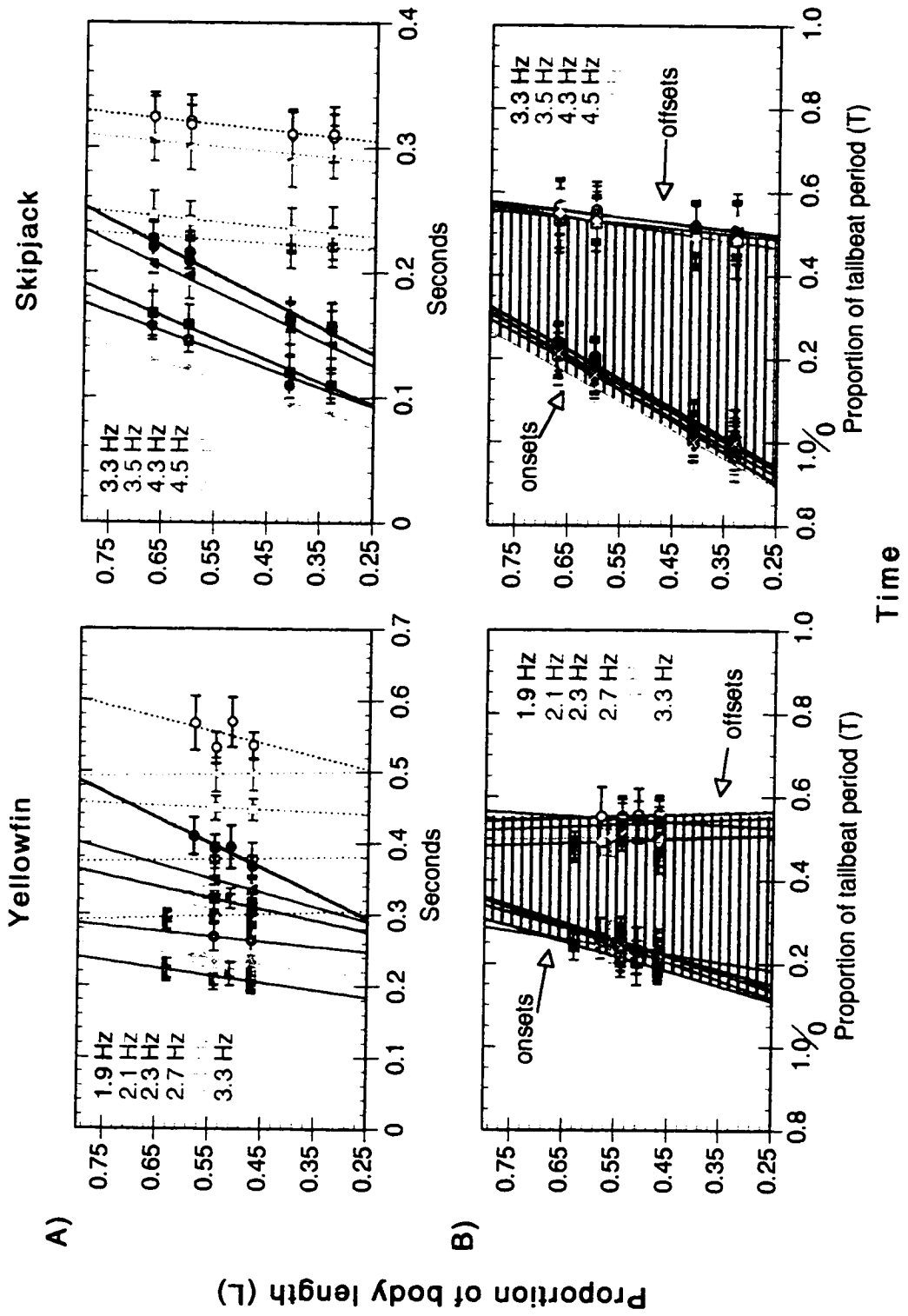
Fig. 2.2: Tailbeat frequency as a function of water velocity in four yellowfin (blue) and three skipjack (red). Points represent means and standard deviations of tailbeats within a swimming bout (each bout consists of 10 to 30 tailbeats). Lines are fit by least squares regressions.

- Fig. 2.3A:** An example of EMG traces (with no post-experimental processing) and tendon buckle force trace from 16 consecutive tailbeats of a swimming skipjack tuna. Locations of EMG electrodes are indicated along the Y-axis. The even spacing in time between EMG bursts or force peaks in each trace indicates steady swimming.
- 2.3B:** Expanded view of 4 tailbeats from a swimming yellowfin tuna. EMG traces have been high-pass filtered and rectified (the first steps of post-experimental processing). Slanted, solid lines are visual aids to indicate the sequential delay in EMG burst onsets moving posteriorly down the fish's body, while the vertical lines show that all the muscles are turning off just as the force peaks at the caudal peduncle.



**Fig. 2.4A:** EMG activation onsets (solid lines) and offsets (dotted lines) in the medial red muscle of one yellowfin and one skipjack at various TBFs, plotted in absolute time (seconds) after peak force from the previous tailbeat. Note that the regression lines at faster speeds have steeper slopes, showing that the EMG trains must travel faster (as expected) to elicit these faster TBFs. Distance between onset and offset lines represents burst duration. Points are means and standard deviations of tailbeats within a swimming bout. Data have been extrapolated across the full length of the medial red muscle (0.25- 0.80 L).

**2.4B:** EMG onsets and offsets from Fig. 2.4A, normalized to tailbeat period (T). Graphs show approximately one tailbeat cycle, with time of peak force in the tail tendons (on the same side as the EMG electrodes) arbitrarily set to 0.5 T. Now all the regression lines for the muscle activation sequences are superimposed, demonstrating that muscle activation and deactivation maintain the same phase within the tailbeat cycle, independent of swimming speed. (For both A and B: all least squares regressions for onset and offset lines were done with time as the dependent variable; axes were then switched in order to illustrate slopes as length/time.)



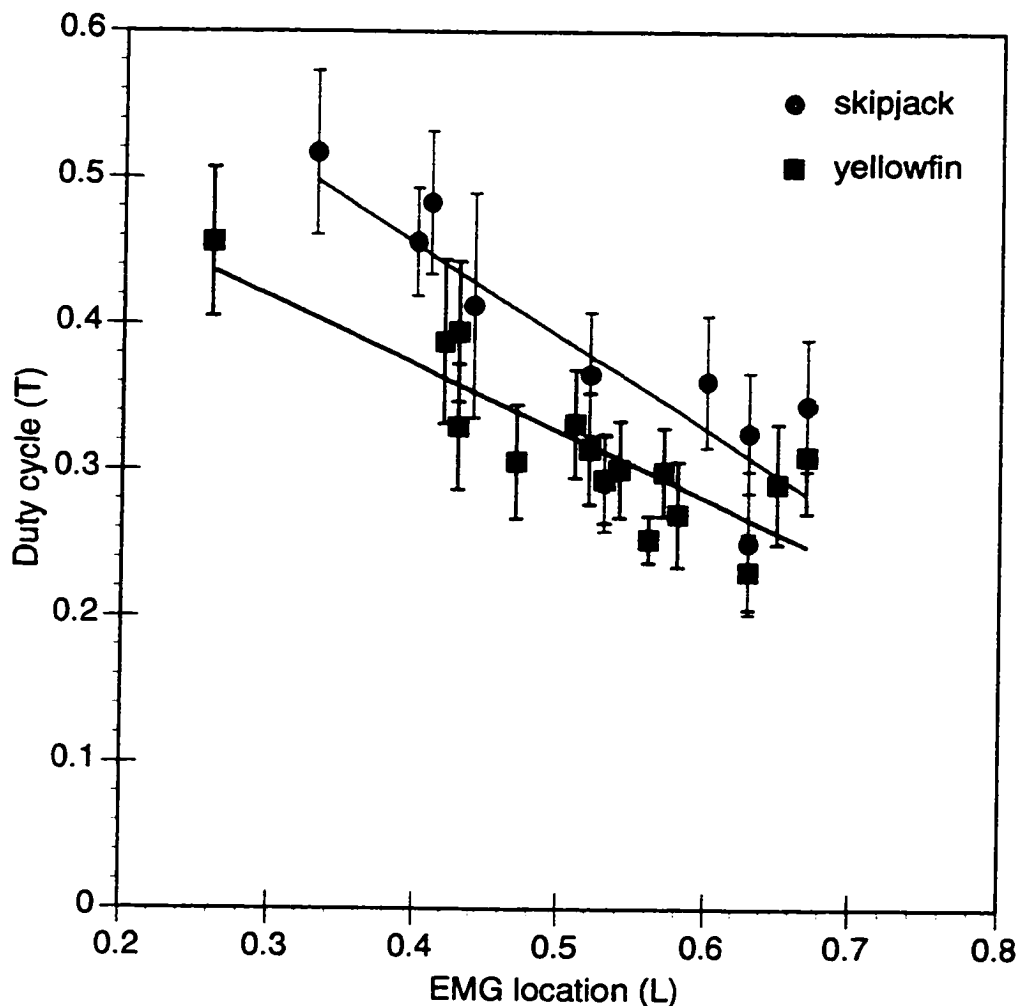
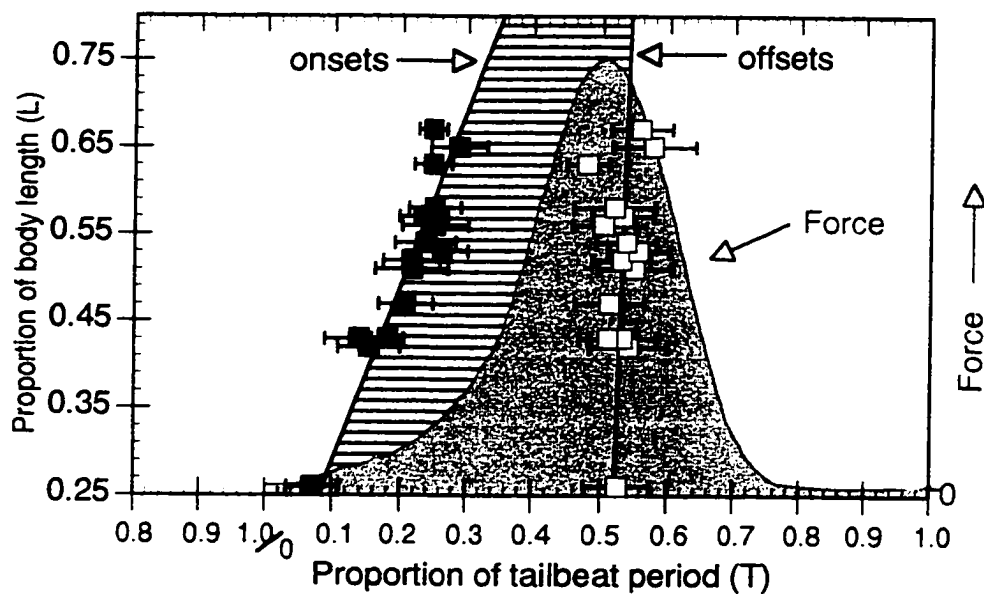


Fig. 2.5: EMG duty cycle in medial red muscle as a function of muscle location: four yellowfin (blue) and three skipjack (red), across all swimming speeds, normalized to  $T$ . This shows that duty cycles decrease in more caudal locations, but at a given location, the period of muscle activation remains a constant proportion of the tailbeat cycle, regardless of TBF. Skipjack exhibit somewhat longer duty cycles than yellowfin (see also Fig. 2.6). (Points and error bars are means and standard deviations of all tailbeats from all speeds at each location.)

**Fig. 2.6:** Summary of muscle activation data (medial red muscle) for four yellowfin (A) and three skipjack (B) across all swimming speeds. Superimposed on each plot is a trace of force development and relaxation measured by the caudal tendon transducer during one tailbeat, to illustrate the association between muscle activation and force. Peak force in the tail tendons (on the same side of the fish as the recorded EMGs) has been set at 0.5 T; 0 T corresponds to peak force on the opposite side of the tail sweep. In both species, peak force is reached just before all the muscle mass on that side is deactivated. The yellowfin have complete segregation of muscle activity between sides, while the skipjack have very slight overlap (anterior muscles on one side are turning on before contralateral posterior ones have shut off). Individual points and error bars along the EMG onset and offset regression lines represent means and standard deviations of all tailbeats from all speeds at that location (10-30 tailbeats per swimming bout per speed; 3-8 speeds per fish).

## A) Yellowfin:



## B) Skipjack:

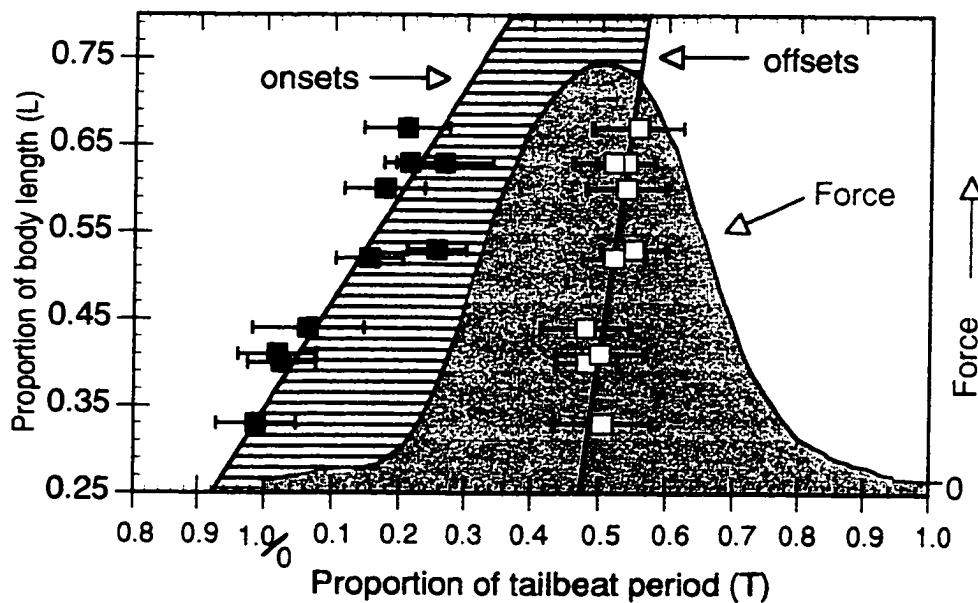
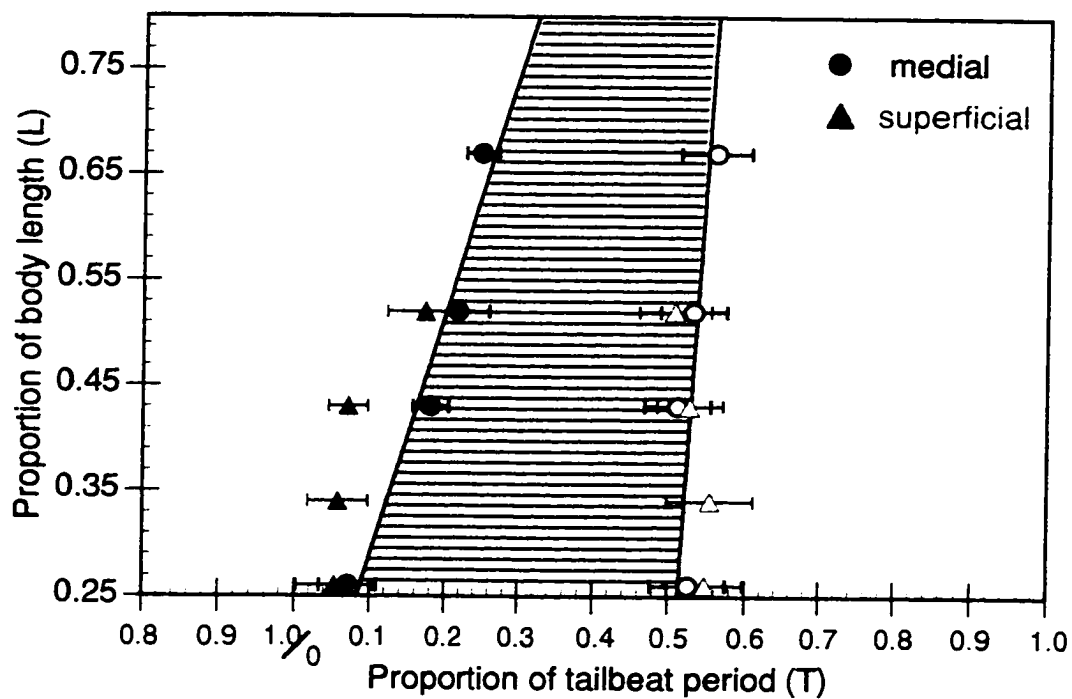




**Fig. 2.7:** Comparison of medial (black circles) and superficial (red triangles) red muscle activity in one yellowfin (A) and one skipjack (B). Timing normalized to  $T$ , with peak force again set to  $0.5 T$ . The skipjack plot only shows data for the first two anterior sites, as no activity was observed in the more posterior sites except during brief bursts of unsteady swimming. In the yellowfin, EMG activity was recorded superficially as far back as  $0.52 L$  during cruising; only the electrode at  $0.67 L$  was silent at these speeds. The yellowfin plot shows that at some axial locations, the superficial red is activated earlier than the medial red in the same transverse plane; offsets are nearly simultaneous. This results in a longer duty cycle for the superficial muscle (relative to the medial) at these axial locations.

## A) Yellowfin:



## B) Skipjack:

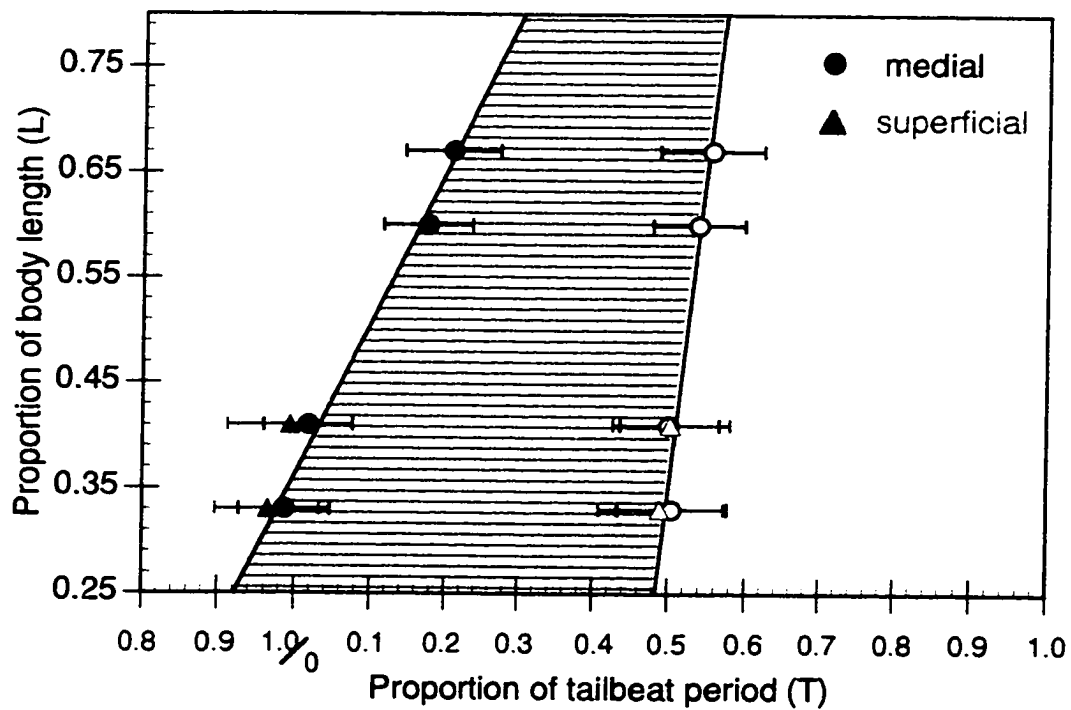
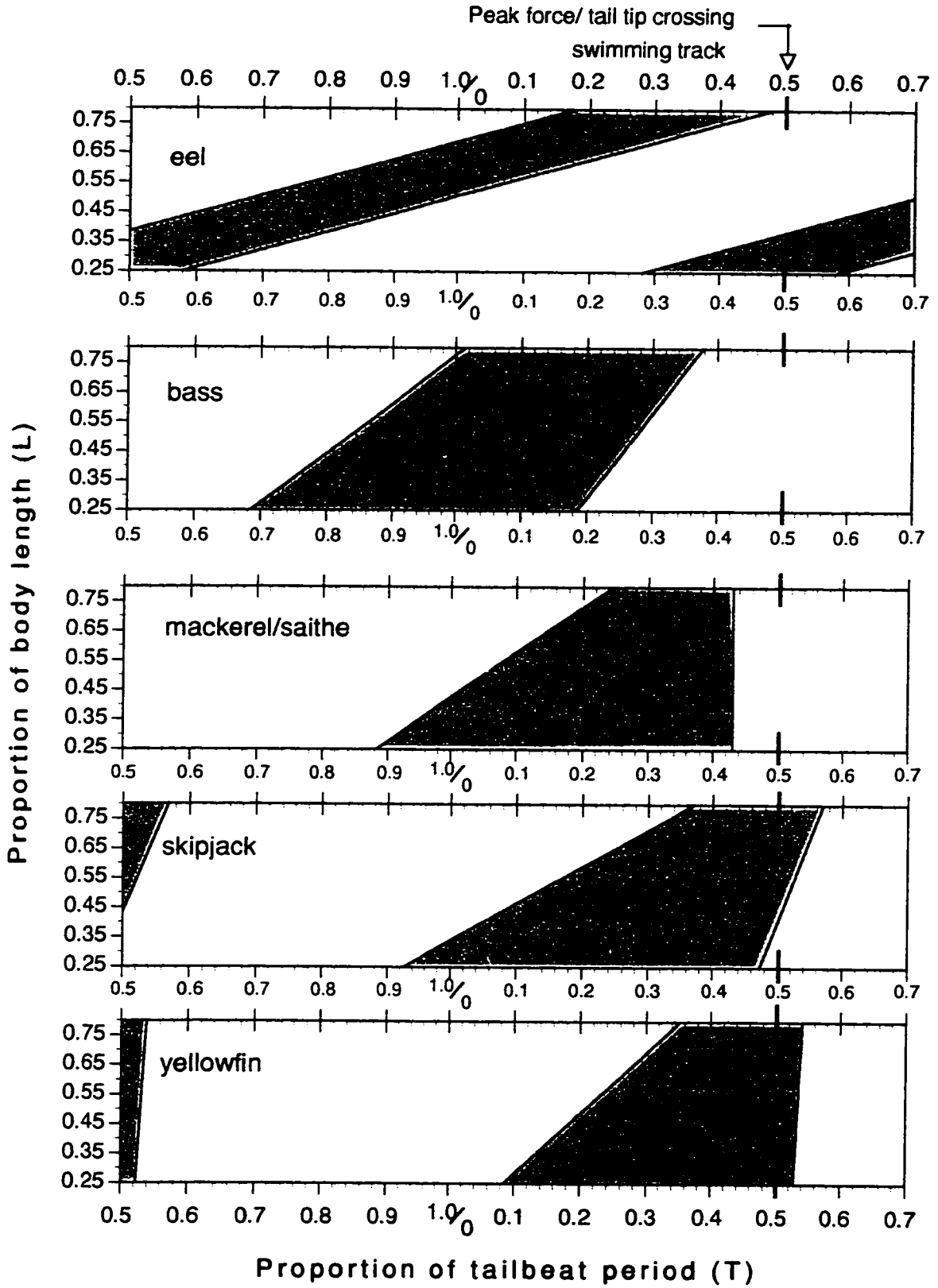


**Fig. 2.8:** Comparison of tuna medial red muscle activation and red muscle activation (superficial) from other species. Green wedges indicate activity during one tail sweep (= half a cycle), with peak force (or when the tail tip crosses the swimming track) for that sweep set at  $0.5 T$ . The ordinate range corresponds to the longitudinal extent of medial red muscle in the tunas. Tuna data are the regressions from Fig. 2.6; data for the other species were derived from the following: eel: Gillis, pers. comm.; largemouth bass: Jayne and Lauder, 1995a&b; mackerel/saithe: Wardle and Videler, 1993. (See text for details.)



## References

- Alexander, R. M. (1969). The orientation of muscle fibres in the myomeres of fishes. *J. Mar. Biol. Ass.* **49**, 263-290.
- Beamish, F. W. H. (1978). Swimming capacity. In *Fish Physiology*, Vol. VII (ed. W. S. Hoar and D. J. Randall), pp. 101-187. New York, etc: Academic Press.
- Biewener, A. A., Blickhan, R., Perry, A. K., Heglund, N. C. and Taylor, C. R. (1988). Muscle forces during locomotion in kangaroo rats: force platform and tendon buckle measurements compared. *J. exp. Biol.* **137**, 191-205.
- Bone, Q. (1978a). Myotomal muscle fiber types in *Scomber* and *Katsuwonus*. In *The Physiological Ecology of Tunas* (ed. G. D. Sharp and A. E. Dizon), pp. 183-205. New York, etc.: Academic Press.
- Bone, Q. (1978b). Locomotor muscle. In *Fish Physiology*, Vol. VII (ed. W. S. Hoar and D. J. Randall), pp. 361-424. New York, etc: Academic Press.
- Breder, C. M. (1926). The locomotion of fishes. *Zoologica* **4**, 159-297.
- Brill, R. W. and Dizon, A. E. (1979). Red and white muscle fibre activity in swimming skipjack tuna, *Katsuwonus pelamis* (L.). *J. Fish Biol.* **15**, 679-685.
- Coughlin, D. J., Valdes, L. and Rome, L. C. (1996). Muscle length changes during swimming in scup: sonomicrometry verifies the anatomical high-speed cine technique. *J. exp. Biol.* **199**, 459-463.
- Dewar, H. (1993). Studies of tropical tuna swimming performance: thermoregulation, swimming mechanics and energetics. Ph. D. dissertation, Scripps Institution of Oceanography, University of California, San Diego.
- Dewar, H. and Graham, J. B. (1994a). Studies of tropical tuna swimming performance in a large water tunnel: I. Energetics. *J. exp. Biol.* **192**, 13-31.
- Dewar, H. and Graham, J. B. (1994b). Studies of tropical tuna swimming performance in a large water tunnel: III. Kinematics. *J. exp. Biol.* **192**, 45-59.
- Fierstine, H. L. and Walters, V. (1968). Studies in locomotion and anatomy of scombroid fishes. *Memoirs of the Southern California Academy of Sciences* **6**, 1-31.

- Gillis, Gary B. Dept. of Ecology and Evolutionary Biology, University of California, Irvine, California 92697.
- Gillis, G. B. (1996). Undulatory locomotion in elongate aquatic vertebrates: anguilliform swimming since Sir James Gray. *Amer. Zool.* **36**, 656-665.
- Graham, J. B., Dewar, H., Lai, N. C., Korsmeyer, K. E., Fields, P. A., Knower, T., Shadwick, R. E., Shabetai, R. and Brill, R. W. (1994). Swimming physiology of pelagic fishes. In *Mechanics and Physiology of Animal Swimming* (ed. L. Maddock, Q. Bone and J. M. V. Rayner), pp. 63-74. Cambridge: Cambridge University Press.
- Graham, J. B., Dewar, H., Lai, N. C., Lowell, W. R. and Arce, S. M. (1990). Aspects of shark swimming performance determined using a large water tunnel. *J. exp. Biol.* **151**, 175-192.
- Graham, J. B., Koehn, F. J. and Dickson, K. A. (1983). Distribution and relative proportions of red muscle in scombrid fishes: consequences of body size and relationships to locomotion and endothermy. *Canadian Journal of Zoology* **61**, 2087-2096.
- Jayne, B. C. and Lauder, G. V. (1995a). Speed effects on midline kinematics during steady undulatory swimming of largemouth bass, *Micropterus salmoides*. *J. exp. Biol.* **198**, 585-602.
- Jayne, B. C. and Lauder, G. V. (1995b). Are muscle fibers within fish myotomes activated synchronously? Patterns of recruitment within deep myomeric musculature during swimming in largemouth bass. *J. exp. Biol.* **198**, 805-815.
- Jayne, B. C. and Lauder, G. V. (1995c). Red muscle motor patterns during steady swimming in largemouth bass: effects of speed and correlations with axial kinematics. *J. exp. Biol.* **198**, 1575-1587.
- Jayne, B. C. and Lauder, G. V. (1996). New data on axial locomotion in fishes: how speed affects diversity of kinematics and motor patterns. *Amer. Zool.* **36**, 642-655.
- Johnston, I. A. (1983). Dynamic properties of fish muscle. In *Fish Biomechanics*. (ed. P. W. Webb and D. Weihs), pp. 36-67. New York: Praeger Publishers.
- Joseph, J., Klawe, W. and Murphy, P. (1988). *Tuna and Billfish-Fish Without a Country*. La Jolla: Inter-American Tropical Tuna Commission.

- Knower, T., Shadwick, R. E., Wardle, C. S., Korsmeyer, K. E., and Graham, J. B. (1993). The timing of red muscle activation in swimming tuna. *Amer. Zool.* **33**: 30A.
- Korsmeyer, K. E., Lai, N. C., Shadwick, R. E. and Graham, J. B. (1997). Heart rate and stroke volume contributions to cardiac output in swimming yellowfin tuna: response to exercise and temperature. *J. exp. Biol.* **200**, 1975-1986.
- Lighthill, M. J. (1969). Hydromechanics of aquatic animal propulsion. In *Annual Review of Fluid Mechanics*, Vol. 1 (ed. W. R. Sears and M. Van Dyke), pp. 413-446. Palo Alto: Annual Reviews, Inc.
- Lighthill, M. J. (1971). Large amplitude elongated-body theory of fish locomotion. *Proc. R. Soc. Lond. B* **179**, 125-138.
- Lindsey, C. C. (1978). Form, function, and locomotory habits in fish. In *Fish Physiology*, Vol. VII (ed. W. S. Hoar and D. J. Randall), pp. 1-100. New York, etc: Academic Press.
- Magnuson, J. J. (1978). Locomotion by scombrid fishes: hydromechanics, morphology, and behavior. In *Fish Physiology*, Vol. VII (ed. W. S. Hoar and D. J. Randall), pp. 239-313. New York, etc: Academic Press.
- Rayner, M. D. and Keenan, M. J. (1967). Role of red and white muscles in the swimming of the skipjack tuna. *Nature* **214**, 392-393.
- Rome, L. C. and Sosnicki, A. A. (1991). Myofilament overlap in swimming carp. II. Sarcomere length changes during swimming. *Am. J. Physiol.* **260**, C289-C296.
- Shadwick, R. E., Steffensen, J. F., Katz, S. L. and Knower, T. (1997). Muscle dynamics in fish during steady swimming. *Amer. Zool.* (in press).
- van Leeuwen, J. L. (1995). The action of muscles in swimming fish. *Exp. Physiol.* **80**, 177-191.
- Videler, J. J. (1993). *Fish Swimming*. London: Chapman & Hall.
- Wainwright, S. A. (1983). To bend a fish. In *Fish Biomechanics* (ed. P. W. Webb and D. Weihs), pp. 68-91. New York: Praeger Publishers.
- Wardle, C. S. (1985). Swimming activity in marine fish. In *Physiological Adaptations of Marine Animals* (ed. M. Laverack), pp. 521-540. Cambridge: Company of Biologists, Ltd.

- Wardle, C. S. and Videler, J. J. (1993). The timing of the EMG in the lateral myotomes of mackerel and saithe at different swimming speeds. *J. Fish Biol.* **42**, 347-359.
- Wardle, C. S. and Videler, J. J. (1994). The timing of lateral muscle strain and EMG activity in different species of steadily swimming fish. In *Mechanics and Physiology of Animal Swimming* (ed. L. Maddock, Q. Bone and J. M. V. Rayner), pp. 111-118. Cambridge: Cambridge University Press.
- Wardle, C. S., Videler, J. J. and Altringham, J. D. (1995). Tuning into fish swimming waves: body form, swimming mode and muscle function. *J. exp. Biol.* **198**, 1629-1636.
- Webb, P. W. (1975). *Hydrodynamics and Energetics of Fish Propulsion*. Ottawa: Department of the Environment, Fisheries and Marine Service.
- Webb, P. W. (1993). Swimming. In *The Physiology of Fishes* (ed. D. H. Evans), pp. 47-73. Boca Raton: CRC Press.
- Westneat, M. W., Hoese, W., Pell, C. A. and Wainwright, S. A. (1993). The horizontal septum: mechanisms of force transfer in locomotion of scombrid fishes (Scombridae, Perciformes). *Journal of Morphology* **217**, 183-204.
- Winter, D. A. (1990). *Biomechanics and Motor Control of Human Movement*. New York: John Wiley & Sons, Inc.



## **Chapter 3: Kinematics**

### **Abstract**

Kinematic analyses were conducted on steady swimming activity in yellowfin and skipjack. The progressing waves of midline curvature and lateral displacement were characterized through digital analysis of video records and coupled with EMG data to determine phase relationships. The phase between muscle activation and muscle strain (relative length change) has been shown in many fishes to be critically important in determining dynamic muscle function. In order to assess dynamic muscle function in tunas, it was necessary to first determine if midline curvature could be used to predict strain in the myotomal cone muscle. After characterizing the timing between the traveling activation and midline curvature waves in tunas, it was concluded that midline curvature is not an accurate indicator of strain in the myotome cone muscle. Rates of the progressing activation, curvature, and displacement waves were also compared. Because activation and curvature travel down the body at the same rate, it was predicted that in tunas, dynamic muscle function does not vary by axial position down the body. Lastly, the position in the tail sweep at which peak force occurs in the caudal tendons was determined. In yellowfin, peak force occurs as the tail tip sweeps through the track of forward motion, whereas in skipjack, peak force occurs later, when the tip is about half way between the midpoint and the lateral extreme of its sweep.

## Introduction

The second stage in the analysis of tuna swimming is to couple body movement with muscle activation. Chapter 2 laid the groundwork by providing the temporal sequence of muscle activation during steady, cruising swimming. The next step is to characterize the kinematics, or motions through time, resulting from the muscle contractions and the body's interaction with the water. By correlating the movements of the fish in the video records with the synchronized EMG records, it is possible to determine the phase relations between the progressing activation and bending waves. This information can then be used to infer dynamic muscle function at different axial locations.

An important consideration in any study of axial fish locomotion is to determine how muscle functions in the generation of work used for thrust, and whether muscle function varies with location. That is, does muscle produce so-called "positive" work (i.e., the muscle generates work on its surroundings) or "negative" work (i.e., the muscle absorbs external work done on it), and does this function vary according to axial location along the body? In the case of tunas, this is a particularly intriguing problem because most of the thrust is produced by the tail, which is spatially separated from the force-generating muscle mass. Because work is the product of force and excursion, it will be maximal when force and excursion are

maximized. Optimization of these two factors is in turn highly dependent on muscle activation state relative to strain phase.

During the reciprocating movements of axial locomotion, muscle undergoes rhythmic lengthening and shortening cycles. These oscillating patterns of length change (strain) can be represented as a sine wave. In one cycle, muscle rest length is defined to occur at  $0^{\circ}$ , the muscle then stretches to its maximum length at  $90^{\circ}$ , shortens back through rest length ( $180^{\circ}$ ) to its minimum length at  $270^{\circ}$ , and finally lengthens back to its starting rest length at  $360^{\circ}/0^{\circ}$ . Much of what we know about muscle function in fish has been derived only recently from *in vitro* work loop experiments, in which force is measured from a bundle of isolated muscle fibers as it is mechanically cycled sinusoidally under varying regimes of strain and stimulation phase (e.g., short-horned sculpin, *Myoxocephalus scorpius*: Johnson and Johnston, 1991; saithe, *Pollachius virens*: Altringham *et al.* 1993; scup, *Stenotomus chrysops*: Rome *et al.* 1993; largemouth bass, *Micropterus salmoides*: Johnson *et al.* 1994; yellowfin tuna, *Thunnus albacares* and bonito, *Sarda chiliensis*: Altringham and Block, 1997). Johnson and Johnston (1991) provide an elegant illustration (their Fig. 4) of the magnitude and type of work produced when muscle is stimulated at different points in the strain cycle (with all other variables such as amount of strain and intensity of stimulation kept constant). The authors show that over the course of a full cycle, maximum net positive work is produced by the muscle if activation begins at about  $30^{\circ}$  (that is, as the fiber is lengthening between rest length and maximum length). This is due to an intrinsic property of muscle whereby greater force is

developed when muscle is stretched while active (Lieber, 1992). Conversely, the muscle will experience the greatest net negative work (i.e., absorb work done on it) if activation onset occurs at about  $210^\circ$ . Whether a muscle performs net positive or net negative work during a cycle (tailbeat) dictates its function within the system.

Physiologically, positive work means the muscle performs work on its surroundings (e.g., skeleton, connective tissues, water), while negative work will stiffen the muscle (due to the resistance of active muscle to lengthening), causing it to absorb external work and serve as a force transmitter. Because the type of dynamic muscle function is critically dependent on the phase relation between stimulation and strain, *in vivo* locomotion studies are needed to supply EMG data and strain estimates from kinematics.

What evidence is there to suggest that muscle function might vary according to axial position within a swimming fish? EMG and kinematic studies conducted on several different species of fish have shown that in those with tail blades (e.g., mackerel, *Scomber scombrus*; carp, *Cyprinus carpio*; saithe; scup), the wave of sequential muscle activation travels down the body faster than the resulting bending wave (reviewed by Wardle and Videler, 1994; Wardle *et al.* 1995; Shadwick *et al.* 1997). The predicted consequence of the differing rates of travel is that with increasing distance down the body, the traveling waves become increasingly out of phase, with activation occurring earlier in the strain cycle posteriorly. Hence, it has been hypothesized that dynamic muscle function must vary by location. For example, near the head, activation might begin just before the muscle reaches its peak length

and then continue during shortening (resulting in net positive work), while at the most posterior locations, the majority of the duty cycle would coincide with muscle lengthening (resulting in net negative work). Wardle and Videler (1993) have concluded that in saithe and mackerel, most of the force for thrust production is generated by the anterior muscle (producing net positive work), while the muscle near the tail is stiffened (net negative work) to transmit the anteriorly-generated force to the tail blade. In contrast, Rome *et al.* (1993) concluded that in the scup, all muscle produces net positive work, with the greater portion in fact being generated by the posterior muscle, due to the larger amplitude strains. There is still much to be learned about dynamic muscle function in different species of fish, with different swimming modes. An analysis conducted on such a specialized swimmer as a tuna should extend this knowledge.

For this investigation of dynamic muscle function in tunas, the EMG patterns have now been discerned (Chapter 2). What is needed next is a kinematic descriptor of the other parameter, muscle strain. Studies in other fishes have shown that strain in superficial muscle can be accurately predicted from midline (backbone) curvature at the same axial location (e.g., carp: Rome and Sosnicki, 1991; largemouth bass: Jayne and Lauder, 1995 and 1996; scup: Coughlin *et al.* 1996; Pacific mackerel, *Scomber japonicus*: Shadwick *et al.* 1997). In essence, the body can be treated as a bending beam, because contraction of a muscle block causes local bending. One of the goals of the present study was to investigate whether midline curvature is also likely to be an accurate indicator of strain in muscle of the myotome cones. The tuna anatomy,

which incorporates aerobic muscle within these nested cones, provides a good model for probing this question at steady, cruising speeds.

Thus, for yellowfin and skipjack, kinematic analyses were first performed to characterize the midline curvature and lateral displacement waves traveling down the body. Next, these data were linked with the EMG data to determine the phase between activation and bending at different axial locations. This information was then used to make inferences about dynamic muscle function down the length of the body.

Besides examining muscle function, the other goal of this kinematics study was to describe the tail movements in relation to force development in tunas. In particular, the purpose was to discern where in the tail sweep peak force occurs. For the first time in any fish, this type of assessment was made possible by the ability to measure internal forces experimentally during swimming, using a buckle force transducer on the caudal tendons. Some investigators (Lighthill, 1971; Wardle, 1985) have predicted that peak force should occur when the tail tip reaches maximum velocity, as it passes through the midpoint of its sweep from one side to the other. Coupling swimming kinematics with direct force measurements in these tunas has provided the first empirical evidence to test this prediction.

## Materials and Methods

Experimental protocol: Care and handling of fish, surgery, swimming procedures in the water tunnel, and EMG methodology were all as described in Chapter 2. Details concerning the tendon buckle are presented in Chapter 4.

The dorsal aspect of the fish, viewed from a mirror mounted at  $45^{\circ}$  above the working section of the tunnel, was filmed with a Sony model CCD-FF3 Video 8 Handycam video recorder at 60 Hz. A reflective background grid of adhesive Scotchlite™ (3M), marked off in 10 cm squares, was attached to the bottom of the working section. Because this material reflects directly back to the light source, it was possible to film at high shutter speeds (1/4000 sec) by placing a fiber optic light right next to the camera lens (Wardle and Videler, 1993). This arrangement mitigated the disturbance to the fish that would have occurred with the use of high wattage lamps, but it meant that the fish was filmed in silhouette. Therefore, small Scotchlite™ markers were usually sutured to a few locations along the dorsal midline for tracking during analysis. The video was synchronized to the computer records of EMG and tendon force with a pulsing red light emitting diode placed in the video field. The voltage square wave emitted with each pulse was recorded to a separate computer acquisition channel alongside the EMG and force traces.

Analysis: After a segment of steady swimming was chosen, video fields were digitized onto a Macintosh Quadra 700 from a Panasonic model AG-7355 video cassette recorder, using a RasterOps 24STV interface board and MediaGrabber

software (RasterOps Corporation, Santa Clara, CA). Distances in the images were calibrated using the background grid, with the minor magnification factor (due to the fish swimming several cm above the grid) corrected based on known measurements of the fish taken after the experiment. Because it was not possible to see the dorsal midline in the silhouettes, the outline of each side of the fish was digitized (using NIH Image software) by recording the x-y coordinates of 15-20 points spanning from the origin of the pectoral fins to the peduncle (Fig. 3.1). A 4th order polynomial curve fit was applied to each series, and then the coefficients for the right and left sides were averaged to generate the equation for a curve describing the shape of the midline in that field. Following the procedure of Shadwick *et al.* (1997), the midline equations from the series of video fields were then used to calculate curvature (defined as the reciprocal of the radius of curvature) as a function of time for several sites along the midline, using software written by Dr. Bradley Shadwick (University of California, Berkeley). This program was also used to calculate the lateral displacement (= the excursion to the left and right of the swimming track) of several midline positions through time. Curvature and displacement waves were smoothed with a low-pass digital filter using AcqKnowledge® software (BIOPAC Systems, Inc.). Filter cut-offs were chosen which did not diminish the wave amplitude or introduce any phase shift. In all figures, positive curvature values denote convexity of the right side of the body, and positive values of lateral displacement indicate excursion of a point on the midline to the right side of the forward swimming track.



Rates of the traveling curvature and displacement waves (in L/s) were calculated by dividing the longitudinal distance between the first and last EMG sites by the average time delay (from several tailbeats) between maximum curvature or displacement at the 2 sites. Activation rate was calculated the same way, using the time delay between EMG onsets at the 2 sites. The propulsive wavelength  $\lambda_b$  (= the wavelength of the traveling displacement wave) was calculated as the product of tailbeat period (T) and rate of the traveling displacement wave (V). Stride length, or distance traveled in one tailbeat, was calculated as the product of T and forward swimming speed, U.

Movements of the peduncle (at a point midway between the widest span of the lateral keel) and tail tip (= tip of the upper tail blade lobe) were digitized separately and correlated with the buckle force records to determine a kinematic reference for peak force.

Because the fish were filmed in a mirror, the left side (with the EMG wires and buckle) appears as the “right” side in the video images. Thus, for ease of discussion, the designation of the right side in all figures and text will refer to the apparent orientation of the body in the images, with the understanding that this is the side with the EMG electrodes and buckle.

## Results

### Description of propagating waves of midline curvature and lateral displacement :

Values of midline curvature and lateral displacement calculated for several axial locations were tracked through time to describe the traveling waves passing down the fish during swimming (Fig. 3.2). Midline curvature at any given axial location is used to indicate muscle strain at that site. Positive values indicate convexity of the right side (muscle lengthening) and negative values denote concavity (muscle shortening). Lateral displacement refers to the movement of a point on the midline to the left and right of the swimming track; positive values indicate excursion to the right. The first axial location is for a marker at the leading edge of the first dorsal fin, the next 3 sites are the locations of the 3 EMG electrodes, and the posterior-most site is the end of the muscle mass, at about the pre-peduncular joint.

Although Fig. 3.2 only shows data from a skipjack, the general trends for midline curvature and lateral displacement are the same for both species: the amplitudes increase with more posterior locations, and there is a phase delay between curves from one site to the next, reflecting the sequential rostral-caudal activation patterns. Fig. 3.3 (for both yellowfin and skipjack) illustrates that the amplitudes of curvature and displacement increase gradually across the first two-thirds of the fish's length, but then increase dramatically just before the peduncle. Thus, most of the bending and lateral movement propelling the fish forward occur close to the tail blade.

Phase relationships among traveling waves of muscle activation, midline curvature, and lateral displacement of the midline:

Fig. 3.4 shows the timing relationships among muscle activation, midline curvature, and lateral displacement at 3 EMG electrode sites in a yellowfin and a skipjack. At any site, maximum curvature precedes maximum lateral displacement, a natural consequence of traveling sine waves of increasing amplitude (Jayne and Lauder, 1996; Katz and Shadwick, 1997). Given the assumption that midline curvature indicates local muscle strain (based on observations in other fishes: Rome and Sosnicki, 1991; Jayne and Lauder, 1995 and 1996; Coughlin *et al.* 1996; Shadwick *et al.* 1997), this means that at a given axial location in tunas, muscle attains its maximum length before reaching its farthest lateral excursion from the swimming track. This pattern is typical of axial fish locomotion.

What sets these tunas apart from other fishes is the timing of muscle activation relative to midline curvature. The most striking observation is that at each site, the muscle is not activated until after the midline there has bent to its most convex and started to straighten. The delay between maximum midline convexity and EMG onset is more pronounced in the skipjack than in the yellowfin. If midline curvature does in fact reflect muscle strain, then in both these species the muscle is already shortening before it is activated, which would produce very little positive work. This seemingly unexpected result is indirect evidence that in tunas, local midline curvature and myotomal muscle strain are probably not in phase. The implication is that activation at a given axial location in the myotomal cones does not result in backbone bending at

that location (as it would in a bending beam, or superficial muscle), but rather at a more posterior location.

The phase relations shown graphically in Fig. 3.4 are quantified in Table 3.1. Each species shows a similar delay between midline curvature and lateral displacement at a particular location, but there is a trend towards increasing delay moving posteriorly. The increasing lag is due to the displacement wave traveling slower than the curvature wave (Table 3.2). Comparing the phase between muscle activation and lateral displacement of the midline to the same side, skipjack EMG onset is approximately coincident with peak displacement, while yellowfin EMG onset precedes it.

Rates of traveling waves of activation, curvature, and displacement:

The yellowfin and skipjack show similar rates (normalized to L/s) of activation, curvature, and displacement (Table 3.2). Mean curvature rate in the yellowfin is somewhat higher than in the skipjack, but the range of values overlap when variability is taken into account. The ratio of activation rate to curvature rate (A:C) in each species is close to one. This is in contrast to observations in other fishes with tail blades, in which muscle activation travels faster than midline curvature (Wardle and Videler, 1994; Wardle *et al.* 1995; Shadwick *et al.* 1997). However, in agreement with data from other fishes, the activation wave in these tunas travels down the body faster than the lateral displacement (propulsive) wave.

The ratio between the speed of the body through the water and the rate of the propulsive wave ( $U:V$ ) is an indicator of how efficiently lateral displacements of the body are translated into forward movement. These ratios are similar in yellowfin and skipjack, as are the values for stride length and the propulsive wavelength.

Kinematic reference for peak force at the tail blade:

In the yellowfin, peak force is registered as the tail tip is sweeping across the swimming track (Fig. 3.5A). In the skipjack, the tail tip has swept beyond the track of forward motion when peak force is recorded (Fig. 3.5B). The phases are quantified in Table 3.3 for 3 yellowfin and 2 skipjack. Within the time resolution afforded by the video frame rate (60 fields/s), the phase between peak force and the tail tip crossing the swimming track is on average  $1^{\circ}$  in the yellowfin. (The best precision that can be placed on an event is half a video field, or 0.00834 s, which at these tailbeat periods corresponds to  $\pm 9^{\circ}$ , where 1 tailbeat cycle =  $360^{\circ}$ .) In the skipjack, peak force occurs much later in the tailbeat cycle, near  $50^{\circ}$ , when the tail tip is about half way on its excursion between the swimming track and its maximum displacement to the right side (= the side with the force transducer).

## Discussion

### Significance of muscle activation-midline curvature phase:

In much of the recent literature on axial fish locomotion, the timing of muscle activation relative to the muscle's strain cycle has been shown to be of great importance in determining whether the muscle will do positive work or negative work during propulsion. The kinematics of midline curvature has proven to be a good predictor of superficial muscle strain in a variety of fishes, as verified by *post mortem* sarcomere length measurements (Rome and Sosnicki, 1991), sonomicrometry (Coughlin *et al.* 1996), and videoradiography (Shadwick *et al.* 1997). The link between midline curvature and muscle strain is reliable for superficial fibers because they are oriented approximately parallel to the backbone, so the body can be treated as a bending beam for strain calculations (Shadwick *et al.* 1997). Investigators have taken advantage of this relationship by correlating kinematics with EMG data to predict superficial muscle function at different axial locations.

In contrast, an important outcome of the present study has been to suggest that for the muscle of the nested myotome cones, curvature of the midline does not appear to be an accurate predictor of local muscle strain. This conclusion is drawn because if curvature reflected strain, it would predict that the muscle was already partially shortened before being activated (Fig. 3.4). Based on data from muscle work loop experiments in other fishes (e.g., Johnson and Johnston, 1991; Altringham

*et al.* 1993; Rome *et al.* 1993; Altringham and Block, 1997), very little positive work would be derived from a muscle that was activated after having already shortened by 30-50% (i.e., at a phase of 120-140° in the strain cycle). In fact, recent work loop experiments by Altringham and Block (1997) on yellowfin medial red muscle show that optimal activation phase (for maximum power) should occur near 60° in the strain cycle (at physiological muscle temperatures). In other words, as observed in many fishes, activation should begin before the muscle has reached its maximum length (at 90°) in order to derive the most net positive work.

One explanation for why midline curvature does not reflect local myotomal muscle strain would be that the backbone is being deformed by contractions of muscle farther forward. Evidence in support of this type of mechanism has been shown by Covell *et al.* (1991), who used sonomicrometry to study white muscle during fast starts in rainbow trout. Their data showed that backbone bending preceded local muscle shortening. While a fast start is not the same as steady axial swimming, their data do demonstrate that the complicated fiber geometries of elongated myotomes, and their attachments to myosepta and skeleton, are able to cause backbone bending at a remote site. Indeed, the arrangement of the tuna anatomy, with the bulk of the force producing muscle mass located forward on the body, spatially removed from the thrust producing tail, predicts that muscle action must somehow be directed toward the rear. Most likely, the purpose in having such highly elongated myotomes, which span up to 13 vertebrae in the yellowfin and 17 in the skipjack (personal observations), is to direct the effects of anterior muscle contractions to more

posterior locations on the backbone. Ultimately, because kinematics cannot be used to predict strain in the myotome cones at the activation site, the specific relation between activation and strain in tunas (and, hence, an assessment of dynamic muscle function as well) awaits the use of sonomicrometry.

Kinematic parameters compared with other teleosts and a previous study of yellowfin:

Stride lengths calculated for yellowfin and skipjack (0.62 and 0.67 L, respectively; Table 3.2) are in close agreement with data from other teleosts (Videler, 1993) and with previous yellowfin data (Dewar and Graham, 1994). The ratio of U:V is an indicator of how efficiently lateral displacements of the body are translated into forward propulsion through the water. The values of 0.6 for yellowfin and 0.7 for skipjack are comparable to those reported for other teleosts (Videler, 1993) but higher than the value of 0.4 reported by Dewar and Graham (1994) for similarly sized yellowfin (their study did not include skipjack). A possible explanation for the differing yellowfin ratios is that similarly-sized yellowfin in Dewar and Graham's 1994 study swam at a slower range of speeds (26-74 cm/s) than the fish in the present study (56-90 cm/s). Their fish swam at a mean U of 48 cm/s, which was approximately equal to the minimum U required to maintain hydrostatic equilibrium ( $U_{\min}$ ). Many of the swimming speeds were well below this  $U_{\min}$ . The authors noted that such a low efficiency value was unexpected for this highly specialized swimmer, and postulated that the slow U could have accounted for it, due to whatever mechanisms the fish used to increase lift and maintain hydrostatic equilibrium.



Finally, the propulsive wavelength,  $\lambda_b$ , was found to be approximately 1 L for both tuna species in the present study, which is again comparable to other teleosts but lower than the average value of 1.24 L reported previously for similarly sized yellowfin (based on the same references above). Again, it is possible that the slower speeds used by the yellowfin in the Dewar and Graham (1994) study may have caused them to use a somewhat different gait than the yellowfin in this work, which might in turn result in a somewhat different  $\lambda_b$ . The discrepancies could also be attributed to variations in experimental protocols. The kinematic analyses in our study were based on video recordings with twice the frame rate and higher shutter speeds (4000/s vs. 200/s) than those used by Dewar and Graham (1994), and 15-20 points per image were digitized to calculate the bending waves instead of 4.

Significance of muscle activation and midline curvature rates in tunas:

Kinematic analyses of these 2 tuna species show that the waves of muscle activation and midline curvature travel at approximately the same rate (Table 3.2). These results are in contrast to findings in other fishes with tail blades, in which the activation proceeds more quickly than the resultant curvature wave (reviewed by Wardle and Videler, 1994; Wardle *et al.* 1995; Shadwick *et al.* 1997). This rate discrepancy led to the prediction that dynamic muscle function would vary by axial position. Because there is no rate difference in tunas, however, there is no evidence to suggest that muscle function might vary with location. A prediction can then

further be made that muscle along the entire body length will produce net positive work. Such a scenario would generate maximal work for transferal to the tail blade.

Kinematic reference for when peak force occurs at the tail blade:

Another contribution of this study has been to discover what position in the tail sweep coincides with peak force in the caudal tendons. This has never been experimentally determined before in any fish because there was no way to measure internal muscle forces. Coupling the time course of force development (registered by the tendon buckle) with the tail tip kinematics has shown that in the yellowfin, peak force occurs just as the tip sweeps across the track of forward motion through the water. This is what Lighthill (1971) and Wardle (1985) predicted, based on the fact that the tail tip should reach its maximum velocity at this point in the tail sweep. Tail tip velocity can be deduced from the traces in Fig. 3.5. Each point on a line comes from one video field, so all points are spaced equally in time (0.01668 sec). As the tip passes through the swimming track, the spatial distance between points is the greatest, indicating maximum velocity.

In contrast to yellowfin, peak force in the skipjack occurs later in the tail sweep, when the tip is about half way towards maximal displacement (average of  $50^{\circ}$ , Table 3.3). Possible explanations for the phase differences between tail tip position and peak force in these 2 species may be linked to differences in tail morphology. In general, skipjack tails have a higher aspect ratio, while yellowfin tails have a greater sweepback angle (Magnuson, 1978). Consequently, the distance between the

peduncle (where the buckle is positioned) and the tips of the tail lobes is longer in the yellowfin. This is illustrated by the greater phase lag between movements of the peduncle and tail tip in the yellowfin compared to the skipjack (Fig. 3.5). The greater sweepback in the yellowfin tail results in the center of thrust being located farther back on the tail blade than in the skipjack (Magnuson, 1978). Because force is being recorded from the same anatomical location in both species, it is conceivable that differences in the location of the center of thrust at the tail could result in different phase relations between peak force and kinematics of the tail tip.

In tunas as well as in other fishes, more research is needed to understand how variations in body morphology, dynamic muscle function, and interactions with the surrounding water combine to define a particular swimming mode.

**Fig. 3.1:** Montages of captured video fields spanning approximately one tailbeat in a yellowfin (A) and a skipjack (B). Image order is left to right; each image is 1/60 sec; every third video field is shown. The view is of the dorsal aspect in silhouette, as filmed from a mirror. In the first image of each montage, a series of white dots is shown along the left and right sides of the fish to illustrate how the outlines are digitized. After 4th-order polynomial curves are fit to these outlines in each image, the coefficients are averaged to describe a line corresponding to the curve of the midline (backbone).

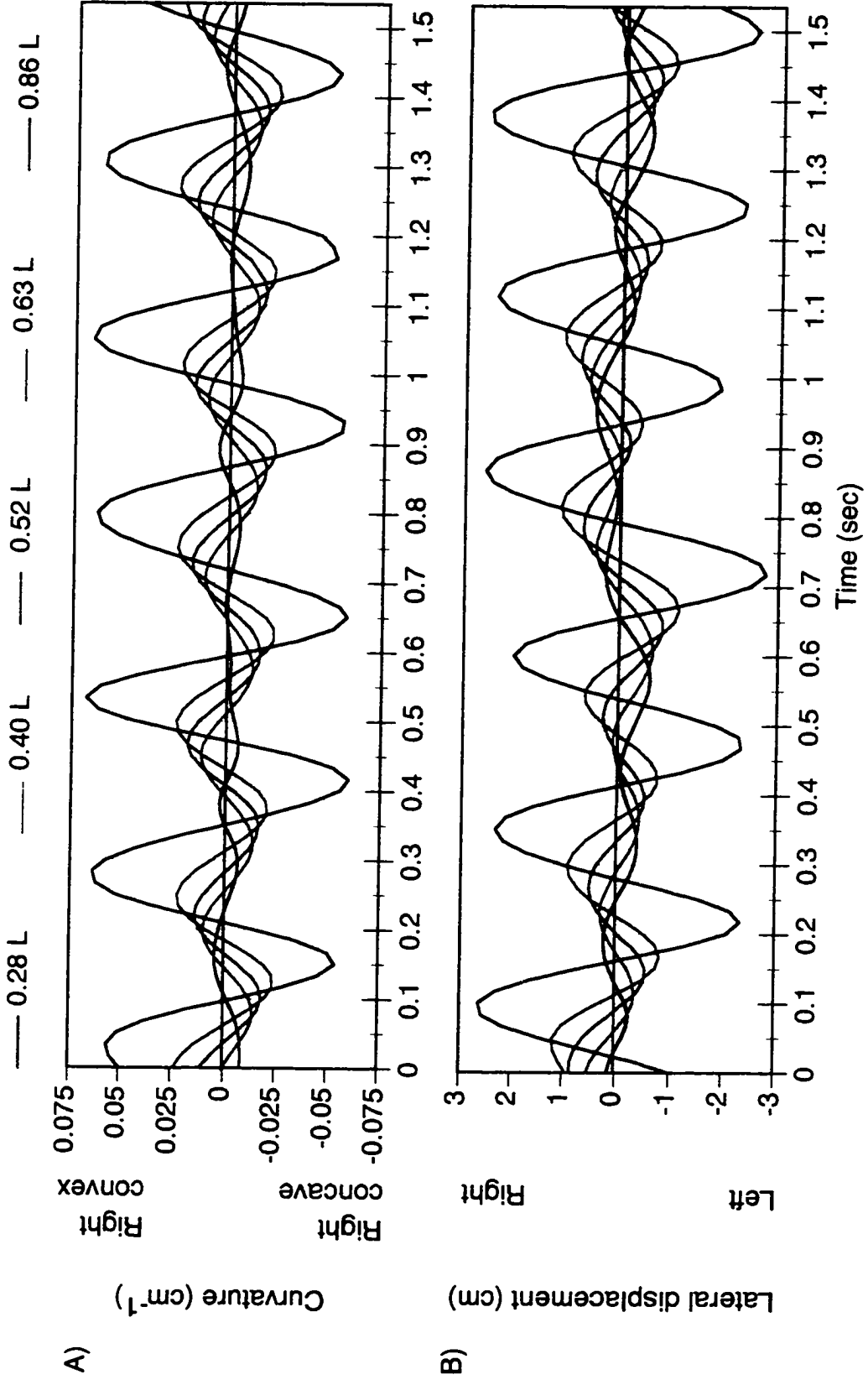
A) Yellowfin



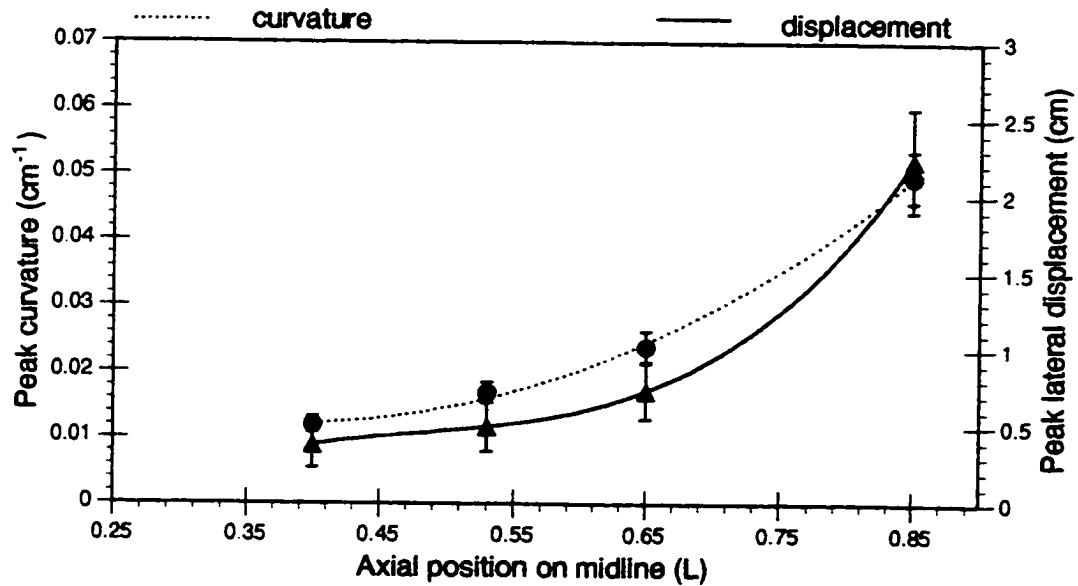
B) Skipjack



**Fig. 3.2:** Traveling waves of midline curvature (A) and lateral displacement (B) for 5 axial locations on a 41 cm skipjack. Six consecutive tailbeats are shown from a swimming bout at 2.7 L/s, with a TBF of 3.9 Hz. The direction of swimming is to the left, so the direction of the posteriorly-propagating bending waves is to the right. The horizontal 0 line denotes the swimming track (the track of forward movement of the body through the water).



Yellowfin:



Skipjack:

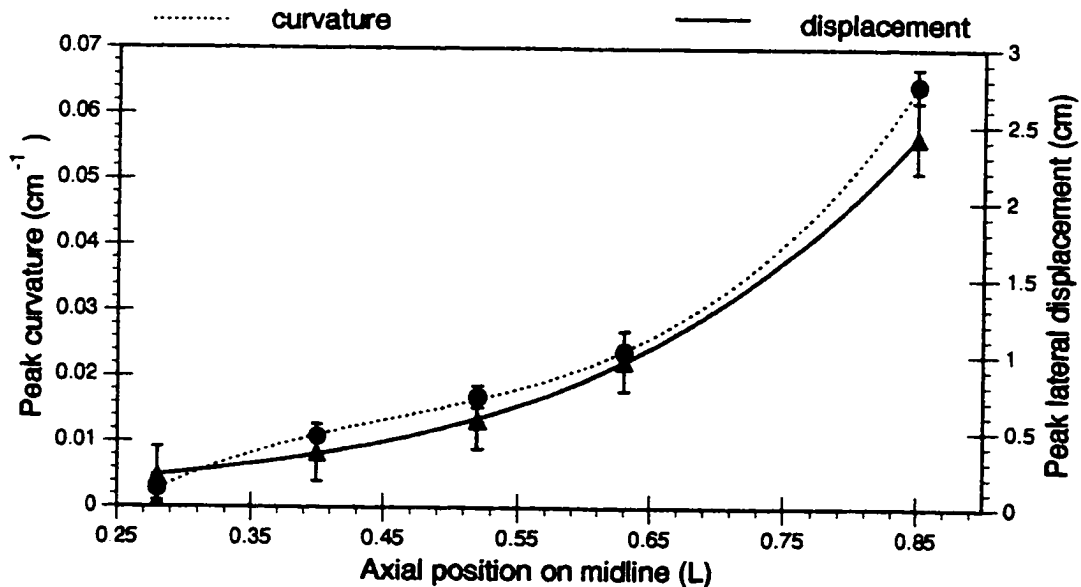
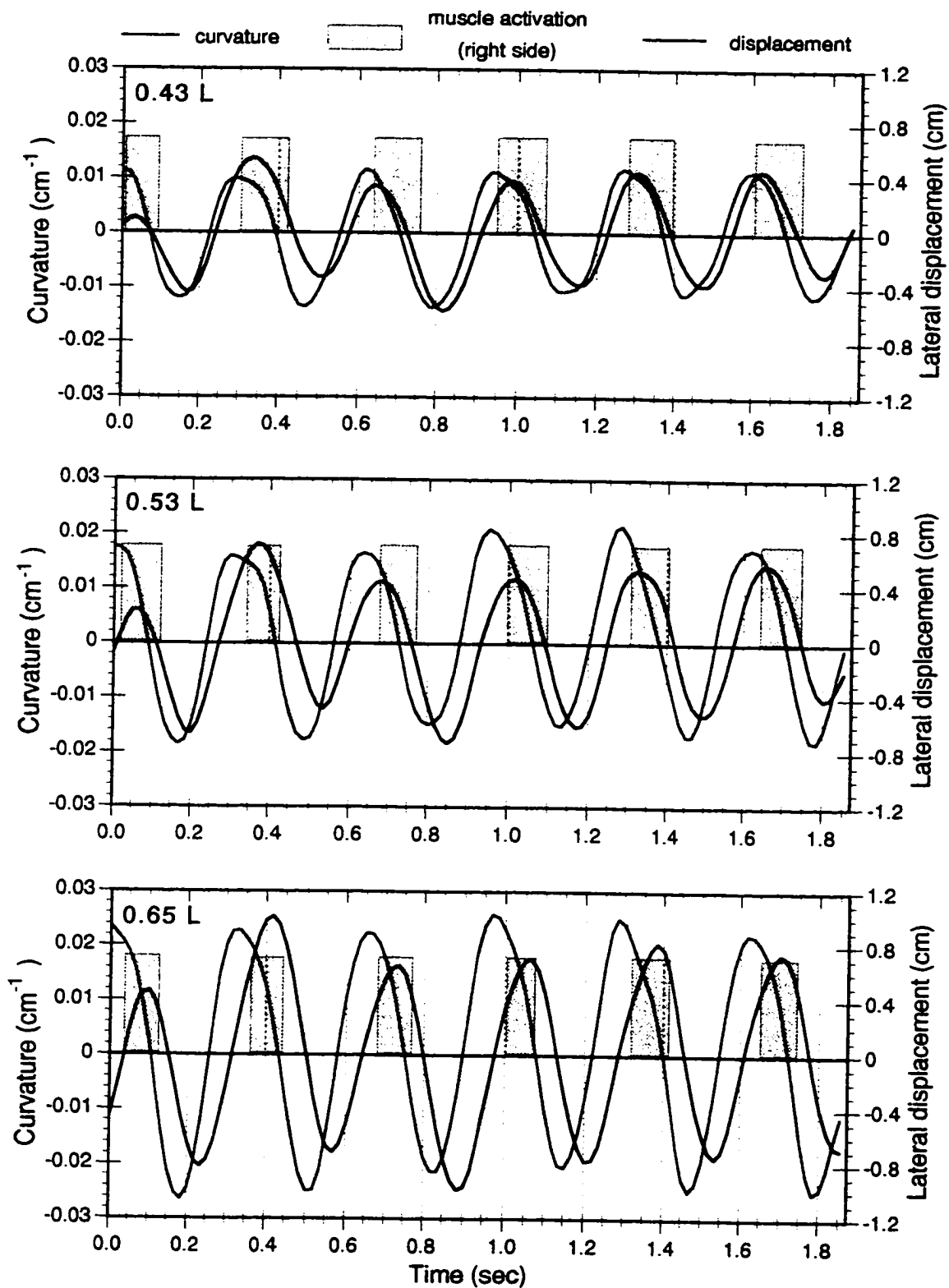


Fig. 3.3: Amplitude envelopes of midline curvature and lateral displacement. Maximum amplitudes are shown as a function of axial position. Curvature is indicated by the dotted lines; lateral displacement by the solid lines. Points and error bars are means and standard deviations from 5 tailbeats. Yellowfin = 40 cm; skipjack = 41 cm.



**Fig. 3.4:** Phase of muscle activation, midline curvature, and lateral displacement at 3 axial locations in a 40 cm yellowfin (A) and a 41 cm skipjack (B) (same individuals used in Fig. 3.3). The 3 sites on the yellowfin are at 0.43, 0.53, and 0.65 L and on the skipjack at 0.40, 0.52, and 0.63 L. Muscle activation of the right side is indicated by the green filled boxes, curvature by the blue lines, and lateral displacement by the black lines. As in Fig. 3.2, positive values of curvature indicate convexity of the right side, and positive values of lateral displacement denote excursion of the midline to the right of the swimming track (as indicated by the horizontal line at 0 on the ordinates).

## A) Yellowfin:



B) Skipjack:

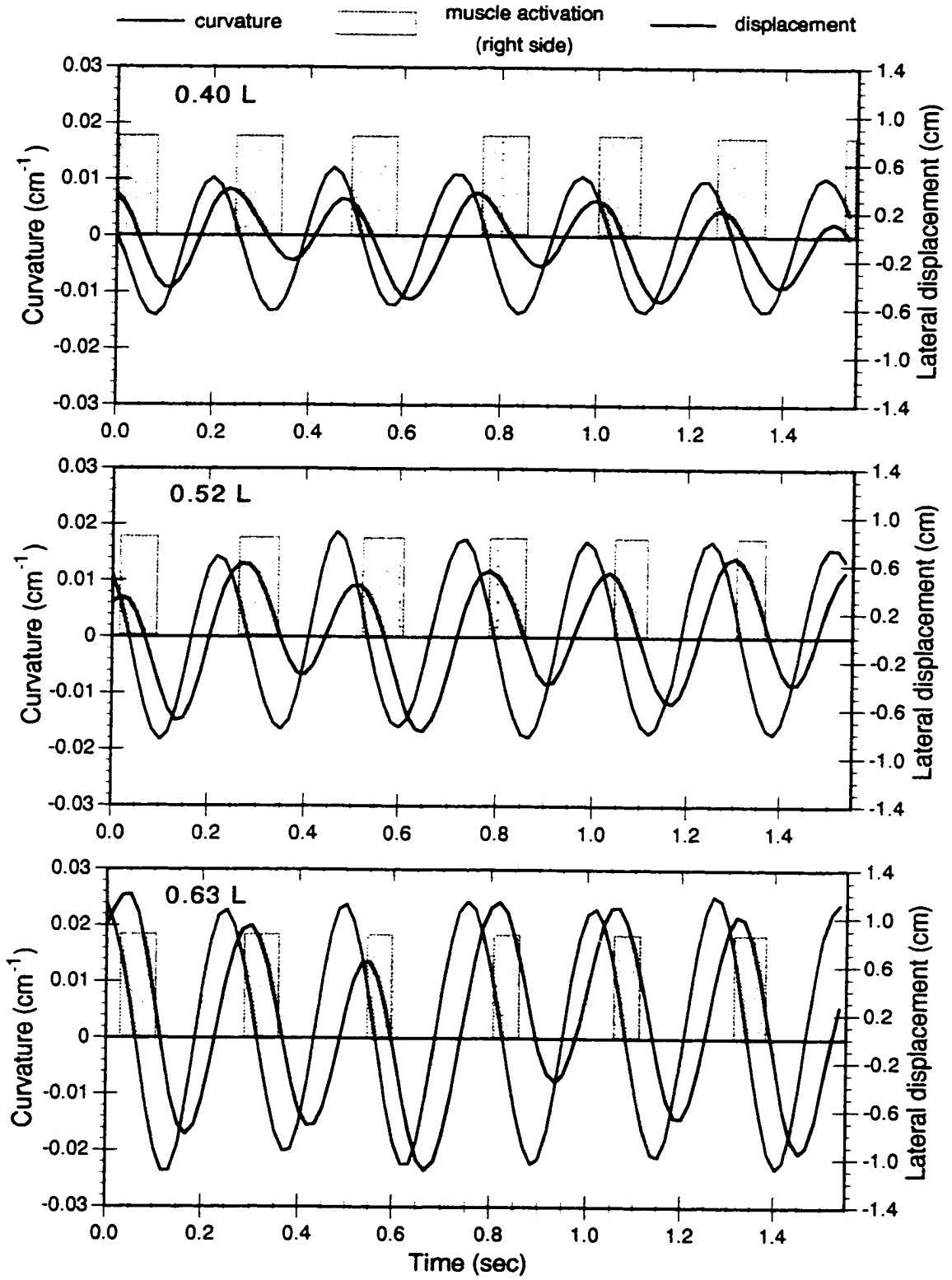


**Table 3.1:** Phase delays among midline curvature, lateral displacement, and EMG onset for the yellowfin and skipjack in Fig. 3.4. Phase delay times are expressed first as a proportion of the tailbeat period (T) and then in degrees, where one tailbeat period represents  $360^{\circ}$  (i.e., the delay in terms of T is multiplied by 360 to give the delay in degrees). In A, means and standard deviations were calculated using the times of maxima and minima for curvature and displacement (seen as peaks and troughs in Fig. 3.4) across the 5 tailbeats in the yellowfin and 6 in the skipjack (n=10 for yellowfin, 11 for skipjack). In B and C, means and standard deviations were calculated only from the values to the right side, since the EMG data were only from that side (In B and C, n = 5 and 6, respectively, for both species). In C, negative delays in the skipjack indicate that lateral displacement preceded EMG onset.

**A) Phase delay between curvature and displacement:**

	Location (L):	Delay normalized to tailbeat period (T)		Delay in degrees:	
		Mean	(Std. Dev.)	Mean	(Std. Dev.)
yellowfin:	0.43	0.115	(0.046)	41	(17)
	0.53	0.139	(0.046)	50	(17)
	0.65	0.226	(0.059)	81	(21)
	0.85	0.294	(0.053)	106	(19)
skipjack:	0.40	0.134	(0.035)	48	(13)
	0.52	0.181	(0.016)	65	(6)
	0.63	0.189	(0.028)	68	(10)
	0.86	0.260	(0.028)	94	(10)

**B) Phase delay from maximum curvature to EMG onset on the same side:**

	Location (L):	Delay normalized to tailbeat period (T)		Delay in degrees:	
		Mean	(Std. Dev.)	Mean	(Std. Dev.)
yellowfin:	0.43	0.041	(0.022)	15	(8)
	0.53	0.103	(0.028)	37	(10)
	0.65	0.098	(0.016)	35	(6)
skipjack:	0.40	0.154	(0.045)	55	(16)
	0.52	0.201	(0.025)	72	(9)
	0.63	0.160	(0.037)	58	(13)

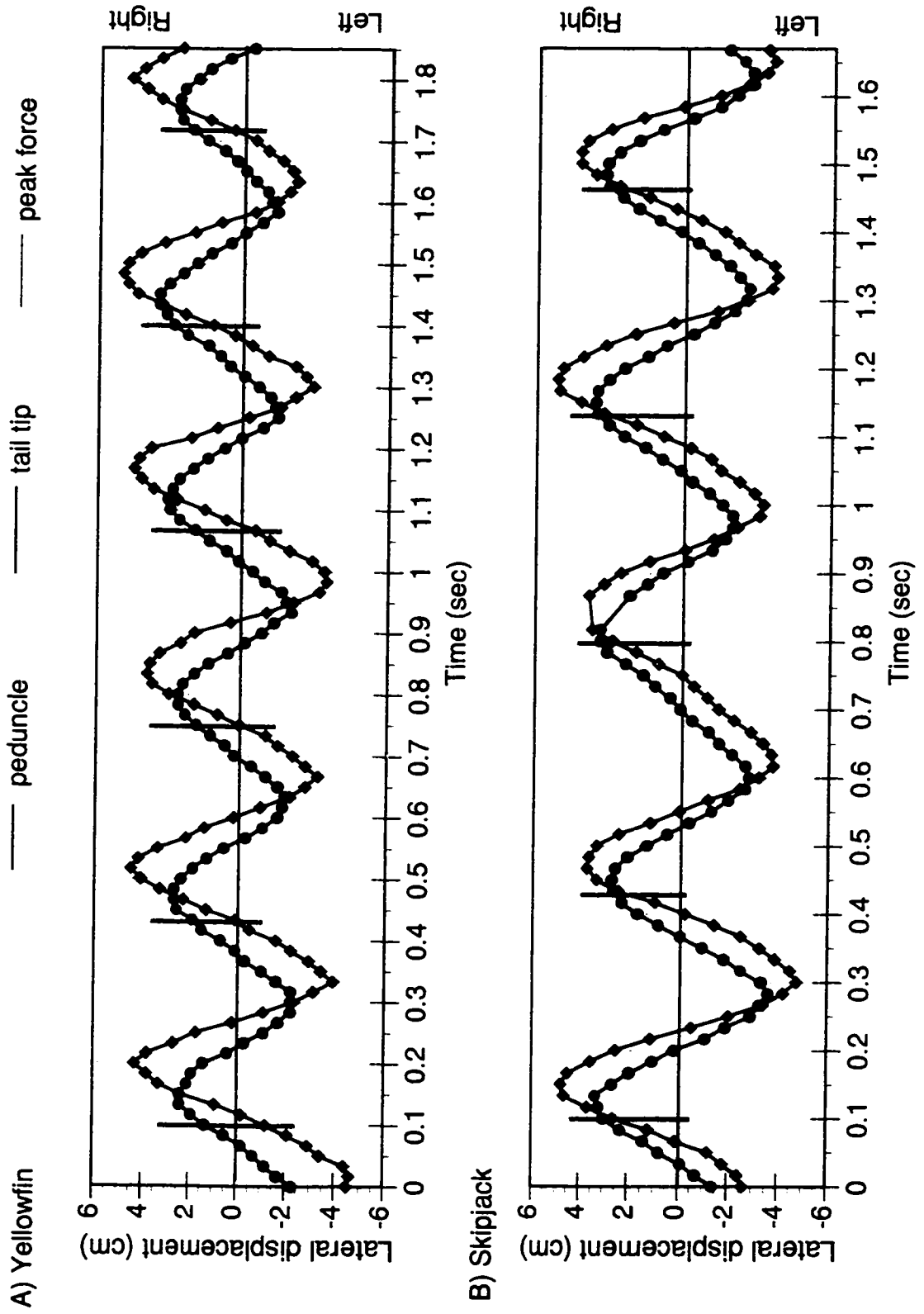
**C) Phase delay from EMG onset to maximum lateral displacement to the same side:**

	Location (L):	Delay normalized to tailbeat period (T)		Delay in degrees:	
		Mean	(Std. Dev.)	Mean	(Std. Dev.)
yellowfin:	0.43	0.071	(0.035)	26	(13)
	0.53	0.043	(0.043)	15	(15)
	0.65	0.179	(0.019)	64	(7)
skipjack:	0.40	-0.033	(0.028)	-12	(10)
	0.52	-0.016	(0.033)	-6	(12)
	0.63	0.028	(0.017)	10	(6)

	U	TBF	T	Stride length (L)	Mean rate (L/s) of traveling wave (Std. Dev.):			Ratio of			$\lambda_b$ (L)	
	(L/s)	(Hz)	(sec)		Activation A	Curvature C	Displacement V	A:C	A:V	C:V		U:V
<b>Yellowfin</b> (40 cm)	1.9	3.1	0.323	0.62	4.7 (.7)	5.8 (1.1)	3.2 (.7)	0.80	1.45	1.81	0.59	1.03
<b>Skipjack</b> (41 cm)	2.7	3.9	0.256	0.69	4.6 (.8)	4.8 (.7)	3.8 (.4)	0.97	1.22	1.26	0.70	0.97

Table 3.2: Propagation rates of waves of muscle activation, midline curvature, and lateral displacement. Rates were calculated across the distance between EMG sites 1 and 3. In the yellowfin, this distance was between 0.43 and 0.65 L; in the skipjack, between 0.40 and 0.63 L. Mean rates and standard deviations were calculated from 5 tailbeats.

**Fig. 3.5:** Occurrence of peak force in the caudal tendons relative to lateral movements of the peduncle (blue lines) and tail tip (black lines). Time of peak force on the right side only (the side with the force transducer) is indicated in each tailbeat by a red vertical line. A: 40 cm yellowfin; B: 38 cm skipjack.





Fish ID	L (cm)	U (L/s)	T (s)	Limit of time resolution <sup>1</sup> (degrees)	Phase between tail tip crossing the swimming track and peak force <sup>2</sup> Degrees (Std. Dev.)
<b>Yellowfin:</b>					
TA1202	40	1.4	0.370	8	9 (14)
		1.9	0.323	9	0 (8)
TA1207	43	1.6	0.313	9	-5 (6)
		2.1	0.333	9	6 (9)
TA315	43	1.7	0.345	9	-6 (4)
					Mean for yellowfin: 1° (7)
<b>Skipjack:</b>					
KP1203	38	2.2	0.345	9	47 (17)
KP331	41	2.7	0.256	12	52 (10)
					Mean for skipjack: 50° (4)

<sup>1</sup> The proportion of a tailbeat cycle occupied by half a video field:  $=(0.00834/T) \cdot 360$

<sup>2</sup> A negative value indicates that peak force occurs before the tail tip crosses the swimming track.

Table 3.3: Phase relationship between when the tail tip crosses the swimming track and peak force is registered in the caudal tendons (using data from Fig. 3.5). Phase delay is expressed in degrees, where one tailbeat period (T) = 360°. Means and standard deviations are from 6 tailbeats in the yellowfin, 5 in the skipjack.

## References

- Altringham, J. D. and Block, B. A. (1997). Why do tuna maintain elevated slow muscle temperatures? Power output of muscle isolated from endothermic and ectothermic fish. *J. exp. Biol.* **200**, 2617-2627.
- Altringham, J. D., Wardle, C. S. and Smith, C. I. (1993). Myotomal muscle function at different locations in the body of a swimming fish. *J. exp. Biol.* **182**, 191-206.
- Coughlin, D. J., Valdes, L. and Rome, L. C. (1996). Muscle length changes during swimming in scup: sonomicrometry verifies the anatomical high-speed cine technique. *J. exp. Biol.* **199**, 459-463.
- Covell, J. W., Smith, M., Harper, D. G. and Blake, R. W. (1991). Skeletal muscle deformation in the lateral muscle of the intact rainbow trout *Oncorhynchus mykiss* during fast start maneuvers. *J. exp. Biol.* **156**, 453-466.
- Dewar, H. and Graham, J. B. (1994). Studies of tropical tuna swimming performance in a large water tunnel: III. Kinematics. *J. exp. Biol.* **192**, 45-59.
- Jayne, B. C. and Lauder, G. V. (1995). Speed effects on midline kinematics during steady undulatory swimming of largemouth bass, *Micropterus salmoides*. *J. exp. Biol.* **198**, 585-602.
- Jayne, B. C. and Lauder, G. V. (1996). New data on axial locomotion in fishes: how speed affects diversity of kinematics and motor patterns. *Amer. Zool.* **36**, 642-655.
- Johnson, T. P. and Johnston, I. A. (1991). Power output of fish muscle fibres performing oscillatory work: effects of acute and seasonal temperature change. *J. exp. Biol.* **157**, 409-423.
- Johnson, T. P., Syme, D. A., Jayne, B. C., Lauder, G. V. and Bennett, A. F. (1994). Modeling red muscle power output during steady and unsteady swimming in largemouth bass. *Am. J. Physiol.* **267**, R481-R488.
- Katz, S. L. and Shadwick, R. E. (1997). Curvature of swimming fish midlines as an index of muscle strain suggests swimming muscle produces net positive work. *J. theor. Biol.* (in press).

- Lieber, R. L. (1992). *Skeletal Muscle Structure and Function*. Baltimore: Williams and Wilkins.
- Lighthill, M. J. (1971). Large amplitude elongated-body theory of fish locomotion. *Proc. R. Soc. Lond. B* **179**, 125-138.
- Magnuson, J. J. (1978). Locomotion by scombrid fishes: hydromechanics, morphology, and behavior. In *Fish Physiology*, Vol. VII (ed. W. S. Hoar and D. J. Randall), pp. 239-313. New York: Academic Press.
- Rome, L. C. and Sosnicki, A. A. (1991). Myofilament overlap in swimming carp. II. Sarcomere length changes during swimming. *Am. J. Physiol.* **260**, C289-C296.
- Rome, L. C., Swank, D. and Corda, D. (1993). How fish power swimming. *Science* **261**, 340-343.
- Shadwick, R. E., Steffensen, J. F., Katz, S. L. and Klower, T. (1997). Muscle dynamics in fish during steady swimming. *Amer. Zool.* (in press).
- Videler, J. J. (1993). *Fish Swimming*. London: Chapman & Hall.
- Wardle, C. S. (1985). Swimming activity in marine fish. In *Physiological Adaptations of Marine Animals* (ed. M. Laverack), pp. 521-540. Cambridge: Company of Biologists, Ltd.
- Wardle, C. S. and Videler, J. J. (1993). The timing of the EMG in the lateral myotomes of mackerel and saithe at different swimming speeds. *J. Fish Biol.* **42**, 347-359.
- Wardle, C. S. and Videler, J. J. (1994). The timing of lateral muscle strain and EMG activity in different species of steadily swimming fish. In *Mechanics and Physiology of Animal Swimming* (ed. L. Maddock, Q. Bone and J. M. V. Rayner), pp. 111-118. Cambridge: Cambridge University Press.
- Wardle, C. S., Videler, J. J. and Altringham, J. D. (1995). Tuning into fish swimming waves: body form, swimming mode and muscle function. *J. exp. Biol.* **198**, 1629-1636.

## **Chapter 4: Forces measured in the caudal tendons of swimming tunas, and the functional role of the tendons as force transmitters.**

### **Abstract**

Muscle force transferred to the tail in swimming yellowfin and skipjack was measured directly by surgically fitting a buckle force transducer onto the pair of deep caudal tendons on the left side. At cruising speeds, powered by the red muscle, mean force among individuals ranged from 1.3-3.8 N in yellowfin and 1.6-4.1 N in skipjack. No clear dependence of force on speed was discernible at cruising speeds in most individuals, although 2 skipjack and 1 yellowfin indicated a trend toward increasing force with speed. Forces recorded for full muscle recruitment by restrained burst swimming, however, were approximately one order of magnitude higher than the cruising forces (41-49 N in yellowfin and 34-45 N in skipjack). The relation between red muscle activation state and force development in the caudal tendons was also explored. Substantial force (on average, 35% and 37% of peak force in yellowfin and skipjack, respectively) is registered in the caudal tendons before the posterior muscle has been activated, implicating the role of intermediate connective tissues in transferring anteriorly-generated force to the caudal tendons and tail. After the

swimming experiments, the tendons were excised and tested mechanically to characterize their biomaterial properties. At cruising speeds, the tendons operate in the region of low stiffness on their stress vs. strain curves. Extension was measured as the tendons were loaded to their *in vivo* forces in a tensile testing apparatus. Force and extension measurements were used to calculate the amount of strain energy stored in the tendons during swimming. When this energy was compared to the total mechanical energy output required for swimming (extrapolated from metabolic data of Dewar and Graham, 1994), it was concluded that the tendons function as inextensible force transmitters, rather than as biological springs, when transferring force from the muscle to the tail.

## Introduction

This research on tuna swimming has been divided into several subcomponents. Chapter 2 (electromyography) discussed the sequential activation patterns of the aerobic muscle during steady, cruising swimming. Chapter 3 then focused on how these particular muscle activation patterns correlate with the movements which define thunniform swimming kinematics. Because the thunniform swimming mode is characterized by thrust being produced almost exclusively by the high aspect ratio lunate tail, the question then becomes: how is the internal force developed by the anteriorly-located muscle mass transferred across the narrow caudal peduncle to the tail blade, to produce external thrust? Anatomically, the prominent linkage is a set of robust tendons, formed from the converging myosepta of the posterior muscle, that course across the bony keel of the peduncle to join the “engine” with the “propeller” (Fig. 4.1). What is not known yet is how much force reaches the tail blade and in what way. The goals of this study were to quantify the forces empirically and then determine the function of the caudal tendons as force transmitters.

Ideally, to quantify total muscle force one would determine how much force each myotome develops when activated. In mammalian and avian systems, muscle force measurement is a fairly tractable problem, as each muscle has a discrete aponeurosis inserting across a joint to the bone to be moved. Force is measured by a transducer on the tendon or the bone and related to the muscle cross-sectional area (e.g., Biewener *et al.* 1988, 1992). Unfortunately, the complicated nesting of folded

myotomes in fish (and especially in tunas, where the myotomes are so elongated) makes this sort of direct force measurement impossible. Each myotome is linked to the vertebrae and skin via a complex combination of myosepta and anterior and posterior oblique tendons (Kafuku, 1950; Fierstine and Walters, 1968; Westneat *et al.* 1993). Because of this arrangement, one cannot quantify myotome force from a transducer on only one tendon, or even determine the muscle cross-sectional area involved in developing force on the skeleton. Furthermore, no single muscle connects to the tail blade, as the caudal tendons are formed by the concentric nesting of myosepta emanating from several posterior myotomes. It is the coordinated transfer of force by the series of myotomes onto skeleton, skin, myosepta, and caudal tendons that culminates in a sweep of the tail blade.

However, the caudal tendons in tunas experience a net force produced by all the myotomes. Therefore, measurements at those tendons provide estimates of the time course and quantity of internally generated force applied to the tail blade to produce external thrust. Tunas provide a unique opportunity for making such measurements because most fishes lack caudal tendons. By surgically implanting a buckle transducer around the deep caudal tendons overlying the peduncle, it was possible to measure forces directly as the tunas swam. The first portion of this study reports on force production as a function of swimming speed, and explores the temporal relationship between muscle activation and force development.

The second component of this study is concerned with characterizing the biomaterial properties of the caudal tendons, to deduce what role they perform as the

transmission linkage to the tail. Tendon is a remarkably conserved material throughout the animal kingdom, comprised of proteinaceous collagen fibers embedded in a mucopolysaccharide matrix (Alexander, 1988). As such, it is strong in tension, yet flexible. In nature, tendon serves one of two primary functions in linking muscle to skeleton: it either acts as a biological spring, by storing elastic strain energy, or it acts as an inextensible force linkage. Its role as an energy-storing spring is demonstrated in the limbs of many large terrestrial animals during fast gaits, such as hopping in kangaroos and running in ungulates such as camels and horses (Alexander, 1984). During foot-fall, kinetic and potential energy must be absorbed to decelerate the body. Instead of being dissipated as heat, much of this energy can be stored as elastic strain energy, absorbed in stretching leg tendons and then largely regained through elastic recoil to re-accelerate the body forward (Alexander, 1988). This saves the animal considerable amounts of metabolic energy.

Bennett *et al.* (1987) and Blickhan and Cheng (1994) considered a similar situation in their examinations of caudal tendon function in 2 species of cetaceans. Analogously to locomotory cycles in terrestrial animals, a dolphin loses potential and kinetic energy at the end of each tail stroke, before the tail reverses direction. The authors postulated that these animals might be able to decrease metabolic cost by storing strain energy in the tendons during deceleration of the fluke and using the recoil energy to help re-accelerate the tail during the next stroke. The two studies arrived at opposite conclusions: Bennett *et al.* (1987) concluded the tendon compliance actually made swimming more costly, while Blickhan and Cheng (1994)



concluded the animals could realize up to 50% metabolic cost savings. However, these widely differing conclusions were the result of not knowing the actual forces the cetacean tendons experience *in vivo*. The authors had to estimate forces based on external hydrodynamic predictions, and they used different assumptions in their calculations. This emphasizes the importance of the tendon buckle in the present study of swimming tunas. With *in vivo* measurements of tendon loading, it is possible to make a more accurate assessment of tendon function.

In general, the role of tendon as a biological spring is relatively uncommon in the animal kingdom. Most tendons in animals experience low stresses (force per unit cross-sectional area) and low strains (relative length change) *in vivo*, and thus act as inextensible force linkages rather than as springs (Ker *et al.* 1988). Because the material composition of tendon is relatively consistent among vertebrates, the key factor determining its function *in situ* is most dependent on its dimensions relative to the loading forces (Ker *et al.* 1988). For a given level of force, tendons that are long and thin experience high stresses and large extensions, and therefore store high levels of strain energy (energy = force x extension). This makes them effective springs. Short, thick tendons, on the other hand, are subjected to low stresses and strains and therefore act as relatively rigid force linkages because they absorb such little strain energy. In tunas, morphological examination reveals a large muscle mass linked to the tail blade by relatively short, robust tendons. Therefore, our prediction was that these tendons function as inextensible force linkages during swimming. However, because tunas are unusual among fishes in having tendons instead of muscle linking to

the tail, the possibility that they might be using these tendons as biological springs could not be overlooked. After all, the cost savings from such springs could be important in these continuous swimmers with high metabolic rates (Dewar and Graham, 1994).

To calculate how much energy a swimming tuna invests in loading its tendons, it is necessary to know not only the forces imparted by the muscle, but also how much the tendons are stretched as the tail sweeps through the water (energy = force x extension). Extension is determined by *in vitro* tensile testing as the tendons are mechanically loaded to the swimming forces. An assessment of *in vivo* tendon function is then made by comparing tendon strain energy with the total mechanical energy required for swimming (extrapolated from metabolic data of Dewar and Graham, 1994). If the amount of energy stored in the caudal tendons represents a large proportion of the total mechanical energy required for each tail sweep, then the tendons are acting as springs. Conversely, if very little energy is absorbed, then this indicates their role as inextensible force transmitters.

## Materials and Methods

### In vivo experiments:

Experimental protocol: Care and handling of fish, surgery, and swimming procedures in the water tunnel were all as described in Chapter 2. Experiments with the tendon buckle force transducer were done in conjunction with EMG electrodes and filming for kinematics. The buckle has been described previously by Biewener *et al.* (1988) and is pictured in the inset of Fig. 4.1. The buckle is fit around the 2 deep tendons such that the tendons pass behind the middle arm, on which the strain gauge is mounted (Fig. 4.1). During swimming, the tendons are pulled and released as the tail blade sweeps through the water. When in tension, the tendons compress the middle arm slightly, resulting in a decreased voltage output from the strain gauge. Voltages are later converted to forces after calibration (see below).

Fish instrumented with the caudal tendon buckle and EMG electrodes swam in the tunnel over whatever range of cruising speeds (powered only by the red, aerobic muscle) they would maintain steadily. It was also important to know the maximal forces a tuna might produce during burst swimming. Because none of the fish could be enticed into burst swimming when subjected to high water flows in the tunnel (see Chapter 2), a few were held gently behind the head, at the end of the experiment. This would prompt the fish to give short bouts of regular, rapid tailbeats at maximal effort (i.e., presumably with the majority of white muscle recruited), without injury.

After each experiment, the fish was euthanized by a sharp blow to the head and the buckle was calibrated with a second transducer while still on the tendons. The calibration procedures were similar in principle to those used by Biewener *et al.* in kangaroo rats (1988). First, all other skeletal and connective tissues were cut at the peduncle, so as to leave the deep tendons through the buckle as the only connection between the main body and the tail blade. A non-compliant string was tied to the tail and connected to the secondary transducer. While the fish's body was held stationary, recordings from both transducers were made as tension to the tendons was applied and released by pulling on the tail with the secondary transducer. Both transducers exhibited linear responses over the range of forces observed in these studies (as verified by calibration with a series of weights exceeding the range of *in vivo* forces). The secondary transducer was calibrated with known weights to convert its output voltages to forces in Newtons (N). Finally, the force response from the secondary transducer was plotted vs. the buckle voltages, and the slope of the resulting best fit line (using least squares linear regression) gave the conversion factor to transform buckle voltages from the swimming records to N. As commonly seen in mammalian tendons, there was very little difference between the loading and unloading curves, so the best fit line through both was used to generate the conversion factor (Biewener *et al.* 1988; Biewener, 1992).

After removing the buckle, the posterior third of the fish was ablated and frozen in tuna saline (1.17% NaCl) with all caudal tendons left *in situ* for subsequent *in vitro* biomaterials testing.

**Analysis:** The video records were first checked to verify that swimming was symmetrical. To determine forces transmitted by the tail tendons at different speeds, the voltage traces from 10-30 consecutive tailbeats during steady swimming bouts (as defined in Chapter 2) were converted to forces and averaged. When necessary, signals were first smoothed with a 10-point moving average. In the cases in which the Wheatstone bridge circuit did not balance at 0 volts, the voltage baseline (i.e., for zero force) was first zeroed before transforming values to N. (The voltage minimum between tailbeats was confirmed as representing zero force by comparing with brief periods when the fish glided.) From the recordings of restrained fish, 2 to 3 bouts of 5-15 consecutive tailbeats with the largest (but consistent) amplitude were chosen to calculate maximal caudal tendon forces.

To integrate the tendon force and EMG data, 3 of the 4 yellowfin and all 3 skipjack presented in Chapter 2 were used for the present study. In addition, another skipjack and 2 other yellowfin were analyzed to determine maximum forces.

**In vitro experiments:**

**Experimental protocol:** After determining the range of forces used by these tunas while swimming, their tendons were cycled mechanically in a tensile testing apparatus to determine the amount of strain experienced when subjected to these forces. The general protocol followed that of Lieber *et al.* (1991) and Pollock and Shadwick (1994). In most cases, the tendons from the right side of the fish (i.e., without the buckle) were used. After thawing in saline (1.17%), the superficial

tendinous sheath was separated from the pair of underlying deep tendons. Next, a section of one deep tendon between the pre-peduncular muscle and the tail blade was cut and removed (this span across the peduncle being where tendon diameter remains nearly constant). After clamping the ends into small aluminum blocks with serrated surfaces, markers (Letraset Letraline<sup>®</sup> tape, 1/16" wide) were glued with Vetbond<sup>™</sup> on either end of the tendon a short distance from the clamps. At all times, the tendon was kept moist by dribbling saline over it. The clamps were then attached to the pulling apparatus, with one held fixed and the other attached to the lever arm of a servo motor (Cambridge Technology, Inc., Series 300 B Lever System, with Model 6400 motor) such that the tendon was oriented in a horizontal position (Lieber *et al.* 1991).

The tendons were cycled sinusoidally to predetermined force limits (10 and 20 N) at rates of 0.5 or 1 Hz from a Macintosh computer using Super Scope II software, ver. 1.3 (GW Instruments, Somerville, MA). [Viscoelastic properties of tendons have been shown to be independent of extension rates between 0.05-11 Hz (Ker, 1981; Shadwick, 1990)]. Strain was measured between the two markers using a Sony CCD-IRIS (Model SSC-M354) video camera coupled to a video dimension analyzer (VDA) (Instrumentation for Physiology and Medicine, Model 303). Rest length ( $l_0$ ) of the tendon was set by imposing a slight pre-tension until there was no slack. The VDA was calibrated to  $l_0$  between the markers. Tendon force and strain signals were digitized onto the computer at 100 Hz per channel after first conditioning the tendons

by cycling 5-10 times to 10 N, until at least 5 consistent consecutive cycles were observed.

**Analysis:** Force and dimension records were imported into AcqKnowledge<sup>®</sup> software and smoothed using a 5-point moving average. The VDA applies a low-pass filter to the output, which introduces a delay to the dimension signal relative to force (in excess of that due to the tendon properties) (Gibbons and Shadwick, 1991). This was corrected by synchronizing the VDA traces with those of the motor lever arm. The most consistent 3-5 consecutive cycles within a record were exported to a spreadsheet, averaged, and plotted as force ( $F$ , in N) vs. tendon extension ( $l$ , in mm). These parameters were normalized to tendon dimensions to give stress ( $\sigma$ ) and strain ( $\epsilon$ ) [where  $\sigma$  (in Pa) = force divided by cross-sectional area (XSA, in  $m^2$ ) and  $\epsilon = \Delta l/l_0$ ]. To determine the XSA of the tendon, the distance between the markers was measured and that section was cut out, blotted dry, and weighed. Dividing mass (kg) by density ( $1,120 \text{ kg/m}^3$ ) and then length (m) gave XSA ( $m^2$ ) (Ker, 1981; Ker *et al.* 1988; Shadwick, 1990). Tendon extension was calculated by multiplying  $\epsilon$  by total tendon length *in situ* (from the anterior end of the keel to the attachment on the caudal fin rays). Energy (mJ) was found from the area under the  $F$  vs.  $l$  loading curve. Hysteresis (the proportion of strain energy lost as heat) was calculated from the difference in areas under the loading and unloading curves of  $\sigma$  vs.  $\epsilon$ . Because tendons have non-linear properties, the elastic modulus ( $E$ ) was determined from the tangent in the stiff region of the loading curve in the  $\sigma$  vs.  $\epsilon$  plots.

## Results

### Relationship between force and swimming speed:

With rare exception, the presence of the buckle force transducer on the caudal tendons did not seem to alter the fish's swimming behavior (as verified by comparing video records from instrumented and uninstrumented fish). In the few cases when erratic swimming was observed, *post mortem* dissection showed the lower (hypaxial) tendon to be worn at the middle arm of the buckle. Those cases were omitted from the present data set.

Fig. 4.2 illustrates typical force traces from a yellowfin and a skipjack. The even peak-to-peak time intervals and the consistent amplitudes indicate steady swimming. The relative timing of force development, peak, and relaxation within any given tailbeat remains constant, independent of swimming speed.

Fig. 4.3 shows the relationship between swimming speed and peak force per tailbeat for 3 yellowfin and 3 skipjack. The forces were measured by the buckle transducer from the pair of deep lateral tendons on the left side. Fig. 4.3A covers the range of cruising speeds achieved by each fish, while Fig. 4.3B shows the maximal forces produced by partially restrained fish. In all experiments, these fish preferred to cruise within a fairly restricted range of TBFs. Two of the 3 skipjack swam with higher TBFs than the rest of the fish; for these and for 1 yellowfin (TA 315), there is a trend of increasing force with increasing speed. For the remaining fish, there is no clear dependence of force on speed. The mean forces for most swimming bouts



clustered around one level for each individual, although that level varied between fish, most likely due to individual differences in total muscle cross sectional area contributing to force. The full span of peak tailbeat forces observed among all 6 fish at cruising speeds was about 3.2 N (a minimum of 1.1 N for TA 315 to a maximum of 4.3 N for KP 507).

The forces shown for 2 skipjack and 2 yellowfin in Fig. 4.3B are estimates of the maximum levels these tunas might produce during burst swimming, when the entire muscle mass (red and white) is recruited. TBFs ranged between 5 and 16 Hz, but are not shown due to the artificial nature of having to restrain the fish. The maximum forces were approximately one order of magnitude greater than those observed at cruising speeds. Even so, they likely underestimate what these fish could achieve when swimming unrestrained.

#### Relationship between muscle activation and tendon force development:

In Chapter 2, Fig. 2.6 showed a sample force trace superimposed over temporal muscle activation along the length of the body. A simplified version has been duplicated here for ease of reference (Fig. 4.4). Force begins to rise in the caudal tendons before the posterior muscle, from which they mostly originate, is even activated. In order to assess the importance of this observation, the percentage of peak force attributable only to activated anterior muscle was quantified. The EMG onset time at 0.65 L (an arbitrarily chosen posterior site) was used as the reference

point to delineate between active and not-yet-activated muscle. The results are presented in Table 4.1.

Activation of myotomal red muscle up to 0.65 L represents approximately 73% of the total muscle length (= 0.25-0.80 L), which correlates to 76% of the red muscle mass in yellowfin and 88% in skipjack (extrapolated from Graham *et al.* 1983). The results show that substantial force is registered at the caudal tendons (and, hence, the tail blade) before the posterior 24% or 12% (yellowfin and skipjack, respectively) of the muscle mass is even activated, let alone had time to develop force. Among the 6 fish, this force level ranges from 25% to 53% of peak force, with the average level equal to 35% for yellowfin and 37% for skipjack, independent of TBF. This is indirect evidence of the role of intermediate connective elements (e.g., skin, myosepta, oblique tendons) in transmitting the forces developed by the anterior muscle to the caudal tendons.

#### Biomaterial properties of tendons:

After the swimming experiments, the tendons were excised and cycled mechanically to determine the amount of extension caused by the *in vivo* forces. Normalizing force and extension to tendon dimensions gives stress ( $\sigma$ ) and strain ( $\epsilon$ ), of which sample curves are illustrated in Fig. 4.5 for 1 yellowfin and 1 skipjack. *In vivo* the tendons operate in a region of relatively low stiffness. The hysteresis loop in each curve shows the proportion of strain energy that is dissipated as heat, and is therefore unrecoverable as elastic recoil when the tendon is unloaded. The hysteresis

of the yellowfin tendon is 23%; that of the skipjack 17%. The elastic modulus ( $E$ , an indicator of stiffness) is 0.46 GPa for the yellowfin tendon and 0.58 GPa for the skipjack when cycled to a force of 10 N (which corresponds to a  $\sigma$  of 3.2 MPa in the yellowfin and 4.2 MPa in the skipjack).

Table 4.2 presents further details of tendon biomaterial properties at cruising forces. Note that *in vivo*, the buckle recorded forces from both deep tendons, whereas for the mechanical tensile tests, only one tendon could be tested at a time. Therefore, buckle force values were divided by 2 to reflect the forces experienced by 1 tendon. Two tendons were tested separately from each fish (in most cases, from the right side, which did not have the buckle. Results from only one tendon are given for KP507, as the other broke during testing). All fish were of similar forklength, so total tendon lengths were also quite similar. However, yellowfin tendons had greater XSAs than skipjack tendons: 3.0-4.0 mm<sup>2</sup> vs. 1.9-2.6 mm<sup>2</sup>. Because both species produced similar forces at cruising speeds, the thicker yellowfin tendons thus experienced less stress than the skipjack tendons (yellowfin range: 0.23-0.58 MPa; skipjack range: 0.48-0.79 MPa).

Strains exhibited by these tendons when loaded to the *in vivo* forces were very small (mostly less than 0.6%). The strains for different tendons were variable partly due to differences in XSA and partly due to the inherent arbitrary nature of defining rest length ( $l_0$ ). Before each experiment, a slight pre-tension was applied until the slackness was removed from the tendon, such that no sagging or buckling occurred during cycling. The amount of pre-tension, and hence  $l_0$ , varied from tendon to

tendon. However, slight differences in starting strains for different tendons are not important when calculating the amount of energy spent by each fish on stretching a tendon. This is because strain energy is derived from the area under the loading curve of force vs. extension; therefore, the flat region of the curve does not contribute significantly to the total area under the curve. The results in Table 4.2 (last column) show that only small amounts of energy are invested by the fish in the cyclic stretching of a tendon at steady, cruising speeds.

Table 4.3 shows stress, strain, and energy input when tendons were loaded to 19 N, which approximates the level of force experienced by a tendon during burst swimming (when all red and white muscle is recruited). Strains were only 3-4 times greater, even though stresses were an order of magnitude greater than for cruising swimming. These smaller strains relative to the greater stresses are indicative of the non-linear material properties of tendons, which become stiffer at higher stresses. The greater stiffness is also indicated by higher elastic moduli ( $E$ ) at the 19 N load:  $E$  ranged from 0.65-0.88 GPa in yellowfin and 0.91-1.17 GPa in skipjack (compared to the values of 0.46 GPa and 0.58 GPa for yellowfin and skipjack, respectively, calculated from a 10 N load, shown in Fig. 4.5). At burst swimming forces, the increased material stiffness required relatively more energy to stretch the tendons: a ten-fold increase in force from cruising to burst swimming required 26-35 times more energy input (except for TA315, which was 61 times greater).

## Discussion

### *In vivo* force measurements:

This study is the first to report direct measurements of internal forces generated by swimming muscle in an active fish. Although the tuna forces measured from the 2 deep tendons do not represent the total force reaching the tail blade (e.g., that from the superficial lateral tendons and skin is not included), they probably represent the major portion of it because the deep tendons comprise the largest portion of the XSA. Interestingly, the internal forces measured in these tunas are similar to the external forces on the tails of swimming bluefish (*Pomatomus saltatrix*), deduced by DuBois and Ogilvy (1978) from pressure recordings. These researchers attached pressure transducers to either side of the upper lobe of the tail fin to measure water pressure on the tail blade during its sweeps. Additionally, they placed forward and lateral accelerometers at the front edge of the first dorsal fin (near the body's pivot point for lateral undulation). Their results for this carangiform swimmer showed that body forces calculated from the accelerometers closely matched the forward component of force calculated from the tail pressure gauges, with values ranging between about 1 and 4 N for peak force (see their Table 1 and Fig. 4). This is the same range of forces registered by the internal buckle in the 6 tunas (Fig. 4.3). The bluefish (48-58 cm) were slightly larger than the tunas, but swam at similar speeds (range 0.3-0.9 m/s, mean of 0.48 m/s, using TBFs between 1.7 and 3.0 Hz).

Thrust forces have been calculated theoretically by Magnuson (1978) for a 40

cm kawakawa (*Euthynnus affinis*) swimming at 5 speeds (see his Table XI). This tuna is morphologically very similar to skipjack. For the 3 slowest speeds which overlap the skipjack speed range, 3.1 - 4.0 L/s, the calculated thrust forces were 0.96 - 4.2 N. These theoretical values, based on tail span and lateral velocity of the tail sweep, agree closely with the internal force measurements from the buckle in similarly sized skipjack in this speed range (Fig. 4.3), even though the TBFs of the kawakawa were twice those of the skipjack. While estimates of internal and external forces are not directly comparable, the similar results from 2 experimental approaches and 1 theoretical indicate that these force estimates are reasonable for fish of this size cruising at these speeds.

Another observation made possible by the buckle was the time course of force reaching the tail blade relative to activation state of the red muscle mass. A substantial amount of force (average 35% in yellowfin and 37% in skipjack) is transmitted to the tail blade by activation of the anterior muscle only-- that is, before the posterior 24% (yellowfin) or 12% (skipjack) of the red muscle mass is activated (based on EMG onset at 0.65 L, Table 4.1). If one further assumes a time delay between activation and beginning of force development of about 5 ms (unpublished results from preliminary muscle twitch studies), that means that the caudal force is actually coming from a slightly shorter span of muscle, between 0.25 L and 0.61 L (or 68% of the muscle mass) in yellowfin and between 0.25 L and 0.63 L (85% of the muscle mass) in skipjack. This suggests that there must be inter-connective tissue linkages [such as among skin, myosepta, oblique tendons, and vertebrae (Wainwright,

1983; Westneat *et al.* 1993)] that transmit forces produced by the anteriorly located muscle to the caudal tendons, without the posterior muscle being active. In other words, the impression often presented in the literature on axial fish locomotion that body bending is the result of myotomes pulling on successive myotomes when they shorten must be incorrect, at least in fish like tunas. As in mammalian and avian systems, fish muscle ultimately acts through tendons on bone, even though the complicated folding of myotomes makes this difficult to visualize. The unique ability to integrate muscle activation data with caudal force measurements in tunas has elegantly demonstrated that force transmission down the body is more complicated than might be apparent at first glance. The largest cross section of the body's muscle mass is situated forward on the body-- too far away to contribute directly to the nested myosepta that form the caudal tendons. Yet it is this large bulk which must contribute the greatest amount of force to power swimming. Therefore, it is reasonable to expect that the tuna body design would include other transmission elements besides the caudal tendons for transferring the anteriorly-generated force to the tail. The observation that force rises in the caudal tendons before the posterior muscle has been activated is the first experimental evidence to demonstrate this.

#### Calculation of tendon strain energy *in vivo* and its possible importance:

The buckle force measurements provided one piece of information necessary to assess the possible role of the caudal tendons in swimming. The other information required for this assessment, tendon extension, was obtained by *in vitro* mechanical

testing. Estimates of strain energy stored in the tendons were compared with the total mechanical energy output during each tail sweep (Table 4.4). Tendon strain energy for each fish was averaged from the values shown in the last column of Table 4.2. To estimate the total strain energy stored on one side, this value was tripled, to account for the 2nd deep tendon and the pair of superficial lateral tendons (which together have a XSA roughly equivalent to one deep tendon).

To estimate the total mechanical energy spent per tail sweep during swimming, the net cost of transport (COT) of 1.58 J/L derived by Dewar and Graham (1994) for similarly sized yellowfin (51 cm) swimming at 2 L/s was used. (The net COT is the total cost to travel a unit distance, minus the component attributable to standard metabolic rate, and as such is an estimate of energy spent on locomotion.) Multiplying net COT by mean swimming velocity ( $U$ , in L/s) gave total power input, which was then converted to mechanical power output by assuming a combined metabolic and mechanical efficiency of 25% (Bone *et al.* 1995). Finally, multiplying mechanical power by the duration of the tail sweep (a tail stroke from one side to the other) gave total mechanical energy output per sweep.

The percent of total mechanical energy used per tail sweep to stretch the tendons is very small: in all cases less than 0.5% (Table 4.4, last column). These low percentages indicate that the tunas are not storing energy in the caudal tendons and then recouping that strain energy from elastic recoil to move the tail. Rather, the caudal tendons are being used as an inextensible, direct transmission linkage to transfer muscle force to the tail.



This is probably not a surprising result for a relatively small animal which swims through a fluid medium where no ground reactive forces are available. Energy storage in the tendons of certain large terrestrial mammals (e.g., ungulates, kangaroos) is cost effective because these animals can use the impact of the foot against the ground as an external energy source to load (stretch) the tendons, and then get much of this stored strain energy back by elastic recoil as the foot leaves the ground. The metabolic cost savings can be greater than 50% at high speeds (e.g., in running humans and hopping kangaroos) (Alexander, 1984). Fish, on the other hand, do not have an analogous external source of energy available to them in their environment. Any tendon loading to store energy would have to be provided by their own musculature. There are inconclusive theoretical interpretations as to whether this mechanism would nevertheless offer cost savings in cetaceans (Bennett *et al.* 1987; Blickhan and Cheng, 1994), which propel themselves via vertical sweeps of a horizontal fluke. However, in the case of the tunas, the experimental evidence is more clear: there is not enough energy being stored in the caudal tendons to represent any cost savings. These fish, swimming by means of lateral sweeps of a vertical tail fin, are better served by the tendon's role as a relatively rigid force transmitter, and the biomaterial properties further reflect this function.

*In vitro* biomaterial properties: comparison of tuna and mammalian tendons:

During aerobic swimming, the caudal tendons in yellowfin and skipjack operate in the region of relatively low stiffness on their stress-strain curves (Fig. 4.5).

When loaded to an estimated burst swimming force of 19 N (approximately an order of magnitude greater than the cruise swimming forces), they typically experienced stresses of between 4 and 10 MPa and strains of 1.4-1.6 % (TA315 falls somewhat outside these ranges). These stress values are similar to the average of 13 MPa found for maximum *in vivo* stresses experienced by a broad range of mammalian limb tendons which are not used as springs, such as digital extensors (Ker *et al.*, 1988). In addition, the elastic modulus of these tuna tendons ranged from 0.65-1.17 GPa, while the hysteresis (H) ranged between 7 and 12% (except one at 25 %), indicating that relatively little energy is lost as heat during a loading/unloading cycle (Table 4.3). These biomaterial properties are again similar to those observed in limb tendons from a diverse sampling of adult mammals tested by Pollock and Shadwick (1994) (average H of 9.3% and E of 1.22 GPa). The only factor in which tuna tendon differs somewhat from mammalian is the magnitude of strain, which is less in the tuna tendons [average of 1.5% between 6-10 MPa vs. an average of 2.5% for a typical mammalian tendon subjected to the same  $\sigma$  (Pollock and Shadwick, 1994)].

The biomaterial properties and dimensions of these tuna tendons are consistent with the theory of Ker *et al.* (1988) which predicts that for a tendon to act as an effective, inextensible force linkage, it should be short and thick relative to the forces imposed, such that it will operate under conditions of low  $\sigma$  and  $\epsilon$ . These operating conditions have now been demonstrated in yellowfin and skipjack, in which tendon XSAs are large relative to the swimming forces. The result is that the tendon itself absorbs very little energy, so that a larger proportion of the muscle force is

directed to the tail to produce external thrust. This direct transmission linkage also provides better control across the joint to move the tail blade. If the tendon had been designed to store energy, by having dimensions to make it more extensible (i.e., long and thin relative to the swimming forces), the trade-off in possible energy savings would have been a loss of tail control, as much muscle shortening would be lost through tendon compliance.

This study's findings concerning caudal tendon function suggest some explanations for why the tuna body plan incorporates tendon instead of muscle to transmit force across the peduncle to the tail. Thick tendons are more effective energy transmitters than muscle, so more of the force developed by the anteriorly-located engine makes it to the propeller. The bony keel increases the mechanical advantage for this force transfer by allowing the tendons to act as pulleys (as suggested by Fierstine and Walters, 1968). To use muscle as a force transmitter in the same capacity requires that it be stiffened, which is achieved by activating it while under tension. This is metabolically more expensive than using tendons. Tendons are also much more space-efficient, allowing the narrowest possible area for the caudal peduncle in front of the tail blade, thereby minimizing resistance to water flow during tail sweeps. Taken as a whole, using this mechanical system of tendons as inextensible force transmitters is no doubt an important factor in enabling these tunas to achieve such high speeds during burst swimming, as well as to travel such long distances efficiently during sustained, cruising swimming.

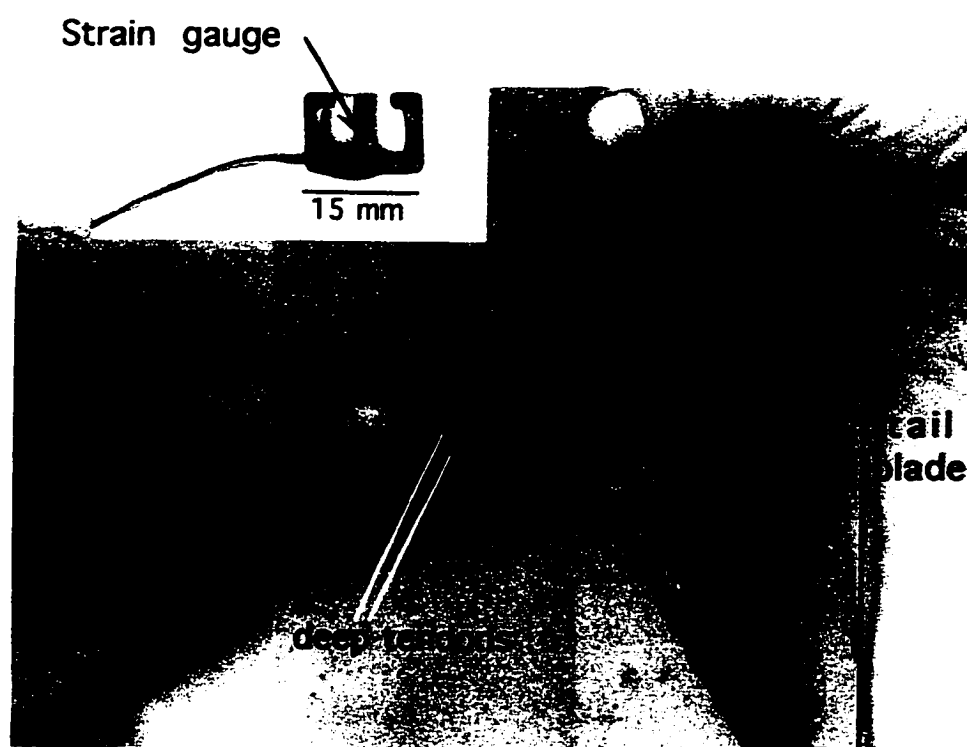
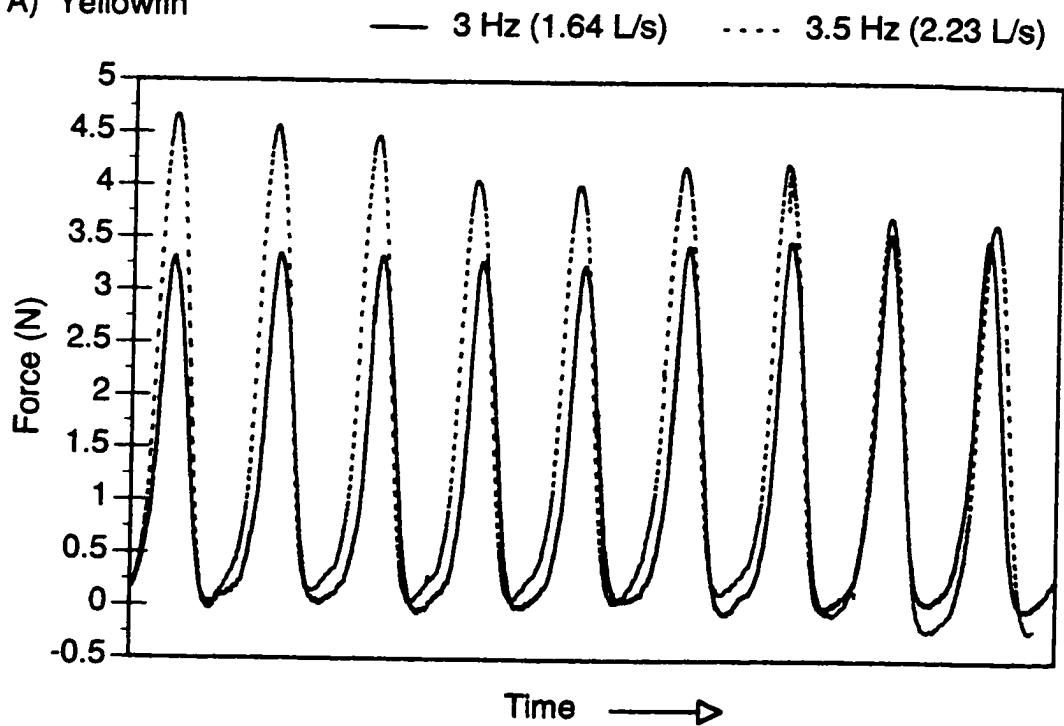


Fig. 4.1: *Post mortem* photograph showing how the buckle force transducer (shown enlarged in inset) fits around the pair of deep tendons traversing the caudal peduncle on the left side. (The skin and superficial tendons have been reflected to expose the underlying structures.)

**Fig. 4.2:** Representative tendon buckle force traces from a 43 cm yellowfin (A) and a 41 cm skipjack (B). Swimming bouts at 2 different speeds are shown for each fish. (The time base has been adjusted to tailbeat period, in order to overlay signal traces.)

A) Yellowfin



B) Skipjack

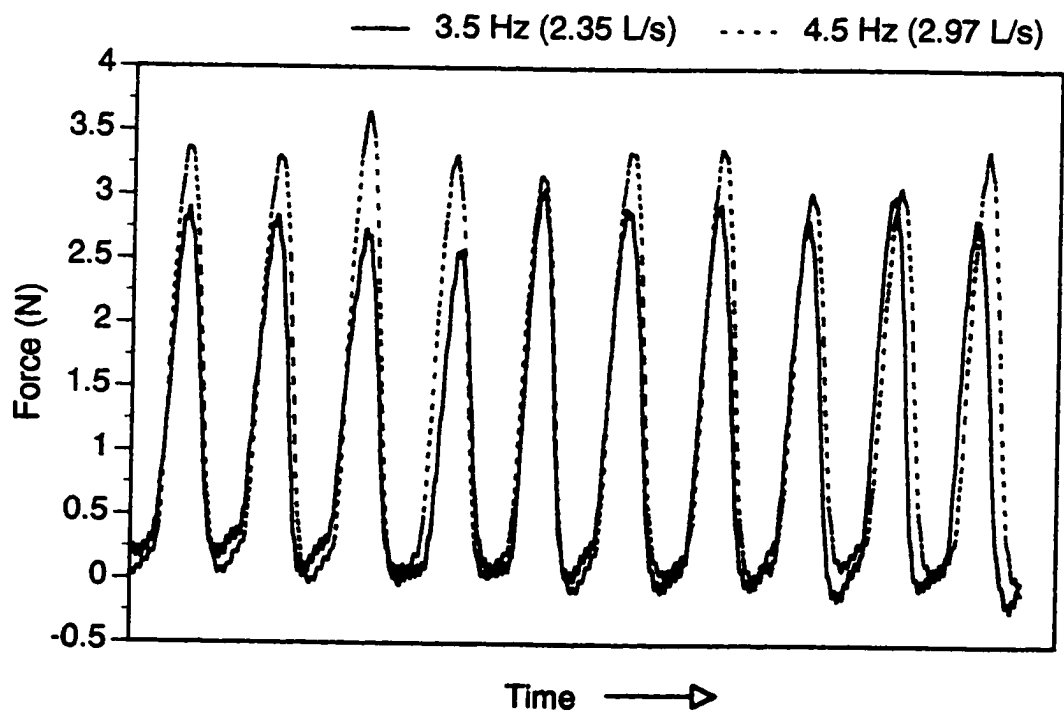


**Fig. 4.3:** Peak caudal tendon forces registered by the buckle transducer during sustained, cruising swimming (A) and restrained burst swimming (B). Force data are from the pair of deep tendons on the left side. Yellowfin are shown in blue; identification labels begin with TA (for *Thunnus albacares*). Skipjack are in red and are labeled with KP (for *Katsuwonus pelamis*). Numbers in parentheses under fish labels are forklength and mass (N/A: mass not available for TA 401). The 2 plots in A show the same force data plotted against swimming speed expressed as either TBF or L/s. Swimming speed is not indicated in B due to the necessity of restraining the fish. Points and error bars are means and standard deviations from 10-30 consecutive tailbeats in A; 5-15 tailbeats in B. The lines in A are the best fits by least squares linear regression.

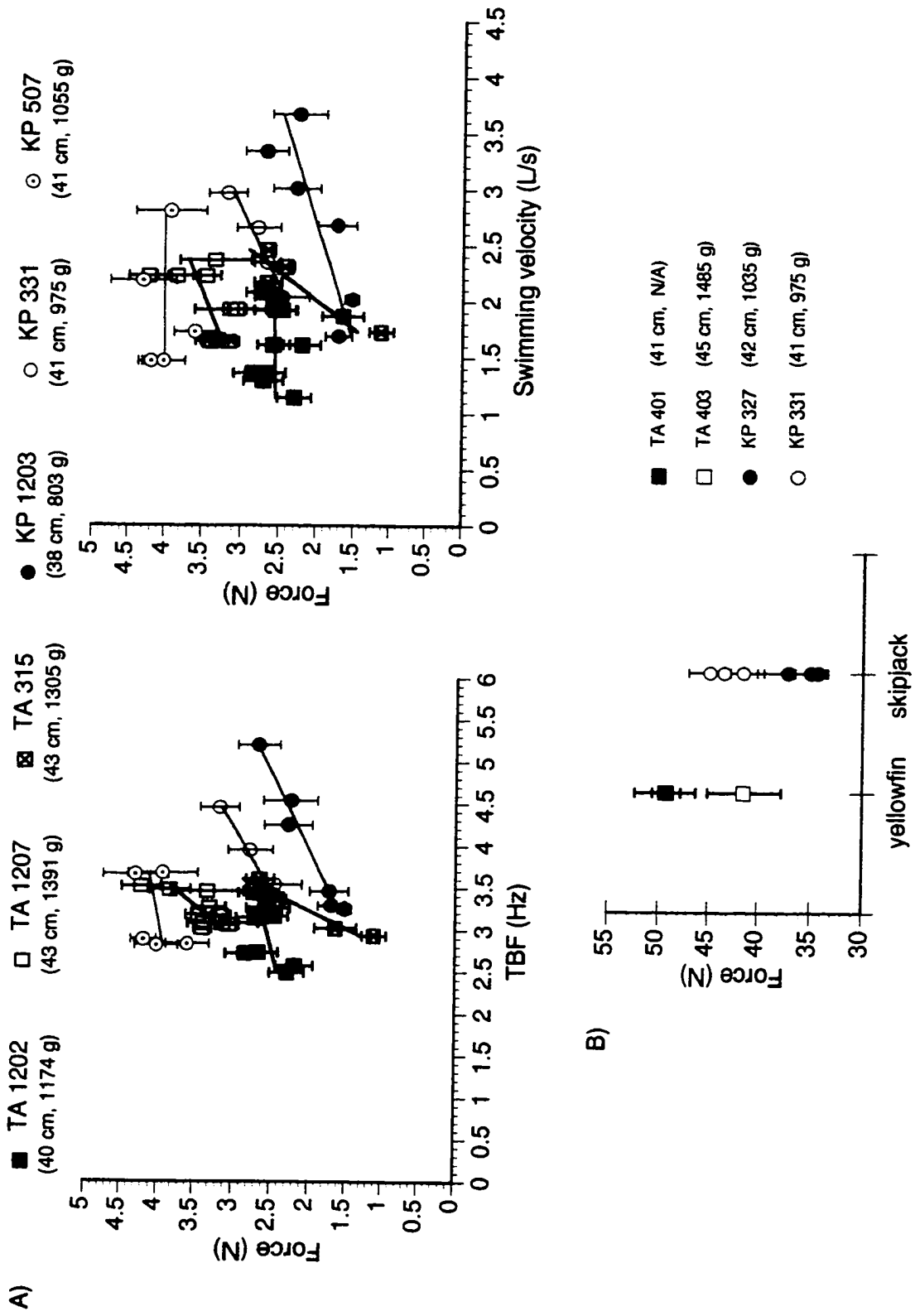
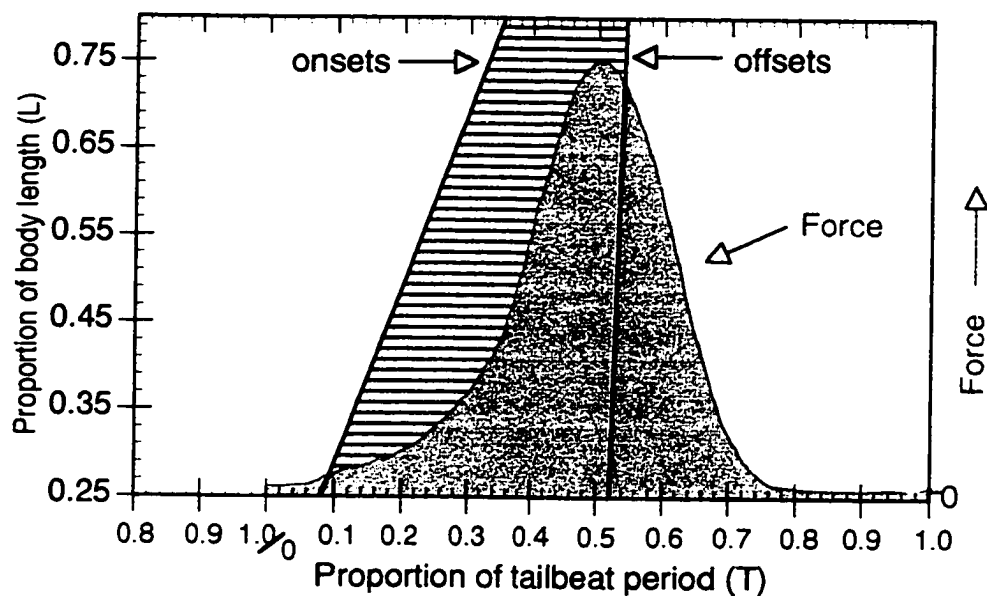




**Fig. 4.4:** Summary of muscle activation patterns for yellowfin (A) and skipjack (B), with superimposed force traces. (See Fig. 2.6 for details.)

**A) Yellowfin:**



**B) Skipjack:**

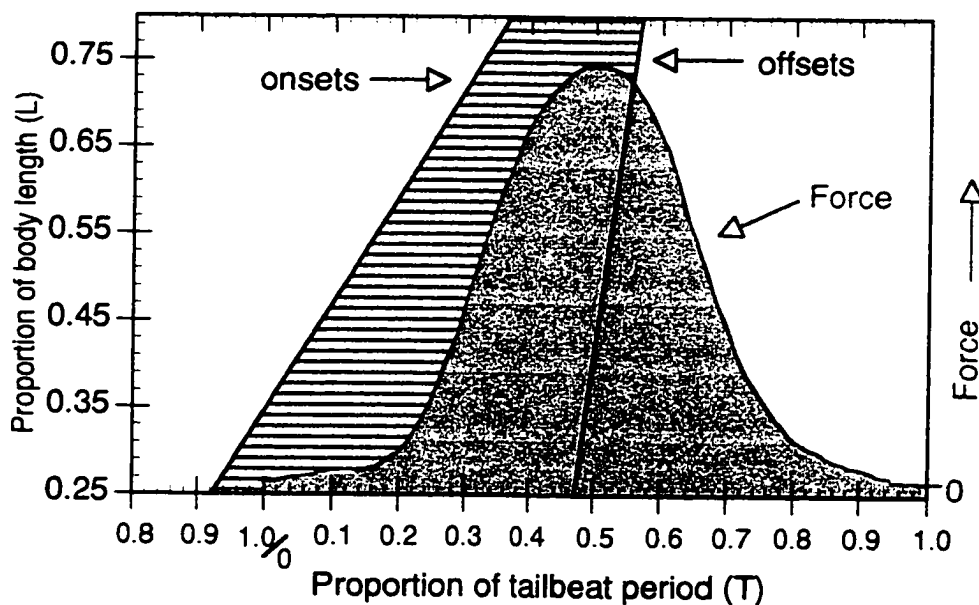


**Table 4.1:** Percentage of peak force registered in the caudal tendons prior to activation of red muscle at 0.65 L. Onset of muscle activation at 0.65 L was determined from the linear regression line of EMG onsets between 0.25 L and 0.80 L, for all fish across all speeds, from the data used in Fig. 4.4. Onset time at 0.65 L is expressed in the table as proportion of a tailbeat period (T) following peak force from the previous tailbeat. From swimming bouts at the slowest and fastest TBFs, forces at 0.65 L onset time were determined from 10-16 tailbeats and averaged (standard deviations shown in parentheses). (Forces were additionally determined at mid-range TBFs for 2 yellowfin.) Finally, the last column shows the average force level occurring at 0.65 L onset time as a percentage of the peak force per tailbeat.

Fish ID	TBF (Hz)	Time of 0.65 L onset (T)	Mean force (N) at 0.65 L onset (Std. Dev.)	Number of tailbeats	Mean peak force (N)	Percent peak force registered before 0.65 L onset
<b>Yellowfin:</b>						
TA1202	2.5	0.80	1.22 (.22)	15	2.30	53
	2.7	"	1.35 (.20)	15	2.68	50
	3.4	"	0.99 (.14)	10	2.74	36
TA1207	3.1	0.79	0.85 (.11)	10	3.06	28
	3.2	"	1.07 (.10)	10	3.45	31
	3.5	"	1.31 (.29)	10	4.23	31
TA315	2.9	0.78	0.28 (.07)	10	1.12	25
	3.6	"	0.74 (.11)	10	2.66	28
<b>Skipjack:</b>						
KP1203	3.3	0.73	0.48 (.11)	16	1.53	32
	5.2	"	1.11 (.30)	16	2.69	41
KP331	3.5	0.74	0.84 (.24)	16	2.91	29
	4.5	"	1.00 (.25)	15	3.43	29
KP507	2.8	0.78	1.68 (.12)	10	4.02	42
	3.7	"	1.91 (.30)	14	3.94	48

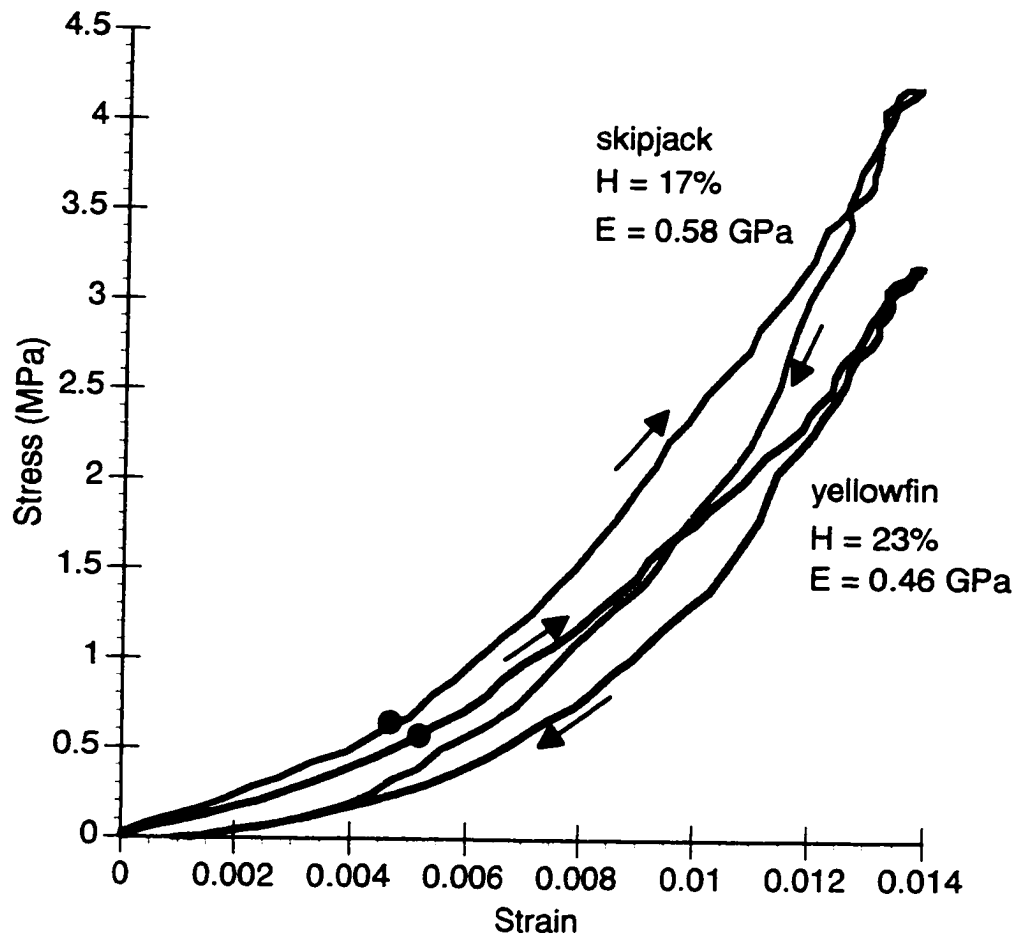


Fig. 4.5: Sample stress vs. strain curves for a caudal tendon from 1 yellowfin (blue) and 1 skipjack (red). The dot on each loading curve shows the stress and strain corresponding to forces experienced by a tendon during sustained, cruising swimming. Arrows indicate loading and unloading; the area within each enclosed loop represents hysteresis (H). The elastic modulus (E) is determined from the tangent slope in the stiff region of each loading curve. The loop for the yellowfin is an average of 5 loading/unloading cycles; that of the skipjack, 4 cycles.

**Table 4.2:** Biomaterial properties of the caudal tendons when mechanically loaded to the average *in vivo* forces measured during cruising.

<sup>a</sup> Measurements were made from the anterior end of the keel (where muscle is just ending) to the tendon attachment site on the caudal fin rays.

<sup>b</sup> Average from all tailbeats, across all speeds (same data set used in Chapter 2). Since tendon buckle recordings were from the pair of deep tendons, values have been divided by 2 to represent forces transmitted by only 1 tendon.

<sup>c</sup> Cross-sectional area of the tendon clamped into the mechanical pulling device, between the 2 markers (where diameter is nearly constant).

<sup>d</sup> Extension is an estimate of how much the whole tendon stretches in the fish when loaded to the average swimming force: i.e., total tendon length \* strain.

Averages and standard deviations of strain were derived from 3-5 consecutive mechanical loading cycles in the tensile testing apparatus.

Fish ID	Tendon ID	Total tendon length in fish* (mm)	Mean force (N) during sustained swimming <sup>b</sup> (Std. Dev.)	Mean TBF (Hz) (Std. Dev.)	XSA <sup>c</sup> (mm <sup>2</sup> )	Stress at <i>in vivo</i> force (MPa)	Strain (% $\epsilon$ ) (Std. Dev.)	Extension <sup>d</sup> (mm)	Energy required to stretch tendon to <i>in vivo</i> force (mJ)	
Yellowfin:	TA1202	R epaxial	43.1	1.28 (.11)	2.97 (.34)	3.2	0.40	0.26 (.026)	0.11	0.082
		L epaxial				3.3	0.39	0.28 (.012)	0.12	0.087
		R epaxial	49.6	1.72 (.18)	3.23 (.19)	4.0	0.43	0.61 (.018)	0.26	0.146
		L epaxial				3.0	0.38	0.57 (.016)	0.24	0.132
TA315	R hypaxial	53.4	1.09 (.32)	3.30 (.27)	3.6	0.43	0.36 (.024)	0.18	0.157	
	R epaxial				3.0	0.43	0.38 (.018)	0.19	0.161	
					3.0	0.56	0.55 (.022)	0.27	0.219	
					3.0	0.56	0.50 (.012)	0.25	0.201	
Skipjack:	KP1203	R epaxial	36.5	1.02 (.23)	4.00 (.79)	1.9	0.32	0.04 (.024)	0.02	0.012
		L epaxial				4.5	0.31	0.05 (.011)	0.03	0.015
		R hypaxial	45.9	1.49 (.19)	3.87 (.44)	2.3	0.23	0.15 (.005)	0.08	0.039
		R epaxial				2.4	0.24	0.14 (.014)	0.07	0.042
KP507	R hypaxial	45.1	2.01 (.14)	3.18 (.45)	2.6	0.66	0.58 (.032)	0.21	0.110	
					2.1	0.52	0.50 (.033)	0.18	0.086	
					2.3	0.48	0.24 (.038)	0.09	0.056	
					2.4	0.48	0.23 (.030)	0.08	0.044	
KP331	R hypaxial	45.9	1.49 (.19)	3.87 (.44)	2.3	0.65	0.48 (.031)	0.22	0.169	
					2.4	0.64	0.42 (.022)	0.19	0.142	
					2.4	0.65	0.35 (.024)	0.16	0.113	
					2.6	0.63	0.37 (.018)	0.16	0.129	
KP507	R hypaxial	45.1	2.01 (.14)	3.18 (.45)	2.6	0.78	0.25 (.017)	0.11	0.131	
					2.6	0.79	0.28 (.023)	0.13	0.130	

Fish ID	Tendon ID	Total tendon length in fish (mm)	XSA (mm <sup>2</sup> )	Stress at 19 N force (MPa)	Strain (% / $\sigma$ ) (Std. Dev.)	Extension (mm)	Energy required to stretch tendon to 19 N force (mJ)	Hysteresis (%)	Elastic modulus (GPa)	
<b>Yellowfin:</b>	TA1202	L epaxial	43.1	3.3	5.77	1.61 (.027)	0.69	3.69	25	0.84
	TA1207	L epaxial	49.6	3.0	6.39	1.57 (.014)	0.78	5.50	12	0.65
	TA315	R epaxial	53.4	4.5	4.18	0.58 (.022)	0.31	2.50	11	0.88
<b>Skiftack:</b>	KP1203	R epaxial	36.5	1.9	10.01	1.50 (.004)	0.55	3.36	7	1.17
	KP331	R epaxial	45.9	2.4	7.92	1.39 (.012)	0.64	4.27	10	0.91

**Table 4.3: Biomaterial properties of caudal tendons when mechanically loaded to 19 N, which approximates maximal burst swimming forces. Averages and standard deviations of strain were derived from 3-5 consecutive mechanical loading cycles in the tensile testing apparatus.**



Fish ID	Forklength (L) (cm)	Mean tendon force (N) during sustained swimming (1 tendon)	Mean energy (mJ) required to stretch tendon to swimming force	Estimated energy (mJ) to stretch all tendons on one side <sup>a</sup>	Mean swimming velocity (U) (L/s)	Mean TBF (Hz)
Yellowfin:						
TA1202	40	1.28	0.112	0.336	1.6	2.97
TA1207	43	1.72	0.191	0.573	2.0	3.23
TA315	43	1.09	0.027	0.081	2.1	3.30
Skipjack:						
KP1203	38	1.02	0.074	0.222	2.7	4.00
KP331	41	1.49	0.138	0.414	2.5	3.87
KP507	41	2.01	0.131	0.393	2.1	3.18
Duration (s) of one tail sweep						
Yellowfin:			Metabolic power input (=net COT x U) <sup>b</sup> (x 1000 = mJ/s)	Mechanical power output (metabolic power input x 25% efficiency)	Mechanical energy (mJ) output per tail sweep	Percent of mechanical energy output per tail sweep spent on stretching tendons
TA1202	0.168	2528	632	106	0.32	
TA1207	0.155	3160	790	122	0.47	
TA315	0.152	3318	830	126	0.06	
Skipjack:						
KP1203	0.125	4266	1067	133	0.17	
KP331	0.129	3950	988	128	0.32	
KP507	0.157	3318	830	130	0.30	

Table 4.4: Data used to calculate the total mechanical energy output per tail sweep, and the percent of this energy output invested in loading the caudal tendons during cruising.

<sup>a</sup> Energy calculated for 1 deep tendon was tripled to estimate total energy including the second deep tendon and the superficial lateral tendons.

<sup>b</sup> Metabolic power input was based on the net cost of transport (net COT) calculated by Dewar and Graham (1994) for a 51 cm yellowfin swimming at 2 L/s: 1.58 J/L.

## References

- Alexander, R. M. (1984). Elastic energy stores in running vertebrates. *Amer. Zool.* **24**, 85-94.
- Alexander, R. M. (1988). *Elastic Mechanisms in Animal Movement*. New York, etc.: Cambridge University Press.
- Bennett, M. B., Ker, R. F. and Alexander, R. M. (1987). Elastic properties of structures in the tails of cetaceans (*Phocaena* and *Lagenorhynchus*) and their effect on the energy cost of swimming. *J. Zool., Lond.* **211**, 177-192.
- Biewener, A. A. (1992). In vivo measurement of bone strain and tendon force. In: *Biomechanics-Structures and Systems* (ed. A. A. Biewener), pp. 123-148. Oxford, New York, Tokyo: Oxford University Press.
- Biewener, A. A., Blickhan, R., Perry, A. K., Heglund, N. C. and Taylor, C. R. (1988). Muscle forces during locomotion in kangaroo rats: force platform and tendon buckle measurements compared. *J. exp. Biol.* **137**, 191-205.
- Biewener, A. A., Dial, K. P. and Goslow, G. E., Jr. (1992). Pectoralis muscle force and power output during flight in the starling. *J. exp. Biol.* **164**, 1-18.
- Blickhan, R. and Cheng, J.-Y. (1994). Energy storage by elastic mechanisms in the tail of large swimmers- a re-evaluation. *J. theor. Biol.* **168**, 315-321.
- Bone, Q., Marshall, N. B., and Blaxter, J. H. S. (1995). *Biology of Fishes*. London, etc.: Blackie Academic and Professional.
- Dewar, H. and Graham, J. B. (1994). Studies of tropical tuna swimming performance in a large water tunnel: I. Energetics. *J. exp. Biol.* **192**, 13-31.
- DuBois, A. B. and Ogilvy, C. S. (1978). Forces on the tail surface of swimming fish: thrust, drag, and acceleration in bluefish (*Pomatomus saltatrix*). *J. exp. Biol.* **77**, 225-241.
- Fierstine, H. L. and Walters, V. (1968). Studies in locomotion and anatomy of scombroid fishes. *Memoirs of the Southern California Academy of Sciences* **6**, 1-31.

- Gibbons, C. A. and Shadwick, R. E. (1991). Circulatory mechanics in the toad *Bufo marinus*. II. Haemodynamics of the arterial windkessel. *J. exp. Biol.* **158**, 291-306.
- Graham, J. B., Koehn, F. J. and Dickson, K. A. (1983). Distribution and relative proportions of red muscle in scombrid fishes: consequences of body size and relationships to locomotion and endothermy. *Canadian Journal of Zoology* **61**, 2087-2096.
- Kafuku, T. (1950). "Red muscles" in fishes. I. Comparative anatomy of the scombrid fishes of Japan. *Jap. J. Ichthyol.* **1**, 89-100.
- Ker, R. F. (1981). Dynamic tensile properties of the plantaris tendon of sheep (*Ovis aries*). *J. exp. Biol.* **93**, 282-302.
- Ker, R. F., Alexander, R. M. and Bennett, M. B. (1988). Why are mammalian tendons so thick? *J. Zool., Lond.* **216**, 309-324.
- Lieber, R. L., Leonard, M. E., Brown, C. G. and Trestik, C. L. (1991). Frog semitendinosus tendon load-strain and stress-strain properties during passive loading. *Am. J. Physiol.* **261**, C86-C92.
- Magnuson, J. J. (1978). Locomotion by scombrid fishes: hydromechanics, morphology, and behavior. In *Fish Physiology*, Vol. VII (ed. W. S. Hoar and D. J. Randall), pp. 239-313. New York, etc: Academic Press.
- Pollock, C. M. and Shadwick, R. E. (1994). Relationship between body mass and biomechanical properties of limb tendons in adult mammals. *Am. J. Physiol.* **266**, R1016-R1021.
- Shadwick, R. E. (1990). Elastic energy storage in tendons: mechanical differences related to function and age. *J. Appl. Physiol.* **68**, 1033-1040.
- Wainwright, S. A. (1983). To bend a fish. In: *Fish Biomechanics* (ed. P. W. Webb and D. Weihs), pp. 68-91. New York: Praeger Publishers.
- Westneat, M. W., Hoese, W., Pell, C. A. and Wainwright, S. A. (1993). The horizontal septum: mechanisms of force transfer in locomotion of scombrid fishes (Scombridae, Perciformes). *Journal of Morphology* **217**, 183-204.

## Chapter 5: Summary and conclusions

This work has integrated electromyography, kinematics, and caudal tendon function in two species of tuna to describe the dynamic physiological design features underlying the thunniform swimming mode. For the first time, temporal red muscle activation patterns have been described in yellowfin and skipjack swimming at steady, cruising speeds. The kinematic spectrum of swimming modes used by a wide variety of fishes from eels to tunas is reflected in a parallel spectrum of underlying EMG patterns. In this continuum from whole-body undulations to more oscillatory motions focused at the posterior end of the body, the tuna EMGs are consistent with a pattern that is more derived relative to the carangiform mode, and at the opposite extreme from the anguilliform mode. In the tunas, muscle activation for each tail sweep proceeds sequentially down one side of the body, while deactivation is nearly simultaneous at all muscle sites. The propagation rate of the activation wave in thunniform locomotion is faster than that exhibited in the other swimming modes--fast enough, in fact, to allow all muscle activation on one side to be completed during a tail sweep in the yellowfin, and nearly so in the skipjack, which has a slightly slower activation rate than the yellowfin. In both species, all muscle on a side is active simultaneously for part of the sweep. Because there is little or no simultaneous contralateral activation, undulation of the body is minimized compared to other swimming modes, and muscle force is directed rearward almost exclusively to the tail.

One of the most novel and important aspects of this research has been the successful measurement of internal muscle forces using a force transducer fitted onto the caudal tendons. Relating muscle activation to force development has shown that in both yellowfin and skipjack, force peaks at the caudal tendons on one side just as the muscle mass on that side is deactivated. Taken in consideration with the minimization of contralateral activity, this suggests that the tuna mechanism is approaching a system in which force development in muscle all down the body is synchronized to deliver an instant of maximal force at the tail. Furthermore, a substantial amount of force develops at the tail before the posterior muscle has been activated, indicating the importance of other tissue interconnections among muscle, myosepta, oblique tendons, skin, and vertebrae in directing anteriorly-generated muscle force to the tail. This design is at the extreme opposite end of the spectrum from eels, in which muscle activation waves are present simultaneously on much of the left and right sides, producing a highly undulatory swimming mode in which sequential segments of the body push in series directly against the water to propel the fish forward.

Kinematic analysis of yellowfin and skipjack swimming has shown several features of their movements to be similar to those reported for many other fishes (e.g., stride length,  $\lambda_b$ , and amplitude envelopes of midline curvature and lateral displacement that increase posteriorly). However, synthesis of kinematics and electromyography in swimming tunas reveals facets of the thunniform swimming mechanism which are quite different from other fishes. For example, midline

curvature has been used extensively in other species as an accurate predictor of local superficial muscle strain. In contrast, the finding in tunas that local muscle activation at any site occurs after the midline has reached maximum convexity suggests that curvature cannot be used to predict local muscle strain in the nested myotome cones of red muscle. The most likely explanation is that activation of the highly elongated myotomes in these tunas results in backbone bending at more posterior locations. Tuna morphology lends support to this idea, as the greatest cross sectional area of the force-producing muscle mass is located anteriorly, far removed from the thrust-producing “propeller”. The highly elongated myotomes in yellowfin and skipjack (spanning 13 and 17 vertebrae, respectively) are important adaptations for directing the muscle force far down the body. The myotomal red muscle in tunas has proved to be an ideal model for bringing to light some of the functional differences between bending caused by contractions within the myotome cones vs. those within the lateral wedge of superficial muscle. Ultimately, though, experimental determination of muscle strain in tuna myotomes, and subsequent inferences concerning dynamic muscle function, await future studies using sonomicrometry.

Another feature contrasting tunas from other “tailed” fishes (i.e., those with a discernible caudal fin) is that the propagating EMG and midline curvature waves travel down the tuna body at the same rate. In other tailed fishes, curvature lags activation, which has led to predictions in the literature that muscle function will vary down the body: varying amounts of net positive or negative work will be produced because activation will occur at different phases within the muscle’s strain cycle.

However, in fishes without tail blades, such as eels and lampreys, activation and curvature propagate at about the same rate, which in turn fosters a train of locally-produced thrust in which sequential sections of the body push directly against the water. For swimming modes in which less of the body is used to push against the water (subcarangiform, carangiform modes), varying degrees of force transfer from front to back are required to focus thrust at more posterior regions of the body. These modes still incorporate some undulatory movements of the body but use increasing amounts of oscillatory movements posteriorly. In these situations, the wave of muscle activation travels more quickly than the curvature wave, and so muscle at different axial sites may produce net positive work or may serve as a force transmitter (negative work) to direct force rearward. In the thunniform mode, however, thrust is focused almost exclusively at the tail, while the activation patterns minimize undulation of the rest of the body. Hence, the activation wave no longer propagates more quickly than the curvature wave. In essence, the whole body now acts in much the same way as a single segment within a tail-less fish. Activation is nearly instantaneous down the length of a tuna, resulting in an instant of maximal thrust by the tail propeller on the water. All muscle is predicted to function in the same way, independent of axial location. Production of net positive work all down the body would maximize thrust at the tail blade, which would support the high speeds these fish are capable of achieving.

Coupling empirical force measurements with kinematics has demonstrated that peak caudal tendon force in a tail sweep of the yellowfin occurs as the tip is

crossing the swimming track, while in the skipjack peak force occurs later in the sweep, when the tip is about half way from the swimming track to its farthest lateral excursion. Before this study with the tendon transducer, it had not been possible to determine at what position in the tail sweep peak force would occur. It has been theorized that it should occur as the tip reaches its maximal velocity, while crossing the swimming track, half way through the sweep before having to reverse direction. For yellowfin this prediction has turned out to be true. The later phase in the skipjack tail sweep can best be explained by differences in tail morphology. The sweepback angle is less in the skipjack tail, so the distance from the peduncle to the location of thrust production is shorter than in the yellowfin. Hence, the tail tip has already moved farther across the swimming track when peak force is registered. More data are needed before it can be determined whether this phase in the skipjack sweep also corresponds to maximum velocity of the tail tip.

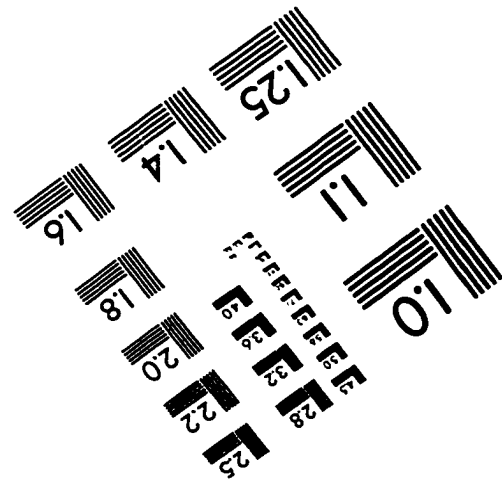
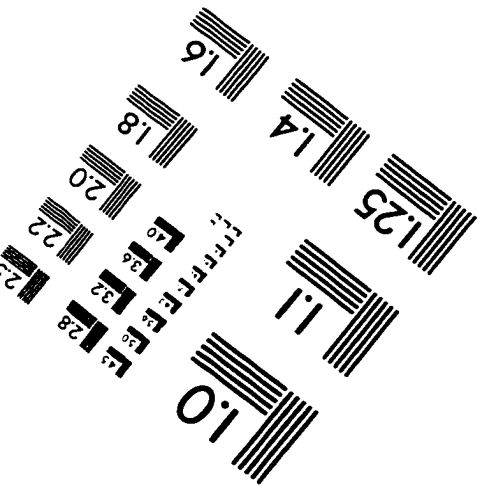
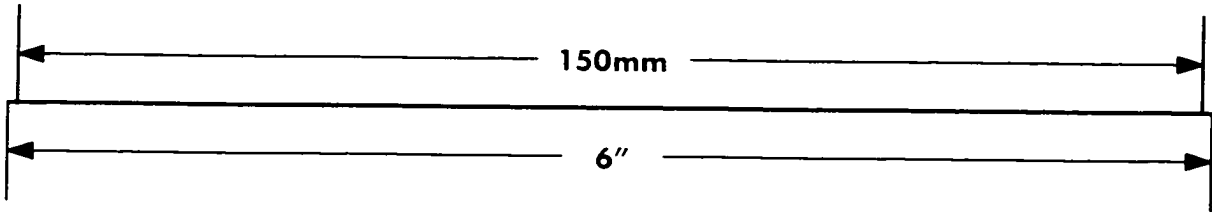
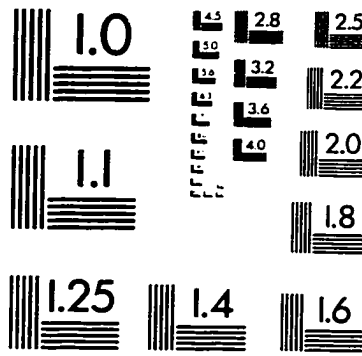
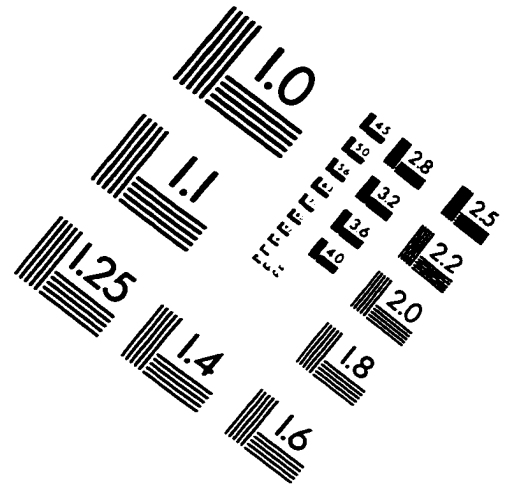
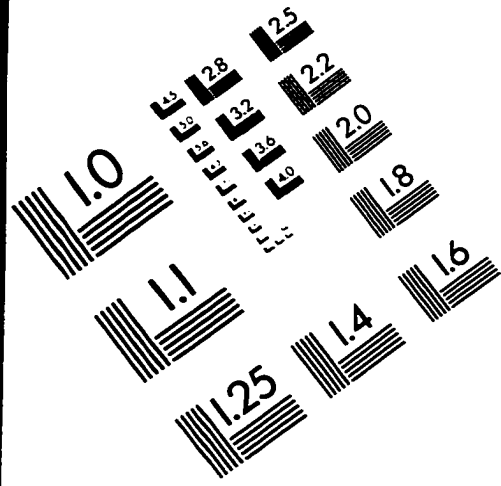
The biomaterial characteristics of the tuna caudal tendons were studied to assess their role as force transmitters *in vivo*-- specifically, to determine if they function as energy-storing springs or inextensible force transmitters. The caudal tendons are thick and short relative to the loads they experience during swimming. Consequently, the stresses and strains they experience are very low, which means they store only a minute amount of energy during swimming. These properties of the tuna tendons are consistent with those of most mammalian limb tendons, indicating that they serve as inextensible, direct linkages to transmit muscle force to the tail blade. Using tendons in this capacity represents the most efficient mechanism for force



transfer, both in terms of minimized space across the peduncle and minimum metabolic costs. Inextensible tendons also provide a high degree of control in moving the tail blade.

This first integrated study of the dynamic features of the thunniform swimming mechanism has pointed out that while yellowfin and skipjack are similar in many respects, even subtle differences in muscle activation patterns and body morphology can result in detectable differences in swimming mode. The interactions between muscle activation and body morphology, and the subsequent interactions between the bending body and the surrounding water, can combine in intricate ways to dictate swimming styles. The ability to study muscle activation within the myotome cones at steady swimming speeds has provided preliminary data to assess dynamic muscle function within this complicated arrangement of fiber geometries. The unique ability to measure experimentally the net muscle force reaching the tail has also contributed to our understanding of the relationship between muscle activation and thrust production. Future work with sonomicrometry (which can be used to measure muscle strain directly), in conjunction with EMG and force measurements, will enable a test of the prediction that muscle produces net positive work all down the body in these tunas. It is hoped that the research presented herein has not only shed light on the dynamics of the thunniform swimming mechanism, but has also broadened our understanding of axial fish locomotion in general.

# IMAGE EVALUATION TEST TARGET (QA-3)



**APPLIED IMAGE, Inc**  
 1653 East Main Street  
 Rochester, NY 14609 USA  
 Phone: 716/482-0300  
 Fax: 716/288-5989

© 1993, Applied Image, Inc.. All Rights Reserved